Evaluation of the global warming impact on the cooling demand in buildings worldwide

Auteur : Verheyden, Antoine
Promoteur(s) : Lemort, Vincent
Faculté : Faculté des Sciences appliquées
Diplôme : Master : ingénieur civil en génie de l'énergie à finalité spécialisée en Energy Conversion
Année académique : 2024-2025
URI/URL : http://hdl.handle.net/2268.2/23353

Evaluation of the global warming impact on the cooling demand in buildings worldwide

Master thesis for the degree Civil Engineer in Energy, specialising in energy conversion by VERHEYDEN Antoine

University of Liège - Faculty of Applied Sciences

Promoter:
LEMORT Vincent

Supervisor:
ZEOLI Alanis

Jury:
LEMORT Vincent
ZEOLI Alanis
GENDEBIEN Samuel
ANDRE Philippe

Academic year 2024 - 2025

Acknowledgement

First, I would like to warmly thank all the people who played a part in making this work possible.

I would like to express my sincere gratitude to my promoter, Prof. Dr. Vincent Lemort, for allowing me to do this work.

I would also like to sincerely express my deepest gratitude to my academic supervisor, Alanis Zeoli for her valuable guidance, insightful advice, expertise, ongoing support, supervision, and constructive feedback throughout this semester.

I would also like to thank the members of the jury for taking the time to read this work and attend its presentation.

I would like to express my gratitude to all the members of the Applied Thermodynamics Laboratory of the University of Liège for warmly welcoming me during this semester and for providing a supportive and enriching environment throughout the course of my Master's thesis.

I thank all the professors I have had over the years for sharing their knowledge. Their passion and commitment have helped me grow academically and personally.

Thank you to my classmates, whose support and encouragement made this academic journey much more enjoyable and meaningful.

Finally, I would like to deeply thank my family and my friends for their unfailing support, who have been a constant source of encouragement throughout those academic years.

Abstract

According to forecast statistics of the United Nations, the global population is expected to grow from 8.2 to 9.7 billion by 2050 and could approach 11 billion by 2100. The number of buildings and habitations is therefore expected to increase proportionally to the population growth. In the European Union, buildings account for 40% of the energy consumption and 36% of the greenhouse gas emissions, with HVAC systems being the biggest contributors. In the actual context of global warming, by the end of the 21^{st} century, the global air temperature is predicted to increase up to 4.8K if global warming issues are not handled carefully regarding the greenhouse gas emissions. As a result, cooling is expected to become the fastest-increasing energy-consuming technology in buildings, making it a key focus for efforts to limit further global warming.

This thesis investigates the impact of global warming on the cooling demand of residential buildings worldwide. A dynamic thermal model was developed and validated to simulate the hourly indoor temperature and cooling loads under various climate conditions. Typical Meteorological Year (TMY) data for present (2001–2020) and future (2041–2060) periods were used to assess the evolution of cooling needs in multiple representative cities across different climate zones.

The results reveal a clear and consistent increase in cooling demand, particularly in regions already subject to warm or humid climates. Increases range from +15 % to over +60 % depending on the city. A sensitivity analysis was conducted to identify the most influential parameters on indoor temperature, such as solar gains, insulation levels, and internal heat sources. The simulation model was validated using real data from monitored test houses, achieving strong statistical accuracy.

In addition, several passive cooling strategies were tested in the model to assess their potential to reduce future cooling loads. Among these strategies were window shading, thermal mass enhancement using concrete layers, phase change materials (PCM), and night-time ventilation. These measures showed significant capacity to reduce future cooling loads, with combined reductions reaching up to 99 % in some cases. However, their effectiveness varied by climate, underlining the need for context-specific design strategies.

This study emphasises the importance of anticipating future energy needs and rethinking building design in a warming world. While passive and active cooling solutions offer promising paths, long-term sustainability will also depend on broader changes in energy consumption behaviours and in the way our cities are designed and organised. Urban layout, building density, green spaces, and materials used play a key role in shaping the thermal performance and energy needs of buildings.

Contents

List of Figures

List of Tables

1 Introduction

"J'entendais parler du réchauffement climatique depuis longtemps. Je me réfugiais derrière une échéance lointaine. Ça devient réel." [Jean-Marc Jancovici, Le monde sans fin (BD) 29 octobre 2021]

In today's world, the population is constantly increasing. According to the United Nations [1], the global population could approach 11 billion individuals by the end of the 21^{st} century. As a result, the number of buildings is also expected to rise. In 2019, the average CO_2 emissions per capita worldwide were 5 tons, compared to 4.3 tons in 1990 [2]. This simultaneous increase in both population and per capita emissions suggests that total greenhouse gas emissions will continue to grow. Consequently, this trend is likely to further contribute to global warming and the rise in average air temperatures. The global air temperature is predicted to increase up to 4.8K considering the Representative Concentration Pathways (RCP) 8.5 of the GIEC by the end of the century due to the constant increase of greenhouse gas emissions worldwide [3, 4]. In this scenario, greenhouse gas emissions and concentrations increase significantly over time, leading to a radiative forcing of 8.5 W/m² by the end of the century. This scenario is in line with the current emission trajectories of greenhouse gases around the world [5]. When looking at the European Union, buildings account for 40% of the energy consumption and 36% of greenhouse gas emissions which puts this sector as one of the biggest emitters of greenhouse gas emissions [6–9]. In the building sector, cooling with HVAC systems is the biggest contributor to energy consumption and greenhouse gas emissions. As the global air temperature is expected to increase in the future, the cooling demand in buildings is going to increase too. As a result, cooling is going to be a key focus for efforts to be made in the building sector to limit its impact and limit global warming [10–12].

This work will first focus on the causes of global warming and their influence on each other. This will demonstrate the snowball effect of the various causes, resulting in the intensification of global warming. The resulting consequences are then discussed to highlight the urgency of addressing greenhouse gas emissions.

In this context, evaluating the impact of global warming on the cooling demand in buildings is highly relevant. As global temperatures continue to rise, the need for space cooling will increase significantly, especially in densely populated or already warm regions. This growing demand not only affects building design and energy consumption but also has critical implications for grid stability, infrastructure planning, and sustainability efforts [13, 14].

A dynamic numerical model will be developed to predict the cooling load of buildings based on a set of key parameters. These parameters will be adapted according to the geographical region in which the building is located, since construction techniques vary globally due to differences in climate and the availability of local resources.

The model will be validated using real-world data to ensure its reliability. A sensitivity analysis will then be carried out to identify the most influential parameters of the building that affect indoor temperature.

Once validated, the model will be used to assess the impact of global warming on building cooling demand worldwide. For that, representative cities will be chosen for the different climates present on Earth. The impact of global warming will be evaluated by comparing the model's results obtained with present-day and future Typical Meteorological Year (TMY) weather files, selected based on the location of each case study.

Finally, the study will explore alternative cooling strategies that are less energy-intensive than conventional active air-conditioning systems. These solutions aim to offer preliminary insights into how the increasing cooling demand could be managed more efficiently. As electricity use rises to meet

this demand, greenhouse gas emissions in the building cooling sector are also expected to grow. Implementing these strategies could help reduce both energy consumption and emissions in the context of a warming climate.

2 Global warming

This chapter provides a comprehensive overview of global warming, from the origins of atmospheric processes and the interactions between greenhouse gases and solar irradiation to the actual and potential future consequences of climate change. This helps to understand why, nowadays in particular, it is crucial to act to reduce anthropogenic greenhouse gas emissions. Additionally, it is important to already think about the fact that the global mean temperature on Earth is increasing and will continue to do so, which will directly lead to an increase in the demand for cooling in buildings worldwide. This work aims to analyse this phenomenon and quantify the projected increase in cooling demand.

2.1 Causes of global warming

2.1.1 Atmosphere

a. Atmosphere layers

The Earth's climate is largely determined by the physics and chemistry of the atmosphere and is illustrated in Figure 1. The lower atmosphere also called the troposphere, from the surface up to about 11-km altitude, is the most crucial zone for humans. Therefore, it is the zone where the variation in the physics and chemistry of the Earth is the most influential. In the troposphere, the temperature decreases with an increase in altitude. This results in cold dense air on top of warm less dense air which is unstable and creates a turbulent zone that mixes the air. The lower atmosphere represents 99% of the atmospheric mass and it is the zone where most of the water vapour is present. The second atmosphere layout is the stratosphere, from 11 to 50 kilometres altitude, where much of the ozone is present and the temperature increases with altitude due to absorption of ultraviolet radiation from the sun in this layer, resulting in a stable zone which corresponds to 1% of the atmospheric mass [15]. The next zones are the mesosphere and thermosphere but their contributions are less important regarding life on Earth and global warming. Therefore, they will not be developed and considered in this work.

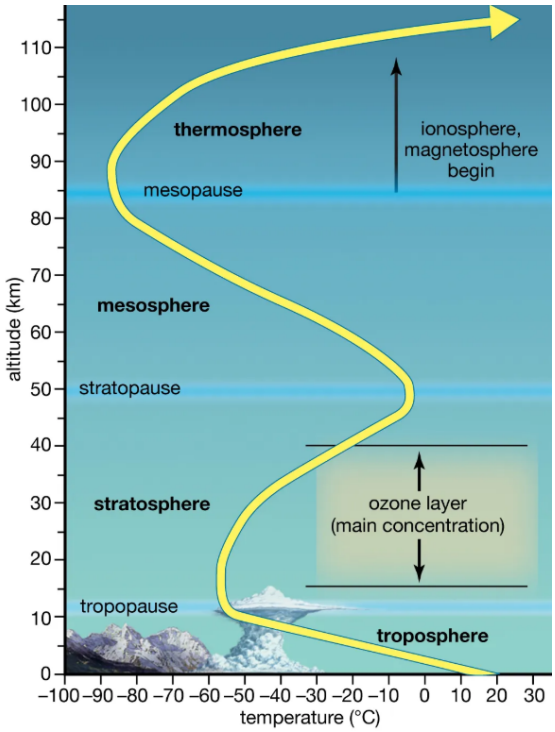

Figure 1: The atmosphere's layers [16].

a. Chemical composition

The atmosphere is a mechanical mixture of gases. Three main gases account for 99.9 % of its volume: nitrogen (78.09 $\%volume$), oxygen (20.95 $\%volume$), and argon (0.93 $\%_{volume}$). However, these major constituents have little influence on the Earth's climate. It is the trace gases, commonly referred to as greenhouse gases, that have the greatest impact. These include carbon dioxide (CO_2), methane (CH_4), carbon monoxide (CO), nitrogen oxides (NO_x), chlorofluorocarbons (CFCs), and ozone (O_3). Water vapour (H_2O) also has a great effect on climate, but its concentration in the atmosphere is highly fluctuant in time as it can go from 0.5% to 4%. The following Table 1 presents the major greenhouse gases present in the atmosphere, where they come from and how they impact the climate. The global warming potential (GWP) is expressed in CO_2-equivalent to provide a common reference for comparing the impact of different greenhouse gases. For example, the emission of 1 kg of methane is equivalent to emitting 25 kg of carbon dioxide.

Chemicals	**Natural source**	**Human source**	**Global warming potential (CO_2-eq)**	**Lifespan in atmosphere (years)**	**Participation in global warming**	**Volume in atmosphere**
H_2O	Water cycle: water evaporates, condenses as clouds, falls as rain or snow, flows or sinks, and evaporates again.	Global warming will accelerate water cycle, dry regions having less rains, humid regions receiving more rains. Also directly emitted by human activities: cooling towers, airplane engines, combustion systems.	/	/	/	0.5 - 4%
CO_2	Carbon cycle: emitted by animals, humans and plant breathing, decay of organic matter, and absorbed by plants (by photosynthesis) and oceans (by planktons and sediments). Note: Human respiration (8 billion people) also contributes to CO_2 release.	Burning carbon-containing materials (e.g. deforestation and burning fossil fuels).	1	5 - 200	65%	0.04%
CH_4	Methane cycle: emitted by decay of organic matter in wetlands, turn into water vapour and CO_2 by reaction in the atmosphere.	Burning natural gas, raising livestock, growing rice and waste landfill.	25	10	17%	0.0002%
N_2O	Nitrous oxide cycle: emitted by bacteria and fungi in soils and oceans.	Use of chemical fertilisers and livestock manure in agriculture, fossil fuel combustion (by coal power plants and internal combustion engines).	298	115	8%	0.00003%
O_3	Ozone-oxygen cycle: formed from oxygen under solar UV radiation in the stratosphere.	At ground level, reaction of NO_x, CO, and particles, (produced by internal combustion engines and industries), in the sunlight.	/	/	/	0.000004%
F-gases	/	Used in refrigerants, aerosols, industrial processes, and electronic components.	5,500 - 22,800	1 - 50,000	10%	0.000000005%

Table 1: Major greenhouse gases, where they come from in nature and by human source, their global warming potential or CO_2-eq, lifespan in the atmosphere, their part in global warming and volume in the atmosphere [17, 18].

2.1.2 Greenhouse effect

The Earth's temperature results from a delicate balance between incoming and outgoing energy. The Earth continuously receives energy from the Sun, mainly in the form of visible light and shortwave irradiation. At the same time, the Earth emits part of this energy back into space as infrared radiation. The average global temperature is maintained when the amount of energy received equals the amount of energy lost. This balance is what governs the Earth's climate system. Life on Earth is possible thanks to the greenhouse effect, illustrated in Figure 2, and defined by Nasa as: *"A process that occurs when gases in Earth's atmosphere trap the Sun's heat. This process makes Earth much warmer than it would be without an atmosphere. The greenhouse effect is one of the things that makes Earth a comfortable place to live."* [19].

Most of the incoming solar ultraviolet radiation passes through the atmosphere without significant interference. However, the most harmful component, UV-C radiation, is almost entirely absorbed by the ozone layer, providing vital protection for living organisms on Earth [20, 21]. Overall, about 70 % of the total solar radiation is absorbed by the Earth's surface (land and oceans) and atmosphere, contributing to their warming. The remaining 30 % is reflected back to space by bright surfaces (clouds, ice,..). Lands and oceans then radiate the energy acquired as infrared radiation (radiation at wavelengths much longer than the radiation from the sun as it is colder) and part of it is absorbed by greenhouse gases and then re-emitted into the atmosphere in all directions, including downwards. The energy that radiates back toward Earth acts as a heating trap and enhances the heating from direct sunlight and therefore warms the atmosphere. This greenhouse effect is beneficial and essential to life on Earth, without it, the Earth would be at least 33°C colder at approximately -18°C instead of the 15°C of today [22, 23].

The Earth is therefore in a dynamic energy equilibrium: over time, all the energy received from the Sun is eventually emitted back into space. However, when the concentration of greenhouse gases increases, the atmosphere retains more of the outgoing infrared radiation. To restore the energy balance, the Earth must radiate more energy. This is only possible by increasing its surface temperature. This phenomenon is known as radiative forcing and is a key driver of global warming.

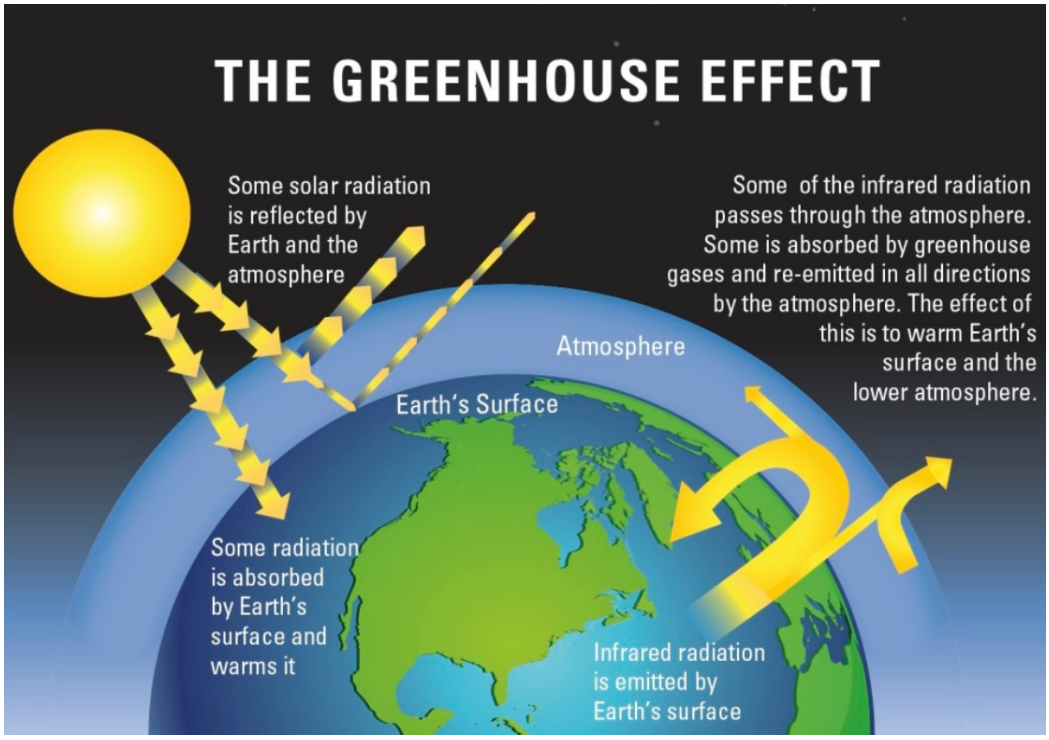

Figure 2: The greenhouse effect [24].

2.1.3 Greenhouse gases emissions and global mean temperature on Earth

Global warming is nowadays a fact. Some people are still sceptical, but the numbers are there, and they will be presented in the following. Since the Industrial Revolution, which began around 1750, humans have been burning fossil fuels (coal, oil and natural gas), which release carbon dioxide (CO_2) and methane (CH_4) into the atmosphere, and cutting down at an accelerated rate carbon-absorbing forests. Two phenomena that artificially increase the concentrations of greenhouse gases in the atmosphere. Between 1750 and 2009, the concentration of methane in the atmosphere increased by 148% due to an increase in human emissions, as can be seen in Figure 3 [22, 25]. These additional greenhouse gases increase the greenhouse effect and therefore elevate Earth's temperatures.

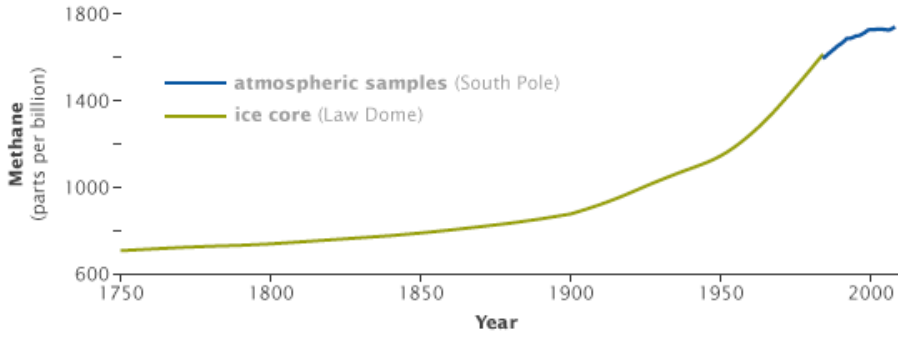

Figure 3: The increase in methane concentration in the atmosphere since the Industrial Revolution [22].

In 2003, a report showed that the global mean temperature had risen by 0.7°C between 1880 and 2001 [26]. Although the exact causes of global warming were still being investigated at that time, a clear correlation had been observed between the increase in global mean temperature and the rise in greenhouse gas emissions. Indeed, from 1880 to 2002, atmospheric concentrations of carbon dioxide and other greenhouse gases increased significantly, from about 275 to 370 parts per million (ppm) [26].

During the Pleistocene and Holocene, the last 2.5 million years, the CO_2 concentration in the atmosphere varied between 180 ppm during ice ages and 300 ppm during interglacial periods as can be seen in Figure 4. The variations in CO_2 concentration were due to slow multi-millennial orbital variations [5]. In December 2024, the atmospheric CO_2 concentration was 425 ppm and has been increasing at a rate of approximately 2 ppm per year during the last 10 years due to human activities as can be seen in Figure 5. The CO_2 concentration in the atmosphere has increased by 50% in less than 200 years *(which corresponds to the Industrial Revolution)* [27].

During the last deglaciation period, global average temperatures increased by 6°C in about 4000 years. From 1850 to 2024, the global mean temperature has increased by 1.55°C in only 174 years, as illustrated in Figure 6 [29, 30].

Since 2021 and the AR6 synthesis report of the Intergovernmental Panel on Climate Change (IPCC), the fact that global warming is due to human activities is unequivocal [5, 31].

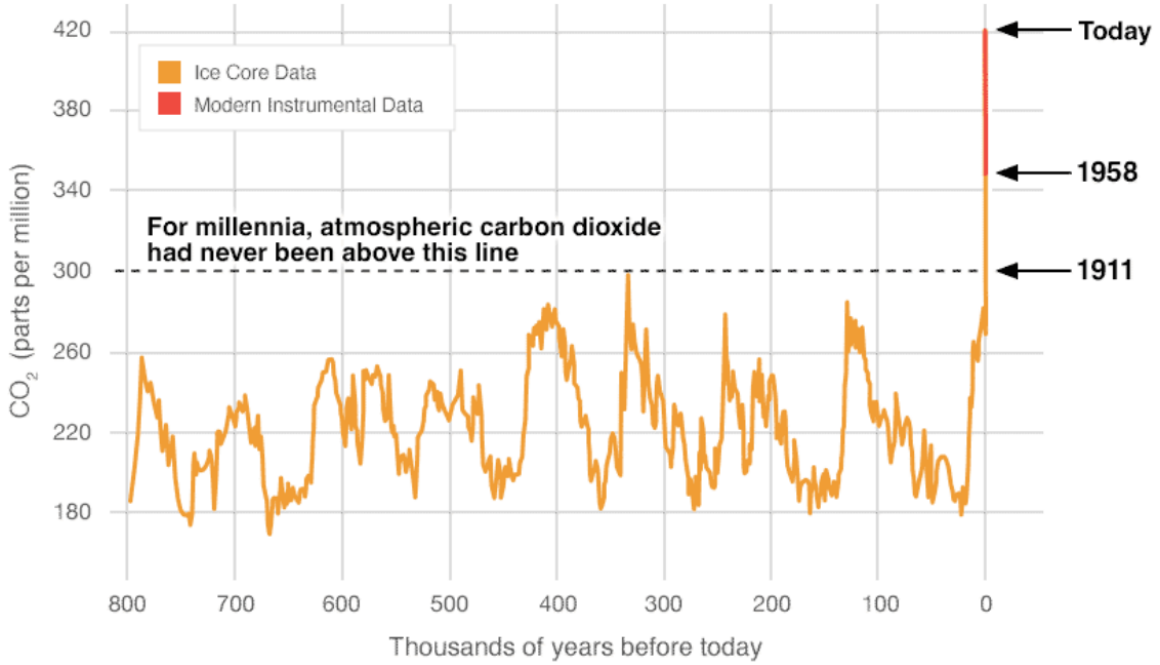

Figure 4: CO_2 concentration evolution during the last 800 thousand years [28].

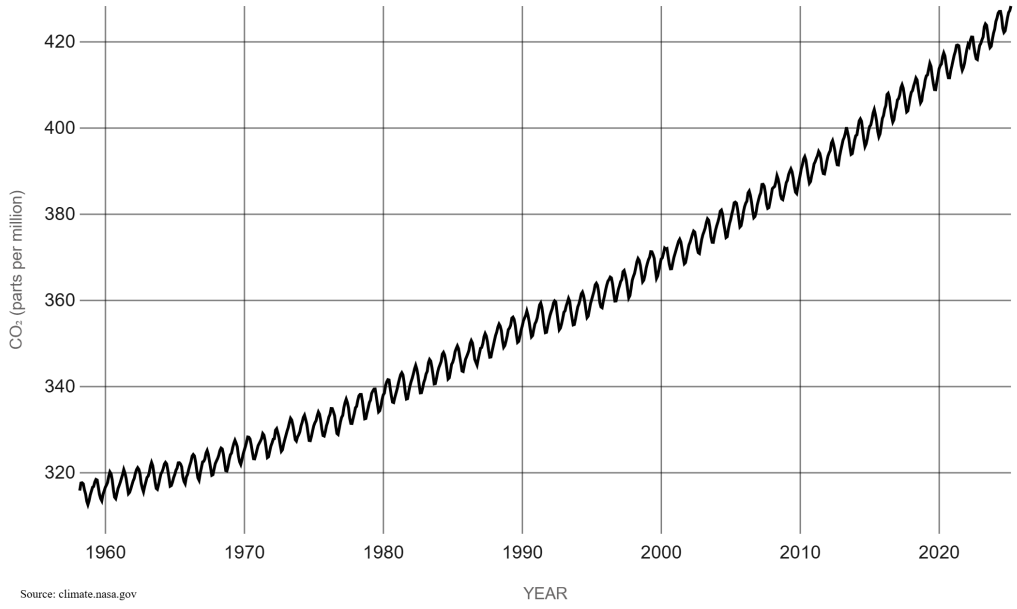

Figure 5: CO_2 concentration evolution since 1958 [27].

2.1.4 Hole in the ozone layer

As aforementioned, the stratospheric ozone layer is a very important gas that forms a thin layer that filters out harmful ultraviolet radiation by absorbing part of it. The UV-C is entirely absorbed, UV-B is partially and UV-A passes through it and reaches the Earth's surface as illustrated in Figure 7. Ultraviolet light damages DNA in animals and plants. It can lead to sunburns and cause cancer and eye damage [23].

Chlorofluorocarbons (CFCs) are long-lived chemical gases that have been used since the 1930s. They were mainly employed as refrigerants in refrigerators and air conditioners, as well as in aerosol cans and solvents for cleaning. In the 1980s, scientists discovered that when CFCs reach the stratosphere,

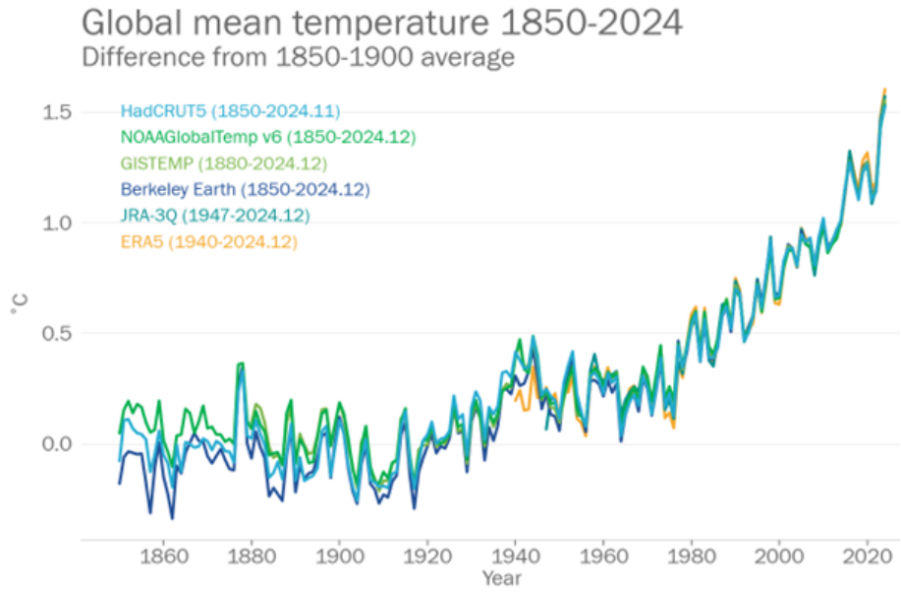

Figure 6: Variation in global mean temperature on Earth from 1850 [29].

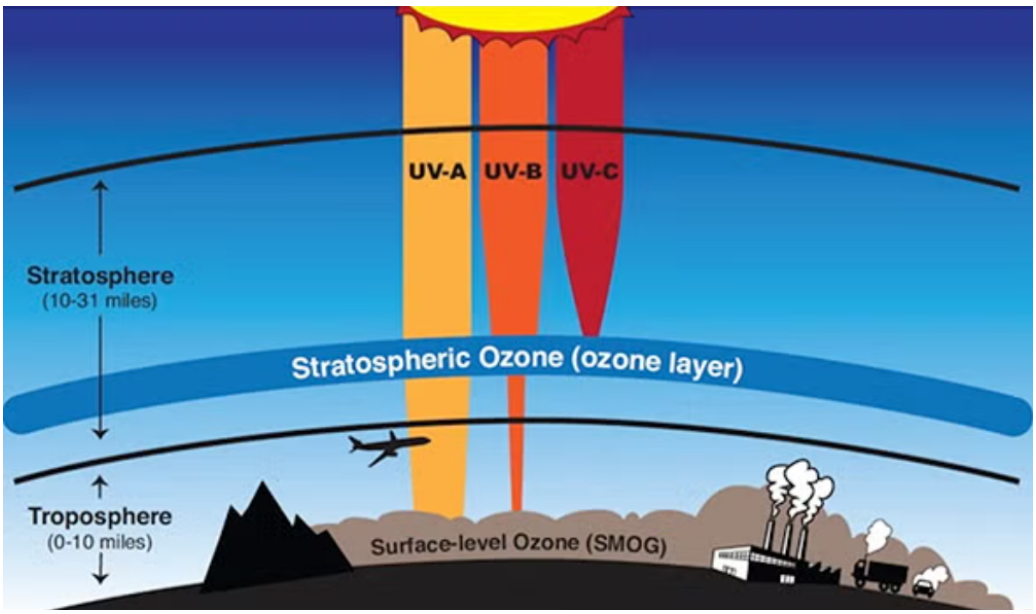

Figure 7: The interaction between the ozone layer and UV radiation [32].

they can break apart under ultraviolet (UV) light. This process releases chlorine atoms, which are highly reactive. Chlorine acts as a catalyst in the destruction of the ozone layer. During the same period, scientists noted large decreases in ozone concentrations in the atmosphere. The largest depletions took place towards the poles and in particular Antarctica due to long, low temperatures (below -78°C) in the stratosphere, which encourage the formation of stratospheric clouds that accentuate ozone depletion [33, 34]. In 1987, an international agreement called the "Montreal Protocol" was concluded to progressively ban CFCs [35]. Approximately 80% of the chlorine present in the stratosphere is due to human activity. At the beginning of the 21^{st} century, CFC concentration in the atmosphere has stabilised. Since then, ozone concentration has been increasing, and the ozone hole is gradually closing above Antarctica. The evolution of the ozone hole is illustrated in Figure 8. Models predict that it should mostly be recovered by 2040 [36]. Since ozone is a greenhouse gas, the recovery of the ozone layer in the stratosphere will have an antagonist effect, which is a further warming of the Earth's atmosphere. Besides, CFCs have been replaced by other fluorinated gases

such as hydrofluorocarbons (HFCs) in refrigerants, which are also powerful greenhouse gases [37].

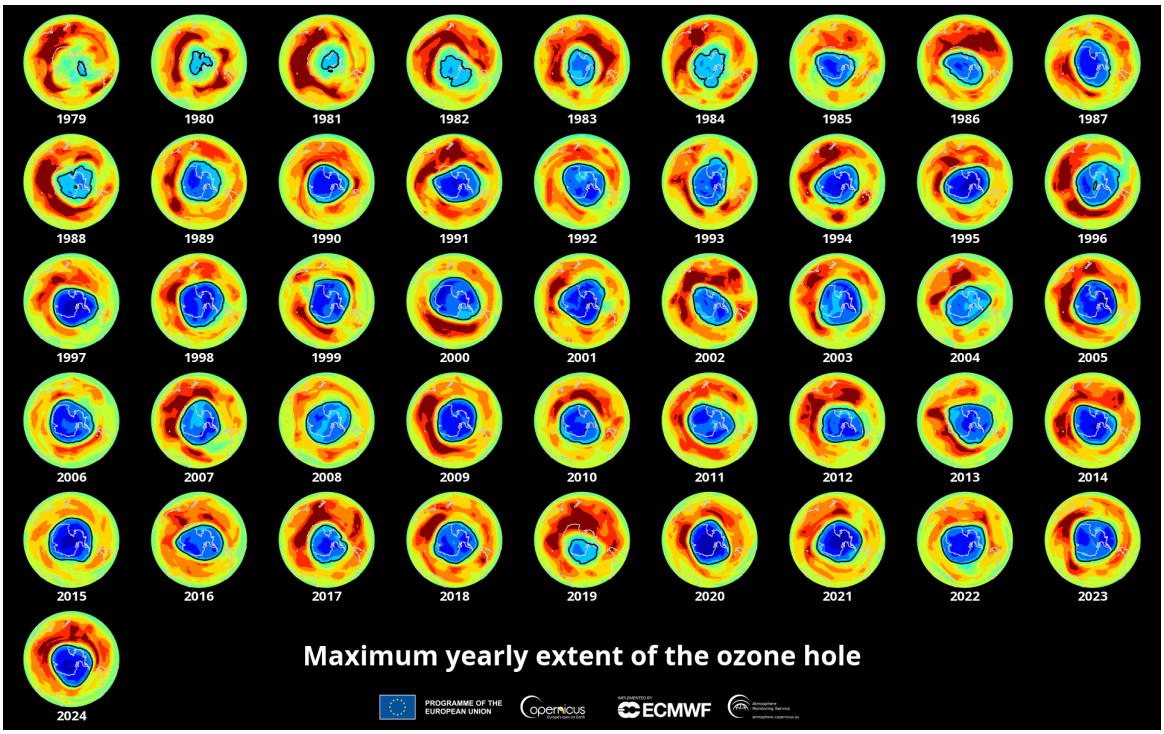

Figure 8: The evolution of the ozone hole since 1979 [33].

2.1.5 Albedo effect

The ability of a surface to reflect solar radiation is called the albedo. A surface with high albedo reflected most of the sunlight like snow or ice. The lighter the surface, the higher its albedo. On the other hand, dark surfaces absorb most of the solar radiation which has a warming effect and are characterised by a low albedo. Therefore, with the melting of snow and ice on Earth particularly in the Arctic and Antarctic, more dark (low albedo) surfaces appear which will lead to more warming and more melting.

2.1.6 Aerosols

Aerosols are small suspended solid or liquid dust particles floating in the atmosphere. They vary in size from nanometers to micrometres and affect climate (absorbing thermal and solar radiation), weather (modifications in cloud reflectivity), and human health differently, depending on their size and composition. Aerosols result from rising sea spray or sand, mineral dust, volcanic ashes, smoke, forest fires, vehicle exhausts, and agricultural and industrial activities after going through chemical reactions in the atmosphere. In general, aerosols have a cooling effect on climate by reflecting sunlight. For example, the gases and ashes emitted in 1991 in the Philippines during the Pinatubo volcanic eruption cooled the region to a temperature of around 0.6°C by shading the incoming solar radiation. This effect could sometimes last for months. Another impact of aerosols is their role in cloud formation by acting as cloud condensation nuclei. An increase in atmospheric aerosol concentration can therefore influence cloud quantity, size, altitude, and even the amount of precipitation.

However, some types of aerosols, such as black carbon (commonly produced by incomplete combustion from vehicle exhausts, biomass burning, and industrial emissions), absorb sunlight like greenhouse gases, creating additional heating of the atmosphere. These aerosols, mostly human-emitted,

contribute to a warming effect. The aerosol can also play an important role in the modification of the albedo: when dust or soot is deposited on ice or snow, it becomes darker, which decreases the reflectivity (albedo). As a result, more sunlight is absorbed, leading to a warming effect that accelerates ice and snow melt. This further amplifies the process, as the exposed ground beneath is even darker, absorbing more heat [23, 38].

2.1.7 Direct anthropogenic CO_2 emissions

According to the IPCC [5] and as can be seen in Figure 9, the current global warming is mainly due to anthropogenic greenhouse gas emissions that increase the greenhouse gas concentration in the atmosphere and lead to an increase in global mean temperature on Earth [31]. Other causes are human land use (deforestation), aerosols, ozone, solar and volcanic activity.

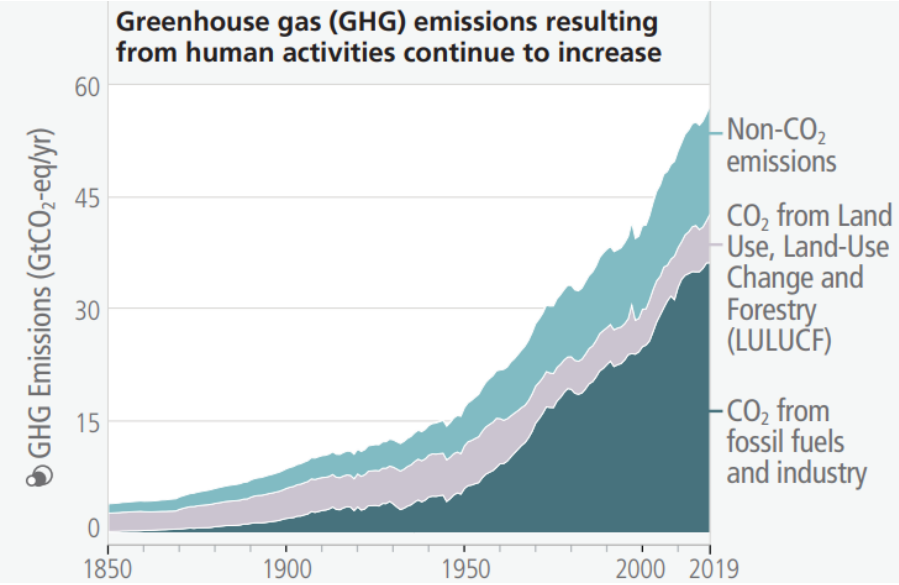

Figure 9: Evolution of the GHG emissions resulting from human activities [5].

In 1900, human activities emitted about 5 billion tonnes of CO_2. In comparison, in 2019, they emitted a bit less than 45 billion tonnes of CO_2. In 2023, greenhouse gas emissions represented 53 billion tonnes of CO_2-eq [39].

According to the IPCC [5], anthropogenic greenhouse gas emissions have increased since the Industrial Revolution due to economic and population growth. Since 1950, the value of all goods and services produced worldwide has multiplied by 14, passing from 11.74 trillion $ to 166.65 trillion $ in 2023 as illustrated in Figure 10 [40].

In the 20^{th} century, the human population has multiplied by 4, from 1.5 to 6.1 billion. In the last 25 years, the human population has increased by 2.1 billion people to 8.2 billion people today [41] [42]. The world population will grow at a rate of 0.85% per year in 2025 and the current population increase is estimated at approximately 70 million people per year [43]. The evolution of the world population and the predictions are illustrated in Figure 11.

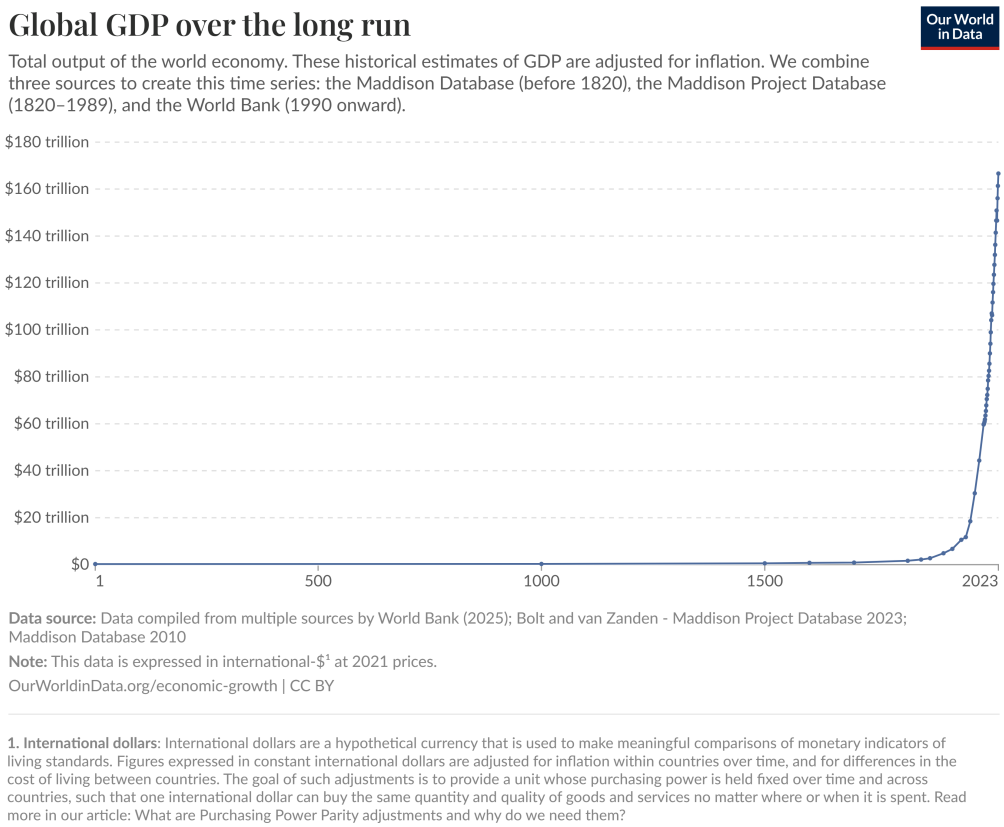

Figure 10: Evolution of the world gross domestic product [40].

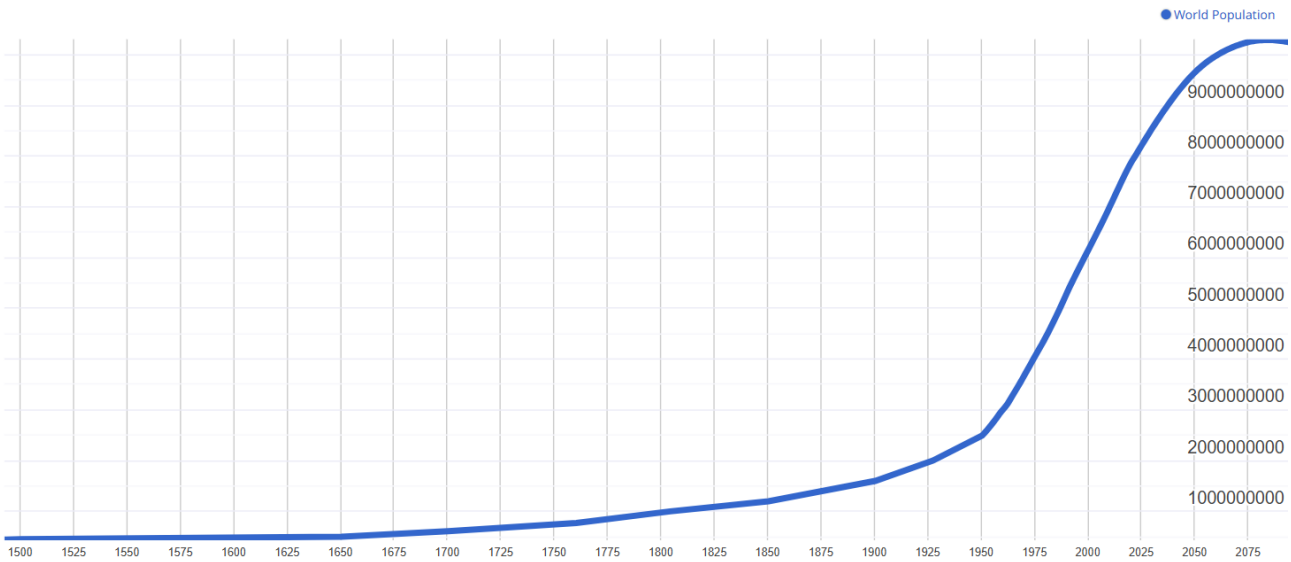

Figure 11: Evolution of the world population [43].

2.2 Consequences of global warming

Climate change is not immediate, there is inertia due to the huge heat capacity of the oceans. The oceans can store over 1000 times more heat than the atmosphere, which significantly delays the full warming effect of increased greenhouse gas concentrations [44]. The increase in temperature nowadays is therefore not directly linked to the increase of greenhouse gas emissions occurring nowadays but to the ones that occurred a few years ago. The climate responds to greenhouse gas emissions with a delay of approximately 10 to 20 years. Accordingly, the current consequences experienced should

be due to emissions that occurred at the beginning of the 2000s. [45–47]

2.2.1 Short-term consequences

a. Temperature rise

As previously mentioned in Tables 2 and 3, RCP 8.5 is the scenario currently being approached, given the greenhouse gas emissions observed in recent years with an increase in temperature in 2100 near 4.8°C as can be seen in Figure 15. This increase in temperature will not be shared equally on Earth. Certain regions, particularly the poles and the mountain chains will be more affected as can be seen in Figure 12.

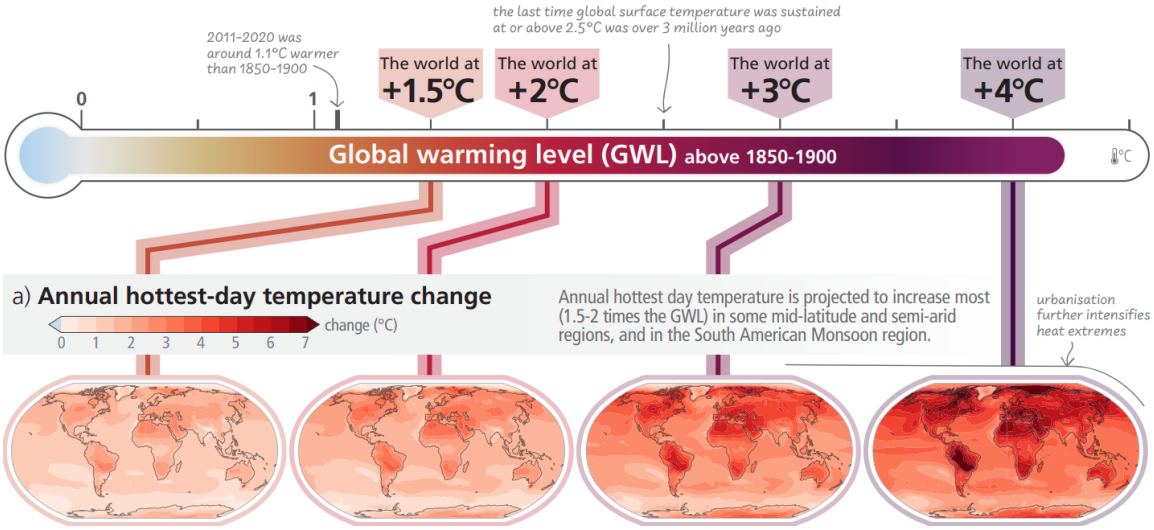

Figure 12: Evolution of the annual hottest day temperature change depending on global warming level [5].

This unequal rise in temperature across the globe does not come without consequences, particularly in regions already exposed to high heat levels. When outdoor conditions become excessively hot, indoor environments also suffer, leading to a variety of negative outcomes for building occupants. One of the first and most direct effects is the degradation of thermal comfort. Although not necessarily life-threatening, discomfort due to overheating can significantly affect daily well-being and lead to dissatisfaction with indoor environments (too hot or too cold, too dry or too humid) [14, 48, 49].

Sleep quality is another area highly sensitive to elevated indoor temperatures. According to the Chartered Institution of Building Services Engineers (CIBSE), temperatures exceeding 24°C at night have been shown to reduce sleep efficiency, increase nighttime awakenings, and delay the time to fall asleep [50, 51]. These disruptions can negatively affect restfulness, productivity and general health, especially if they persist over time [14, 52, 53].

In addition, elevated indoor temperatures also negatively affect mental performance. Overheating has been associated with reduced concentration ability, slower reaction times, and decreased accuracy in performing tasks [54–56]. These effects are particularly problematic in workplaces and learning environments, such as schools, where they can lead to noticeable drops in efficiency. Research shows that this can result in productivity losses that can reach or exceed 10% [57–59]. With the growing prevalence of homeworking, this issue is also becoming increasingly relevant in residential buildings [14, 60].

More importantly, high temperatures can directly threaten health. According to the World Health Organization, prolonged exposure can intensify pre-existing health conditions such as cardiovascular

or respiratory diseases, diabetes, and renal issues [61]. Vulnerable populations, including the elderly, infants, pregnant women, and those with medical conditions, are especially at risk. The consequences are most evident during extreme events like heat waves, which can cause widespread health emergencies. For example, the 2003 European heatwave led to nearly 70,000 excess deaths, with cities such as Paris experiencing mortality rates more than double the norm [14, 62].

b. Sea level rise

The global sea level has already risen by approximately 25 cm since 1900 [63]. Under the RCP 8.5 scenario, the global mean sea level could rise by up to 1 meter by the end of the century as can be seen in Figure 13. Extreme sea level events that previously occurred once per century could become 20 to 30 times more frequent by 2050. This rise will result in increased flooding and coastal erosion, affecting all coastal regions and small islands. Small island nations, such as the Maldives, the Marshall Islands, and the Seychelles, are projected to become uninhabitable with a 1-meter rise in sea level. Major coastal cities, such as Shangai, Hong Kong (China), Mumbai (India), New York (USA), and Tokyo (Japan) will face significant impacts. Additionally, major deltas and rivers will also be affected such as the Nile, the Mississippi, the Mekong, and the Rhine. In total, approximately 1 billion people will be exposed to such risks [5].

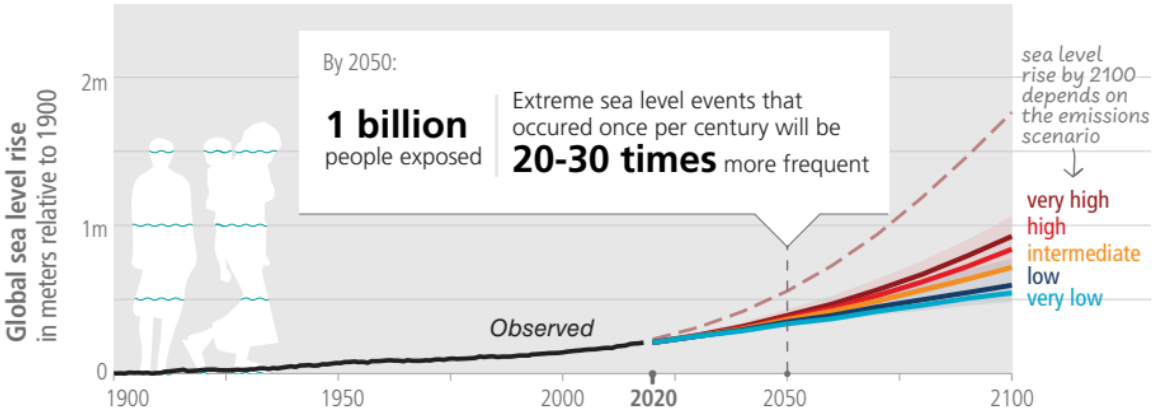

Figure 13: Evolution of the sea level rise (observations and projections based on the IPCC scenarios) [5].

The first cause of sea level rise is thermal expansion [64]. Warmer water takes more place than colder water. As a result, when the ocean gets warmer, the sea level rises [65]. As the increase in temperature will not be shared equally on Earth, the sea level increase will also not be the same everywhere. Another cause is the melting of glaciers and ice sheets in Greenland and Antarctica but this is more of a long-term consequence and will be developed below.

c. Biodiversity

Global warming will lead to mass species extinction due to the loss of their habitat caused by deforestation, forest burning or due to the rise in temperature not tolerated by certain species, especially the marine species. Approximately 50% of tropical marine species will disappear, and a shift in biome will be observed across 35% of the Earth's continents [5].

d. Ocean acidification

Direct measurements of the ocean's chemistry have shown that the oceans have become more acidic. This results from the dissolution of atmospheric CO_2 in the surface water of oceans. As the atmospheric concentration in CO_2 increases, ocean acidification increases. Some marine organisms, such as corals and shellfish, have shells composed of calcium carbonate. In acidic environments, the calcium carbonate dissolves more rapidly leading in dead of the organisms [66–68]. Oceans are considered the second lung of the planet, they absorb more than a quarter of the CO_2 emitted thanks

to corals' photosynthesis [69]. As a result, the acidification of the oceans puts in danger the CO_2 absorption capacity of oceans.

e. Extreme climate events

Hurricane formation will be favoured in a warmer world, as these storms require sea surface temperatures above 26°C to develop [70]. Hurricanes risk to occur more frequently. Flooding will also be more frequent as aforementioned, and approximately 10% of the global land area is expected to experience both more frequent high extreme streamflows and reduced low extreme streamflows, impacting over 2.1 billion people without additional adaptation measures [5]. The frequency and strength of heat waves and droughts will increase, which will also lead to more forest fires [71]. According to the IPCC [5], the global burned area on Earth will increase by 50 to 70% and the fire frequency by approximately 30% compared to 2020. Heat waves and droughts are always accompanied by human deaths; for example, the 2003 heat wave in Europe resulted in at least 30,000 deaths (more than 14,000 in France) [61, 72]. As a result, around 4 billion people are expected to face water scarcity [5].

f. Global consequences

As a result of all these short-term consequences, famines, humanitarian crises and mass migration are expected to occur. On average, more than 26 million people, mainly in Asia, are already displaced each year by climate-related events such as floods, cyclones, etc. according to [73] published in 2015.

2.2.2 Long-term consequences

a. Melting of ice sheets

On average, Greenland has lost 268 billion metric tons per year since 2002 [74]. If Greenland's ice melts completely, the global sea level would rise by 7 meters. Concerning Antarctica, the ice has been melting at an average rate of 137 billion metric tons per year since 2002 [74]. The melting of Antarctica is slower because it is effectively isolated from the rest of the world by circumpolar ocean currents and winds. If all Antarctic ice melts, the global sea level would rise by 58 meters. Regarding the Arctic Ocean, ice is declining at a rate of 12.2% per decade, meaning it is expected to be ice-free in summer before the end of the century [75]. This loss will accelerate global warming as the dark surface of the Arctic Ocean will absorb more solar radiation. This will result in a reduction of the Earth's albedo. The permafrost is land frozen permanently located in the North of the globe (near the Arctic), such as Greenland. The permafrost stores methane at high concentrations coming from decaying organic matter. Climate change is warming up the permafrost, which, when melting, releases the trapped methane. Scientists have estimated that there is at least 2.5 times more carbon within the world's permafrost than there was in the global atmosphere in 2020 [76–79].

b. Amazon rainforest death

Forests and especially rainforests are considered the lungs of the planet, they absorb CO_2 emitted thanks to photosynthesis. For rainforest to survive, it requires a large amount of rain during the wet season and a short dry season so as not to dry out [80]. Global warming will increase the dry season in Amazonia and therefore could lead to forest fires and the replacement of the rainforest by savannah [5]. When forest fires occur, the CO_2 stored is released back into the atmosphere. Moreover, savannah, dry grassland, absorbs much less carbon than rainforests. It is also important to note that deforestation is still occurring in Amazonia due to the expansion of agriculture, gold mining and logging [81]. Between 2001 and 2020, it is 54.2 million hectares of the Amazon forest that have been lost [82]. Such events occur in all rainforests worldwide.

2.3 Projected scenarios of global warming

Concerning the future of global warming on Earth, the IPCC has forecasted four different scenarios, referred to as the Representative Concentration Pathways (RCPs), presented in Table 2. Those pathways evaluate the evolution of human greenhouse gas emissions and temperature worldwide.

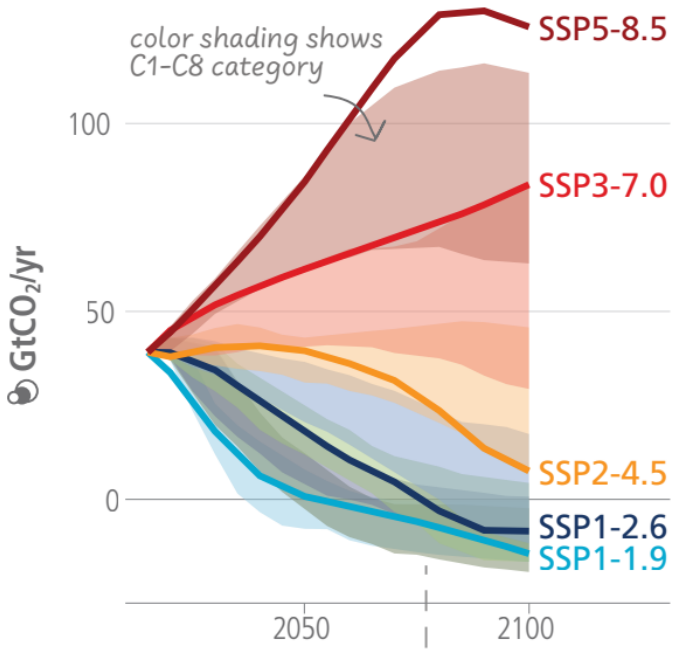

Figure 14: Potential future evolution of CO_2 emissions based on the scenarios of the IPCC [5].

RCPs	Names	Descriptions
RCP 8.5	'Business as usual' scenario	Emissions continue to rise throughout the 21^{st} century.
RCP 7	Stabilization scenario	Emissions peak around 2080, then decline.
RCP 4.5	Stabilization scenario	Emissions peak around 2040, then decline.
RCP 2.6	Voluntary scenario	Emissions peak before 2020, then decline substantially to reach no emissions and capture CO_2 afterwards.

Table 2: The different Representative Concentration Pathways (RCPs) forecasted by the IPCC linked to the anthropogenic GHG emissions.

The Representative Concentration Pathways (RCPs) are greenhouse gas concentration trajectories adopted by the IPCC to project potential climate futures. Each RCP is named after the level of radiative forcing it reaches by the year 2100, expressed in watts per square meter (W/m^2). For example, RCP 2.6 assumes aggressive mitigation efforts, stabilizing radiative forcing at 2.6 W/m^2, while RCP 8.5 represents a high-emission scenario with minimal mitigation, leading to a forcing of 8.5 W/m^2. The higher the number, the greater the expected accumulation of greenhouse gases in the atmosphere, and therefore the stronger the resulting warming effect. Under RCP 8.5, global air temperatures could rise by up to 4.8°C by the end of the century, as illustrated in Figure 15, due to the continuous increase in emissions and atmospheric concentrations of CO_2 and other greenhouse gases, illustrated in Figure 14 [3].

RCP 2.6 has already been exceeded, as CO_2 emissions have continued to rise, leading to a temperature increase surpassing the +1.5°C threshold. This exceedance violates the target set by the Paris Agreement, which aimed to limit global warming below this critical limit [83]. It is important to note that the IPCC scientists have insisted on the importance and necessity of staying below +1.5°C to avoid catastrophic consequences on Earth for human living [84]. In the AR5 report [85], the IPCC estimated the reduction of emissions needed for each scenario and their likelihood of staying below

certain temperature thresholds. Table 3 presents a simplified and rounded version of the values from the AR6 report [5], to ensure clarity and consistency with the latest IPCC data.

RCPs	CO_2-eq concentration in 2100 (ppm)	GHG change relative to 2010		Likelihood of staying below temperature thresholds by 2100 (relative to 1850-1900)			
		By 2050	By 2100	1.5°C	2°C	3°C	4°C
2.6	450	-55%	-100%	Unlikely	Likely	Likely	Likely
4.5	550	-10%	-80%	Unlikely	Unlikely	Likely	Likely
7.0	750	+35%	+30%	Unlikely	Unlikely	Unlikely	Likely
8.5	1,000	+75%	+125%	Unlikely	Unlikely	Unlikely	Unlikely

Table 3: CO_2-eq concentration of greenhouse gases in the atmosphere in 2100 for each RCP scenario, the required emission reductions, and the likelihood of staying below specific temperature thresholds.

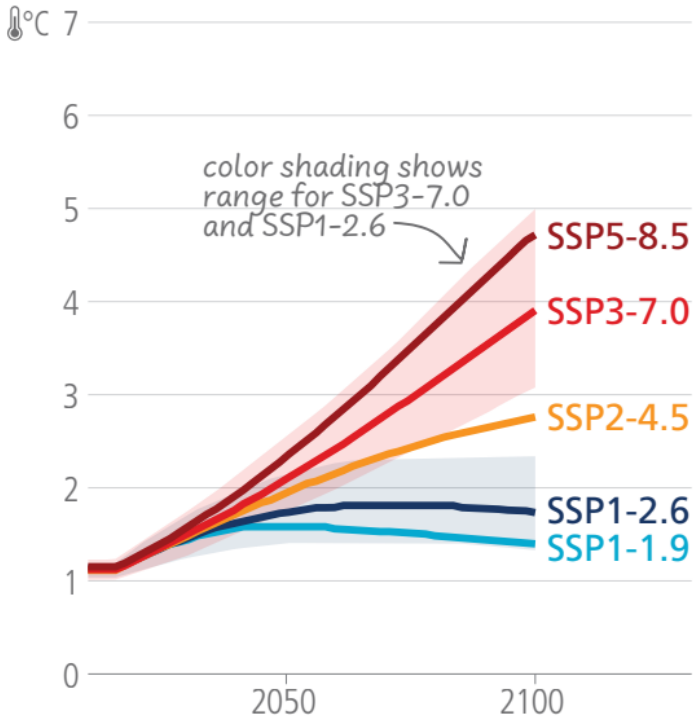

Figure 15: Potential future evolution of the temperature based on the scenarios of the IPCC [5].

2.4 Conclusion

Now that more is known about the causes and consequences of global warming on human living conditions on Earth, it is clear that minimizing future greenhouse gas emissions is crucial to prevent further increases in the planet's average temperature. Since global temperatures are expected to rise, and some regions will be more affected than others due to the uneven distribution of warming, it is essential to identify the areas where this increase will be most significant. In this context, analysing present and future TMY (Typical Meteorological Year) weather files allows for assessing how climate change will influence cooling demand in buildings. This analysis is key to understanding how indoor comfort can be maintained under evolving climatic conditions. Furthermore, it is vital to explore energy-efficient technologies for cooling in order to reduce greenhouse gas emissions associated with cooling production.

3 Meteorological data

To accurately assess the thermal behaviour and energy demand of buildings, it is essential to begin with a solid understanding of the local weather conditions. More specifically, this study requires access to hourly meteorological data, including outdoor temperature, as well as global and diffuse solar irradiation on a horizontal surface, and direct normal irradiation on a surface perpendicular to the sun's rays. Based on these three types of irradiation, it is then possible to compute the equivalent normal irradiation on vertical surfaces for each of the four cardinal directions (north, south, east, and west). These inputs are fundamental, as they directly influence the heat exchanges between the building envelope and its surroundings, as well as the internal gains through windows due to solar exposure.

3.1 Data presentation

Given that the objective of this thesis is to evaluate the impact of global warming on the cooling demand in buildings worldwide, it is essential to use consistent and standardized meteorological data from a selection of representative cities, each reflecting a different climatic zone, covering all the different climates. The studied climatic zones and their corresponding cities are shown in Figure 16. The climate zones are defined according to the American Society of Heating, Refrigerating and Air-Conditioning Engineers (ASHRAE) Standard 169 [86]. To ensure comparability and accuracy, the analysis is based on Typical Meteorological Year (TMY) datasets. TMY's are synthetic annual weather datasets composed of hourly climate data, constructed to reflect average climatic conditions in a given location. Rather than being an actual recorded year, a TMY is built by selecting individual months from a long-term weather dataset, typically spanning at least ten years, where each selected month closely mirrors the statistical behaviour of that month over the full period. The selection process ensures that the final synthetic year is representative of typical climate conditions while smoothing out anomalies and extremes. To identify the most representative months, statistical techniques such as the Finkelstein–Schafer method (1971) are employed, comparing cumulative distributions to ensure a strong fit between selected months and long-term climate trends [87].

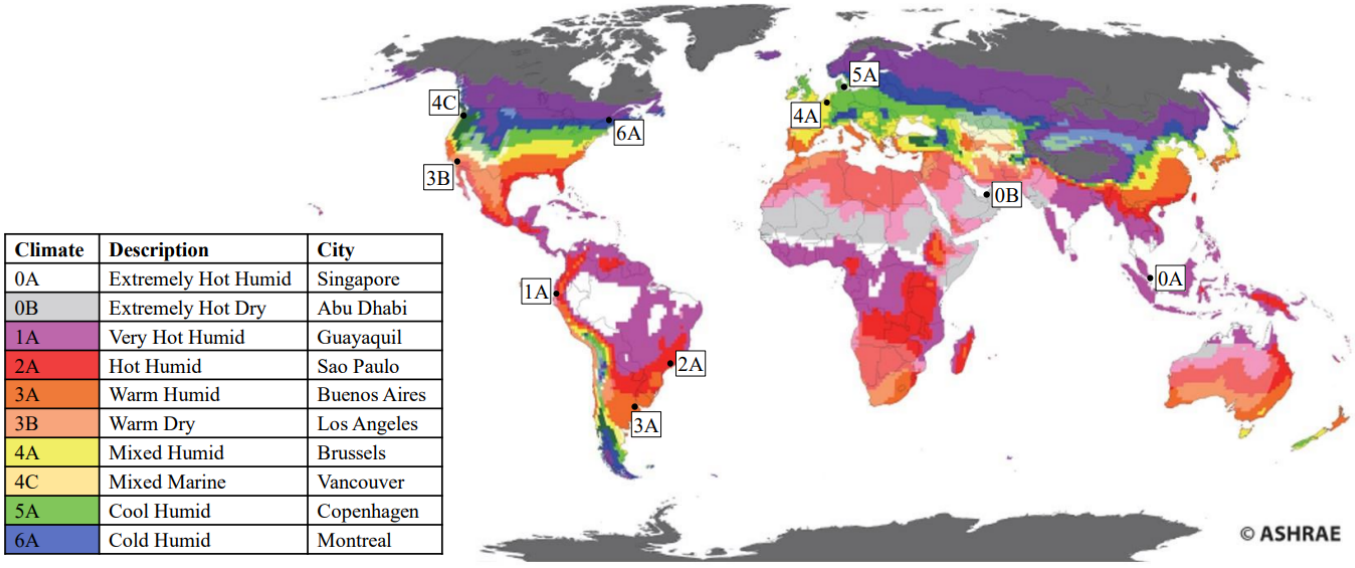

Climate	Description	City
0A	Extremely Hot Humid	Singapore
0B	Extremely Hot Dry	Abu Dhabi
1A	Very Hot Humid	Guayaquil
2A	Hot Humid	Sao Paulo
3A	Warm Humid	Buenos Aires
3B	Warm Dry	Los Angeles
4A	Mixed Humid	Brussels
4C	Mixed Marine	Vancouver
5A	Cool Humid	Copenhagen
6A	Cold Humid	Montreal

Figure 16: World climatic zones classification according to the ASHRAE Standard 169 [88].

The TMY datasets used were generated for the *Annex 80* of the IEA [89, 90], using a high-resolution regional climate model adapted to the specific characteristics of each location. The use of a regional

model allows the production of continuous and homogeneous meteorological data series, both spatially and temporally, depending on the considered period (past or future) [14].

For Belgium TMY datasets, the regional climate model used is the *"Modèle Atmosphérique Régional (MAR)"*, which has been specifically developed and validated for the Belgian region [14]. For the historical climate period (2001–2020), MAR is driven by the ERA5 reanalysis, providing a reliable reconstruction of atmospheric conditions based on observational data [91]. For future climate projections (2041–2060), MAR is forced by outputs from three Earth system models taken from the Coupled Model Intercomparison Project Phase 6 database: BCC-CSM2-MR, MPI-ESM1.2, and MIROC6. This combination enables the generation of future climate scenarios that reflect a range of plausible evolutions, capturing different model sensitivities and uncertainties [91].

Projected climate data are essential for anticipating shifts in heating and cooling demands within buildings. Assessing the expected minimum and maximum outdoor temperatures under future climate scenarios is a critical step in determining seasonal energy requirements. This insight supports the need to rethink building design strategies, ensuring they remain functional and resilient under changing environmental conditions driven by climate change.

In traditionally heating-dominated regions, architectural approaches have long prioritized heat conservation to minimize energy use during cold seasons. However, the steady rise in global temperatures over recent decades due to global warming has revealed a major downside: these designs often lead to significant overheating during warmer months.

As such, it becomes increasingly important to evaluate how buildings will perform under future climate conditions and adjust their design accordingly. While developing cooling systems that can remain efficient for an entire century poses a considerable challenge, the adaptability of buildings can be improved through passive architectural strategies, new materials usage, active heating and cooling technologies, or a hybrid of both. Regardless of the chosen method, periodic updates or system replacements will likely be required throughout the lifecycle of a building.

3.2 Comparison of present and future solar irradiation and mean outdoor temperature

TMY datasets are used to evaluate the impact of global warming on solar gains in buildings and the mean outside temperature. Table 4 presents a comparison of the total annual solar irradiation incident on building windows and mean outdoor temperatures across all studied cities, for two different climate periods: 2001–2020 (current reference) and 2041–2060 (future projection). The calculation considers the four main orientations (north, south, east and west) for solar irradiation, the analysis is expressed in kilowatt hours per square meter of window surface (kWh/m^2) to isolate the climate effect and ensure a consistent comparison as the size of the windows is not taken into account. The construction techniques in a favela of São Paulo, a small village in Vancouver and a building in Singapore are completely different. Therefore, a constant Solar Heat Gain Coefficient (SHGC) of 1 was also applied across all locations for the same reason, to ensure comparability by isolating the climatic effect from building-specific characteristics and the technological development of the building industries worldwide. The mean outside temperature is also analysed. This analysis highlights the areas of the world where solar gains and the mean outside temperature are expected to increase significantly, with direct implications for future building cooling demand.

Although the evolution of annual solar irradiation is not uniform across all cities, some regions experience an increase, while most of the others show a decrease. The mean outdoor temperatures increase consistently in all studied locations. This systematic rise in ambient temperature, regardless of the solar gain trend, indicates a clear shift in thermal conditions. As a consequence, even in cities where solar gains decline, the increased external temperatures will lead to higher indoor cooling needs to

maintain thermal comfort. This underlines the global nature of the challenge: the cooling demand in buildings is expected to rise in all climate zones because of the warming trend, even where solar irradiation remains stable or even decreases. As already discussed in Section 2.2.1, the impacts of global warming are not evenly distributed across the world. This is reflected in the temperature variations presented in Table 4: while Brussels shows a relatively modest increase of only +1.43% in the average outdoor temperature, Vancouver experiences a much more pronounced increase of more than + 21%. Such disparities highlight the importance of region-specific analyses when evaluating future energy needs and climate adaptation strategies for buildings.

City	Irradiation present (kWh/y/m^2)	Irradiation future (kWh/y/m^2)	Irradiation variation (%)	Present mean outside temperature (°C)	Future mean outside temperature (°C)	Temperature variation (%)
Singapore	2932.681	3021.785	3.04	27.95	29.07	4
Abu Dhabi	3704.715	3693.326	-0.23	27.9	29.45	5.56
Guayaquil	4604.873	4372.668	-5.04	27.12	28.5	5.09
São Paulo	2780.585	2959.67	6.44	19.64	21.92	11.61
Buenos Aires	3614.7	3567.059	-1.32	17.8	18.86	5.96
Los Angeles	4091.169	3928.301	-3.98	16.73	17.77	6.22
Brussels	2644.582	2568.962	-2.86	11.21	11.37	1.43
Vancouver	3305.818	3097.706	-6.29	7.69	9.31	21.07
Copenhagen	2487.85	2352.211	-5.45	9.01	9.71	7.77
Montreal	3095.983	3156.755	1.96	7.86	9	14.5

Table 4: Comparison of annual Solar irradiation on building facades (kWh/y/m^2) and mean outdoor temperatures (°C) across multiple cities for present (2001–2020) and future (2041–2060) climate projections.

Temperature variation color scale:

- Low variation (5%)
- Moderate variation (5–10%)
- High variation (10–15%)
- Extreme variation (> 15%)

Furthermore, it is important to note that the percentage variation in the mean annual temperature does not fully capture the severity of potential impacts on building cooling demand. For example, while Singapore and Abu Dhabi show relatively modest increases of around 4 to 5%, these regions already experience very high baseline temperatures. In such hot climates, even small additional warming can push outdoor conditions beyond critical comfort and health thresholds, leading to a disproportionately large increase in cooling needs. These regions are already subject to frequent extreme events such as heat waves or days of high humidity, and further warming is likely to increase the frequency, intensity, and duration of such extremes [14]. Moreover, the present analysis is based on annual temperature averages, which inherently smooth out these short-term but intense temperature spikes. As a result, the true impact of warming, particularly in regions already near critical thresholds, may be underestimated when only considering mean annual values. In contrast, cities like Vancouver or Montreal may show higher percentage increases in mean temperature, but their cooler initial climate makes them less immediately vulnerable to thermal stress. This highlights the non-linear nature of climate impacts: a modest mean temperature rise in already hot regions can have far more severe implications than a larger rise in temperate areas. Therefore, to go further in the analysis, when evaluating the future of building cooling demand, it is essential to go beyond simple average-based metrics and take into account local climate characteristics, the frequency of extreme events, and the physiological thresholds for human comfort.

Meteorological graphs of daily temperature anomalies comparing present (2001-2020) and future projections (2041-2060) in the studied cities are present in Appendix A.4 for a more visual representation.

3.3 Cooling degree days

Considering only the average outdoor temperature for the cooling demand analysis doesn't consider the fact that global warming can increase extreme temperatures in both ways: hotter summers and colder winters, which have a compensating effect. The cooling degree days (CDD) are calculated to counteract this potential compensating effect. They quantify the accumulated delta of temperature above a defined base comfort temperature, over a day, to quantify the need for cooling. The higher the outdoor temperature and the longer the duration of this delta of temperature above the base temperature, the greater the cooling requirement [92].

In this study, CDDs are computed from hourly outdoor temperature data available over a full year. For each hour where the outdoor temperature exceeds the base temperature, the difference is summed and then normalised to express the daily CDD as follows:

$$\mathrm{CDD}_{\mathrm{day}} = \frac{1}{24} \sum_{i=1}^{24} \max(T_{\mathrm{out},i} - T_{\mathrm{base}},\, 0) \tag{1}$$

With :

- $T_{\mathrm{out},i}$, the outdoor temperature at the i hour of the day.
- T_{base}, the reference base temperature equals to 18°C in this case.

The daily CDDs are then summed over a year to have the total cooling degree days over a year.

$$\mathrm{CDD}_{\mathrm{year}} = \sum_{\mathrm{day}=1}^{365} \mathrm{CDD}_{\mathrm{day}} \tag{2}$$

This method provides an indicator of climate-driven cooling needs and allows for direct comparisons between different regions and between past and future climate scenarios, as illustrated in Figure 17.

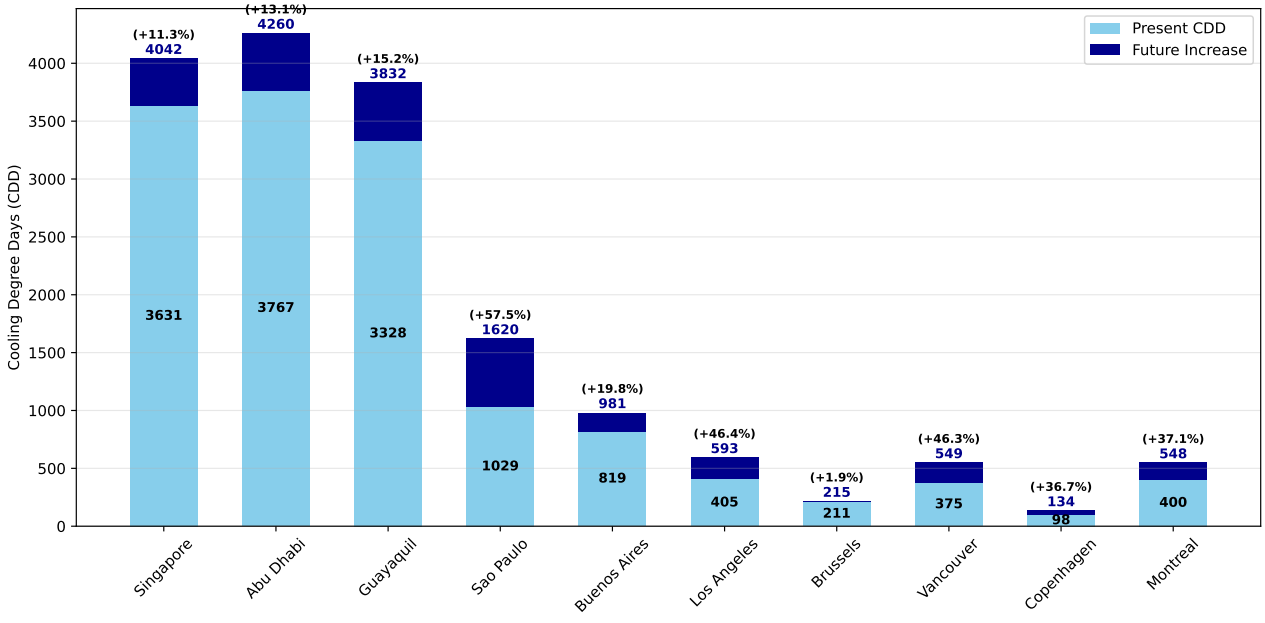

Figure 17: Comparison of present and future cooling degree days for the different studied cities.

The climates 0A, 0B and 1A, represented respectively by Singapore, Abu Dhabi, and Guayaquil, need the most cooling already nowadays, as can be interpreted when analysing the CDD seen in Figure 17. In the future, the cooling demand in such regions will increase, but not significantly. Therefore, the cooling capacity will not need a large increase. In climates such as 2A, 3B, 4C, 5A and 6A, represented respectively by São Paulo, Los Angeles, Vancouver, Copenhagen and Montreal, the cooling demand will increase significantly. For example, in São Paulo, the cooling demand will increase by 57.5%. In such climates, the choice of cooling technologies will significantly impact future electricity demand, as active systems rely heavily on electricity [11, 93]. Therefore, developing passive cooling solutions in these regions is essential to prevent potential grid failures [13].

3.4 Conclusion

The analysis of present and future Typical Meteorological Year (TMY) data reveals a marked increase in average outdoor temperatures and Cooling Degree Days across various climate zones. These findings validate the use of standardised weather files as reliable inputs for dynamic thermal simulations. Moreover, the regional variations observed reinforce the importance of a climate-specific approach when assessing future cooling requirements.

4 Methodology

This chapter presents the equations governing the building simulation model, its validation process, a sensitivity analysis of key building parameters that may significantly influence thermal performance, and the model's adaptation to evaluate the impact of global warming on the cooling demand. The model developed for this study is implemented using the Python programming language. It is a white box model with meteorological and building parameters inputs to compute the cooling demand and indoor temperature as illustrated in Figure 18.

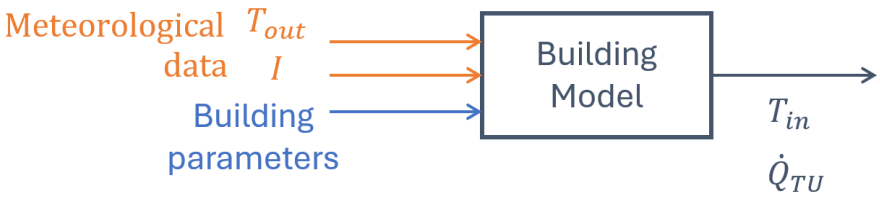

Figure 18: Representation of the model principle.

4.1 Building model

A dynamic heat balance is implemented to model the building's interactions with the outdoor environment. A dynamic heat balance is necessary to fit the much as possible to reality, as different interactions between the building and the exterior will influence each other. The following Figure 19 represents the different interconnected interactions between the inside of the building and the exterior.

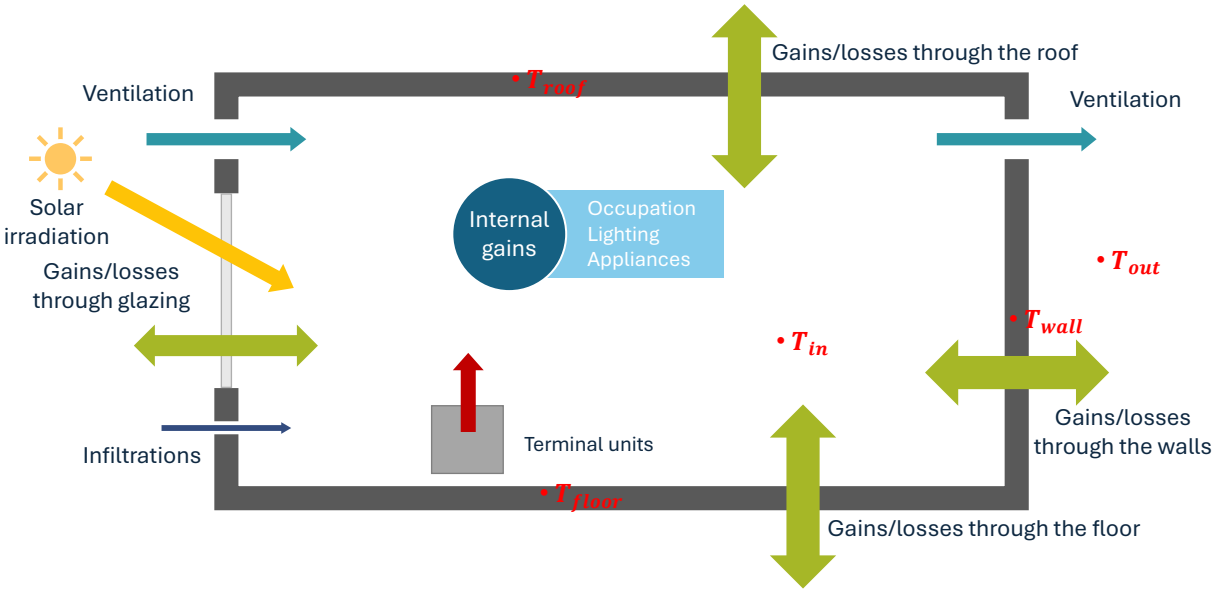

Figure 19: Representation of the heat exchange in a building.

4.1.1 Governing equation for indoor air temperature

The main objective of the model is to calculate the indoor air temperature on an hourly basis and maintain it in a range of acceptable thermal comfort predefined in function of the location of the building. To compute the indoor air temperature, all the interactions of the building with its surroundings need to be taken into account. The global equation governing the model is the following:

$$\frac{dT_{\text{in}}}{dt} = \frac{1}{m_a \, c_{p,\text{air}} \, ICF} \left(\dot{Q}_{TU} + \dot{Q}_{\text{int}} + \dot{Q}_{\text{cond, tot}} + \dot{Q}_{\text{ventilation}} + 0.1 \cdot \dot{Q}_{\text{irrad, tot}} + \dot{Q}_{\text{infiltration}} \right) \quad (3)$$

With:

- m_a : the mass of air inside the building, calculated as $m_a = \rho_{\text{air}} \cdot V$, where ρ_{air} is the air density equals to 1.225 kg/m^3 and V is the interior volume of the building (in m^3).
- $c_{p,\text{air}}$: the specific heat capacity of air equals to 1005 J/(kg·K).
- ICF : the Internal Capacity Factor, a dimensionless coefficient that represents the portion of indoor air that effectively contributes to thermal exchanges, equals 4 for the typical model house.

The term $\dot{Q}_{\text{cond, tot}}$ takes into account the conduction of heat through all possible surfaces between the inside of the building and its environment: walls, windows, floor, and roof. The different conduction equations are the following.

$$\dot{Q}_{\text{cond, tot}} = \dot{Q}_{\text{cond,wall\_in}} + \dot{Q}_{\text{cond,windows}} + \dot{Q}_{\text{cond,floor}} + \dot{Q}_{\text{cond,roof}} \quad (4)$$

With:

$$\dot{Q}_{\text{cond,wall\_in}} = \frac{U_{\text{walls}}}{\theta_{\text{wall}}} \cdot A_{\text{walls}} \cdot (T_{\text{wall}} - T_{\text{in}}) \quad (5)$$

$$\dot{Q}_{\text{cond,windows}} = U_{\text{windows}} \cdot A_{\text{windows}} \cdot (T_{\text{out}} - T_{\text{in}}) \quad (6)$$

$$\dot{Q}_{\text{cond,floor}} = \frac{U_{\text{floor}}}{\theta_{\text{floor}}} \cdot A_{\text{floor}} \cdot (T_{\text{floor}} - T_{\text{in}}) \quad (7)$$

$$\dot{Q}_{\text{cond,roof}} = \frac{U_{\text{roof}}}{\theta_{\text{roof}}} \cdot A_{\text{roof}} \cdot (T_{\text{roof}} - T_{\text{in}}) \quad (8)$$

The other terms of Equation 3 are explained in the following subsections 4.1.2 - 4.1.7.

4.1.2 Solar gains

The solar gains in the building are defined for all the orientations (north, south, west, east) as follows.

$$\dot{Q}_{\text{irrad}} = A_{\text{window}} \cdot \text{I} \cdot SF \quad (9)$$

With A_{window}, the window area in square meters; I, the equivalent normal irradiation on vertical surfaces in W/m^2 and SF, the solar factor of the window, also called the solar heat gain coefficient

(SHGC). The total solar gain ($\dot{Q}_{\text{irrad, tot}}$) in the building is simply the sum of the contributions of the four orientations.

$$\dot{Q}_{\text{irrad, tot}} = \dot{Q}_{\text{irrad, north}} + \dot{Q}_{\text{irrad, south}} + \dot{Q}_{\text{irrad, west}} + \dot{Q}_{\text{irrad, east}} \tag{10}$$

4.1.3 Building envelope

The walls and roof are represented by a 2R-1C circuit in the model as illustrated in Figure 20. R is the thermal resistance of the wall, and C is its capacitance. Two additional parameters, ϕ and θ, are introduced to characterise the dynamic thermal behaviour of the wall. The parameter ϕ represents the fraction of the thermal capacity of the wall that is used effectively over a 24-hour time period, while θ indicates the relative position within the wall where this capacity is accessed. The floor is supposed to be adiabatic and is therefore represented with the same principle by a 1R-1C circuit. The irradiations coming inside the building are considered to be integrally absorbed by the floor. Windows and doors are represented as purely resistive components.

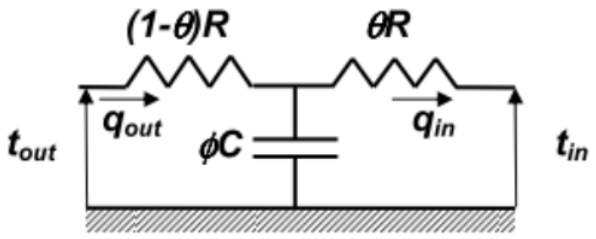

Figure 20: Walls and roof representation as a 2R-1C circuit [94].

The key physical characteristics of the building needed for the model include U, C, θ, and ϕ factors. These values are foundational inputs for the simulation model developed in this section. The U factor, also called the thermal transmittance, represents the rate at which heat is transferred through a building element (such as walls, roof, window, or the floor) per unit area and per unit temperature difference between the interior and exterior environments. It is expressed in watts per square meter per degree Kelvin (W/m^2.K). It indicates the insulation performance of the materials used. A low U factor means that less heat is lost in winter and that less heat is gained in summer. Therefore, a low U factor means a better thermal resistance.

The U factors can be calculated as follows when all the materials used and their respective thicknesses are known:

$$U = \frac{1}{R_{\text{tot}}} \tag{11}$$

With:

$$R_{\text{tot}} = \sum_{i=1}^{N} \frac{e_i}{k_i} \tag{12}$$

Where :

- *e* represents the respective layer thicknesses of the material (for example: concrete, brick, insulation), expressed in meters.
- *k* represents the respective layer thermal conductivity of the material, expressed in watts per meter-Kelvin [W/(m·K)].

The thermal capacitance C expressed in joules per square meter per degree Kelvin (J/m^2.K), can be calculated as follows when all the materials used and their respective thicknesses are known:

$$C = \sum_{i=1}^{N} c_{p,i} \cdot \rho_i \cdot e_i \tag{13}$$

With :

- c_p the specific heat capacity of the material, expressed in Joules per kilogram-Kelvin [J/(kg·K)].
- ρ the density of the material, expressed in kilograms per cubic meter [kg/m^3].

The heat exchange dynamics between the building and its environment are governed by these parameters and the thermal properties of the envelope components. The following equations describe the thermal interactions for the roof, walls, and floor within the model.

$$\frac{dT_{\text{roof}}}{dt} = \frac{(0.1 \cdot \dot{Q}_{\text{irrad, tot}}) + \left(\frac{U_{\text{roof}}}{1-\theta_{\text{roof}}} \cdot A_{\text{roof}} \cdot (T_{\text{out}} - T_{\text{roof}})\right) - \left(\frac{U_{\text{roof}}}{\theta_{\text{roof}}} \cdot A_{\text{roof}} \cdot (T_{\text{roof}} - T_{\text{in}})\right)}{\phi_{\text{roof}} \cdot C_{\text{roof}} \cdot A_{\text{roof}}} \tag{14}$$

$$\frac{dT_{\text{walls}}}{dt} = \frac{(0.3 \cdot \dot{Q}_{\text{irrad, tot}}) + \left(\frac{U_{\text{walls}}}{1-\theta_{\text{walls}}} \cdot A_{\text{walls}} \cdot (T_{\text{out}} - T_{\text{walls}})\right) - \left(\frac{U_{\text{walls}}}{\theta_{\text{walls}}} \cdot A_{\text{walls}} \cdot (T_{\text{walls}} - T_{\text{in}})\right)}{\phi_{\text{walls}} \cdot C_{\text{walls}} \cdot A_{\text{walls}}} \tag{15}$$

$$\frac{dT_{\text{floor}}}{dt} = \frac{(0.5 \cdot \dot{Q}_{\text{irrad, tot}}) - \left(\frac{U_{\text{floor}}}{\theta_{\text{floor}}} \cdot A_{\text{floor}} \cdot (T_{\text{floor}} - T_{\text{in}})\right)}{\phi_{\text{floor}} \cdot C_{\text{floor}} \cdot A_{\text{floor}}} \tag{16}$$

4.1.4 Infiltrations

The heat exchange due to the infiltration through window frames can be expressed as follows.

$$\dot{Q}_{\text{infiltration}} = \frac{V_{\text{infiltration}} \cdot \rho_{\text{air}} \cdot c_{p,\text{air}} \cdot (T_{\text{out}} - T_{\text{in}})}{3600} \tag{17}$$

With:

- $V_{\text{infiltration}}$: the infiltration air flow rate expressed in m^3/h.
- ρ_{air} : the air density equals to 1.225 kg/m^3.
- $c_{p,\text{air}}$: the specific heat capacity of air equals to 1005 J/(kg·K).

Or with the air changes per hour coefficient (ACH) as follows:

$$\dot{Q}_{\text{infiltration}} = \frac{ACH \cdot A_{\text{floor}} \cdot H \cdot \rho_{\text{air}} \cdot c_{p,\text{air}} \cdot (T_{\text{out}} - T_{\text{in}})}{3600} \tag{18}$$

With:

- H: the height of the building in meters.

4.1.5 Ventilation system

Heat can also be lost through the ventilation system. The equation representing heat exchange due to mechanical ventilation in the model is the following.

$$\dot{Q}_{\text{ventilation}} = \left(\frac{V_{\text{mech}}}{3600} \cdot \rho_{\text{air}}\right) \cdot c_{p,\text{air}} \cdot [T_{\text{out}} + \varepsilon_{\text{HEX}} \cdot (T_{\text{in}} - T_{\text{out}}) - T_{\text{in}}] \tag{19}$$

With V_{mech}, the mechanical ventilation air flow rate imposed in the building, expressed in m^3/h. The term $\varepsilon_{\text{HEX}} \cdot (T_{\text{in}} - T_{\text{out}})$ takes into account if there is a heat recovery before extracting the air from the building to replace it with fresh new outside air.

4.1.6 Heating/cooling system

In this study, thermal comfort is ensured through a set point-based control strategy that activates heating or cooling when the indoor air temperature deviates from a defined comfort temperature range. When the indoor temperature T_{in} falls below the lower comfort limit $T_{\text{set, cold}}$, the heating system is activated, providing thermal energy to the building. In contrast, when T_{in} exceeds the upper limit $T_{\text{set, hot}}$, cooling is activated to extract heat from the indoor environment and reduce the temperature of the indoor air.

The thermal energy delivered or removed by the system, denoted $\dot{Q}_{\text{TU}}$, is dynamically calculated based on the distance between the indoor temperature and the comfort limits. The heating and cooling powers are calculated according to the following formulas:

- If $T_{\text{in}} < T_{\text{set, cold}}$, then:

$$\dot{Q}_{\text{TU, heat}} = \max\left(\min\left(C \cdot (T_{\text{set, cold}} - T_{\text{in}}),\ 1\right) \cdot P_{\text{nom, heat}},\ 0\right) \tag{20}$$

$$\dot{Q}_{\text{TU, cool}} = 0$$

- If $T_{\text{in}} > T_{\text{set, hot}}$, then:

$$\dot{Q}_{\text{TU, cool}} = \min\left(\min\left(C \cdot (T_{\text{in}} - T_{\text{set, hot}}),\ 1\right) \cdot P_{\text{nom, cold}},\ 0\right) \tag{21}$$

$$\dot{Q}_{\text{TU, heat}} = 0$$

- Otherwise, no active heating or cooling is applied:

$$\dot{Q}_{\text{TU}} = 0$$

The final thermal power $\dot{Q}_{\text{TU}}$ is defined as:

$$\dot{Q}_{\text{TU}} = \dot{Q}_{\text{TU, heat}} + \dot{Q}_{\text{TU, cool}} \tag{22}$$

$P_{\text{nom, heat}}$ and $P_{\text{nom, cold}}$ represent the nominal capacities of the heating and cooling systems, respectively, and C is a control coefficient that modulates the response of the system based on the temperature deviation. This formulation ensures that the power delivered remains within physical limits and reflects realistic part-load operation. $P_{\text{nom, heat}}$ and $P_{\text{nom, cold}}$ can be calculated as a function of the surface area to cover.

$$P_{\text{nom, heat}} = 100 \text{ W/m}^2 \quad [95–98] \tag{23}$$

$$P_{\text{nom, cold}} = 500 \text{ W/m}^2 \quad [99] \tag{24}$$

4.1.7 Internal gains

In addition to the primary heating system, internal heat gains also come from occupants, lighting, and appliances. These additional heat sources are highly variable and difficult to quantify with precision, as they are strongly dependent on occupant behaviour. For the occupants, it depends on whether they are present in the building and how many of them there are (n_{people}). For lighting and appliances, their contribution depends on several factors, such as whether they are in use, the duration and frequency of operation, weather conditions (principally for lights) and the number and type present. For example, a LED light bulb does not emit the same amount of heat as an incandescent light, and lighting usage tends to increase during winter due to shorter daylight hours. These variables can differ significantly from one household to another, making them inherently personal and context-dependent.

According to the ISO 17772 standard, internal heat gains from occupants, lighting, and appliances are estimated as follows: each person can be represented as a heat source of 100 W, lighting adds 3 W/m² when active, and appliances contribute around 6 W/m². However, these values are not continuously applied throughout the year. Therefore, weighted usage factors have been introduced to account for the realistic operation time of each internal source over a full year.

Based on occupancy assumptions where people are present during evenings and nights on weekdays and all day during weekends, an average presence rate of 67.2% is applied [100]. Similarly, lighting is assumed to be used around 27.4% of the time, primarily during dark hours [100]. Appliances are considered active 14.9% of the time, depending on daily usage habits [100]. These correction factors allow for a more realistic estimation of the internal heat gains in the energy balance of the building. However, actual internal heat gains can differ considerably and introduce a degree of uncertainty into building energy modelling.

Those additional heat sources, when activated, can be represented in the model by the following equation:

$$\dot{Q}_{\text{int}} = (100 \cdot n_{\text{people}} \cdot 0.672) + (3 \cdot A_{\text{floor}} \cdot 0.274) + (6 \cdot A_{\text{floor}} \cdot 0.149) \tag{25}$$

4.2 Building model validation

4.2.1 Test case presentation

The building model is validated using experimental data from twin houses (N2 and O5) located in Holzkirchen, Germany. These houses have been the subject of various tests conducted as part of the IEA Annex 58 initiative, specifically for empirical model validation purposes [94, 101]. Although the validation is based on a specific type of dwelling in a particular climate, the findings are extendable to similar buildings in other regions with an adaptation of the implemented meteorological data. This generalizability is supported by the IEA's selection of the Holzkirchen twin houses, which were chosen to represent typical residential structures.

The test applied to the twin houses to validate building energy models, illustrated in Figure 21, is structured into five distinct phases, each designed to isolate and analyse specific thermal behaviours.

The first phase consists of a seven-day initialisation period during which internal temperatures were maintained at 30°C in both houses using electric heaters, while the blinds on the south façade remained closed. This stage established a uniform thermal baseline. The measured indoor temperature data served as a reference to assess the precision of the model, and the simulation model calculated the internal temperature based on the interactions of the building with the external environment and the recorded heating inputs.

The second phase continued for another seven days with the same indoor temperature set-point. This time, the blinds in one of the test houses (house O5) were opened to let solar irradiation in, allowing the evaluation of the impact of solar gains.

In the third phase, a Randomly Ordered Logarithmic Binary Sequence (ROLBS) of heat input pulses, ranging in duration from 1 to 90 hours, was applied in the living room for two weeks. This sequence was designed to ensure that internal heat gains and solar irradiation were uncorrelated, thereby enabling a more rigorous evaluation of the building model's response to dynamic conditions.

The fourth phase served as a re-initialisation period to set the internal thermal conditions at a temperature of 25°C.

Finally, in the fifth phase, both houses were placed in free-floating conditions: one with blinds open and the other with blinds closed, enabling an analysis of natural indoor temperature evolution without active heating control.

The test took place between August 21^{st} and October 1^{st}. The values of heat injected ($\dot{Q}_{TU}$) for the heating system are provided on an hourly basis in watts. they are derived from the measured data of the electric heater input within the twin houses. Data were recorded at 1-minute intervals throughout all phases of the experiment.

The building parameters of the Twin houses needed for the model computations can be found in Appendix B.1 and B.2.

4.2.2 Definition of indicators used for validation

Statistical indices are commonly employed as key validation tools to assess the accuracy of a building energy model against real-world data. These indices do not provide a calibration methodology but rather serve to quantify the goodness-of-fit between the simulated outputs and measured data. Among the most widely recognised indicators are the Mean Bias Error (MBE) and the Coefficient of Variation of the Root Mean Square Error (Cv(RMSE)). These metrics are recommended by major international standards and protocols such as ASHRAE guideline 14 [102], the international performance measurement and verification protocol [103], and the Measurement and Verification (M&V) guidelines for the U.S. federal energy management program [104].

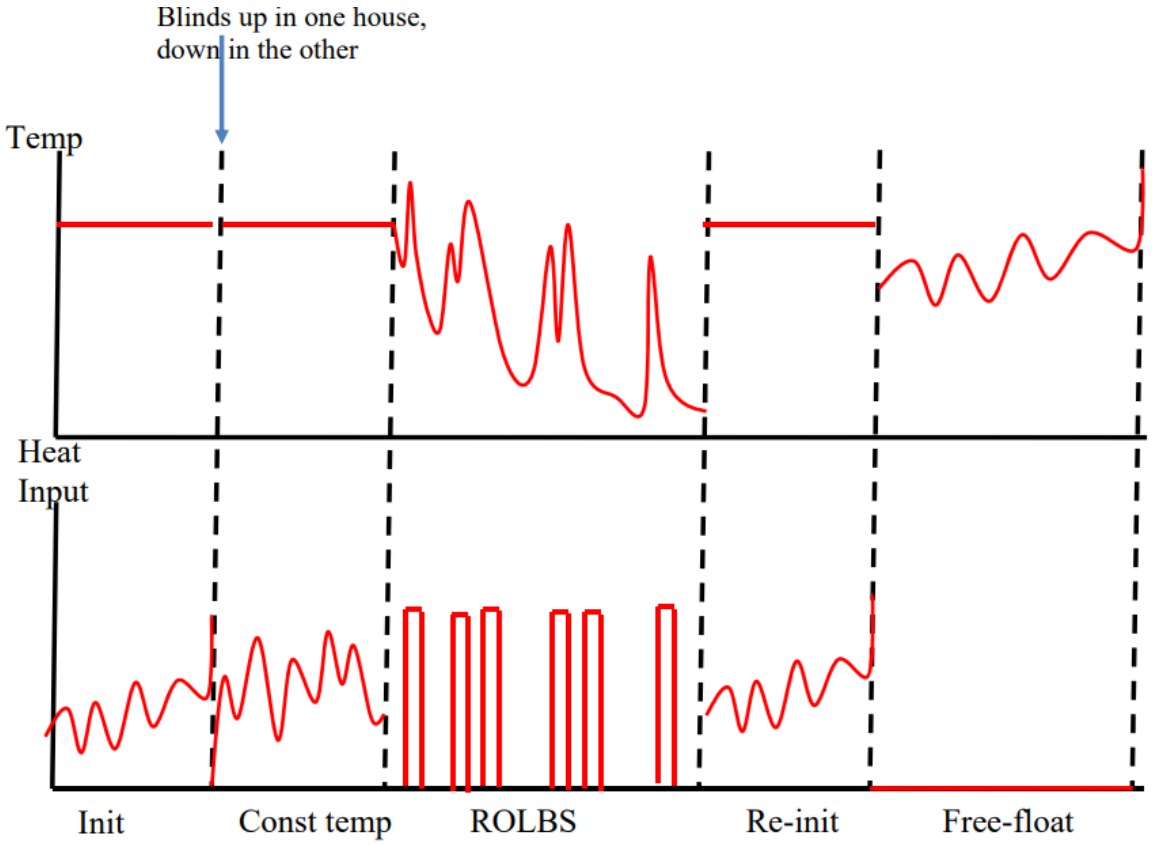

Figure 21: Schematic of the building model validation test procedure [101].

The MBE expresses the average deviation between simulated and measured values. It indicates whether the model tends to over-predict or under-predict measured values. It is calculated by summing the differences between simulated (S) and measured (M) values over all time intervals, then dividing this total by the sum of the measured values:

$$\text{MBE}\ (\%) = \frac{\sum_{i=1}^{N}(S_i - M_i)}{\sum_{i=1}^{N} M_i} \times 100\% \tag{26}$$

Where N is the total number of time intervals considered.

However, MBE alone can be misleading due to potential error compensation between over-estimates and under-estimates. To mitigate this limitation, it is typically used in parallel with the Cv(RMSE), which captures the magnitude of the errors regardless of their direction [105].

The Root Mean Square Error (RMSE) quantifies the dispersion of the residuals (differences between simulated and measured values). The Cv(RMSE) normalises this deviation relative to the mean of the measured values. Therefore, the Cv(RMSE) reflects the relative variability of the model predictions [105].

$$\text{RMSE} = \sqrt{\frac{1}{N}\sum_{i=1}^{N}(S_i - M_i)^2} \tag{27}$$

$$\overline{M} = \frac{1}{N}\sum_{i=1}^{N} M_i \tag{28}$$

$$\text{Cv(RMSE)} = \frac{\text{RMSE}}{\overline{M}} \times 100\% \tag{29}$$

These statistical indices provide a quantitative benchmark to determine whether a model can be validated according to accepted standards [105].

4.2.3 Application of validation methodology

Figure 22 shows the comparison of the indoor temperatures measured at 1-minute intervals and the hourly response of the model for the twin house N2, where the blinds stay closed during all phases of the test, as explained in section 4.2.

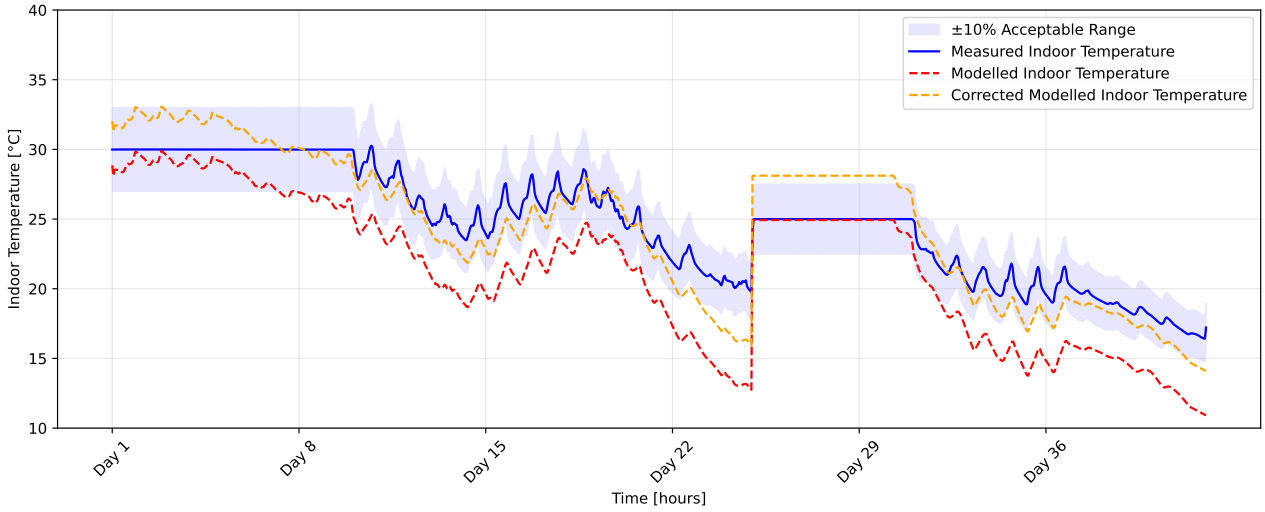

Figure 22: Comparison of measured and modelled indoor temperatures for the N2 house.

The modelled indoor temperature curve (in red) is consistently about 3 K lower than the measured indoor temperature (in blue) throughout all phases of the test. This discrepancy can largely be attributed to several modelling assumptions and sources of measurement uncertainty.

First, it is important to note that interior walls are not represented in the model. The house is simplified as a homogeneous thermal zone without internal partitions. In reality, interior walls contribute to the thermal inertia of the building by absorbing and releasing heat over time. Their omission in the model likely reduces the overall thermal buffering effect, which may contribute to the observed lower modelled indoor temperatures compared to the measured indoor temperatures.

Additionally, to compare modelled and measured temperatures, a mean indoor temperature was derived from the experimental data by averaging the values recorded in each room of the house. This was done by weighting the temperature in each space according to its floor area, ensuring coherence with the single-zone indoor temperature simulated by the model. However, such an approach introduces potential biases. Each room temperature was measured using sensors placed at a fixed height. However, indoor air temperature is rarely perfectly uniform due to stratification and varying heat gains. As a result, the measured values may not fully reflect the average thermal conditions of each room.

Furthermore, this averaging process tends to mask spatial thermal variations between rooms. In practice, rooms may experience significantly different thermal behaviours due to their orientation, window size, or exposure to solar radiation. For example, a south-facing room may overheat during the day,

while a north-facing room remains cooler. These differences are smoothed out in the weighted average, potentially underestimating the real amplitude of temperature variations.

Further uncertainties come from the temperature sensors used inside the rooms and outside, which are subject to accuracy limits and potential calibration drift over time [106]. Similar limitations apply to the measurements of the heating power ($\dot{Q}_{TU}$), which were derived from the instrumentation installed on the electric heaters. These readings may vary slightly depending on the sensor precision and the method used to record the power input.

Together, these factors, ranging from assumptions in data processing to measurement inaccuracies, help explain the systematic difference observed between modelled and measured indoor temperatures and should be considered when interpreting the results of the model validation.

To determine the actual temperature bias, ΔT, between the measured (blue curve) and simulated (red curve) indoor temperatures, it is necessary to account for the modelling assumptions. This bias reflects the systematic difference introduced by those simplifications. The optimal value of ΔT is found by identifying the one that minimises the RMSE value across both validation test cases (twin houses N2 and O5). The value of ΔT that leads to the lowest RMSE is 3.18 K.

In Figure 22, the yellow curve labelled *"Corrected Modelled Indoor Temperature"* corresponds to the original modelled temperature curve (in red) shifted upward by the constant bias of 3.18 K across the entire simulation period. This corrected curve serves only to better visualise the difference between the measured and modelled values. The close alignment between this adjusted curve and the actual measured data provides strong evidence that, despite the hypothesis, the model captures the essential thermal behaviour of the building.

Figure 23 presents the comparison between the indoor temperature measured at 1-minute intervals (in blue), the original simulated temperature at 1-hour intervals (in red), and the corrected simulated temperature (in yellow) created to better visualize the good fit of the modelled values for the twin house O5. In this test case, the blinds were open during certain phases of the experiment, as described in the validation procedure in Section 4.2.

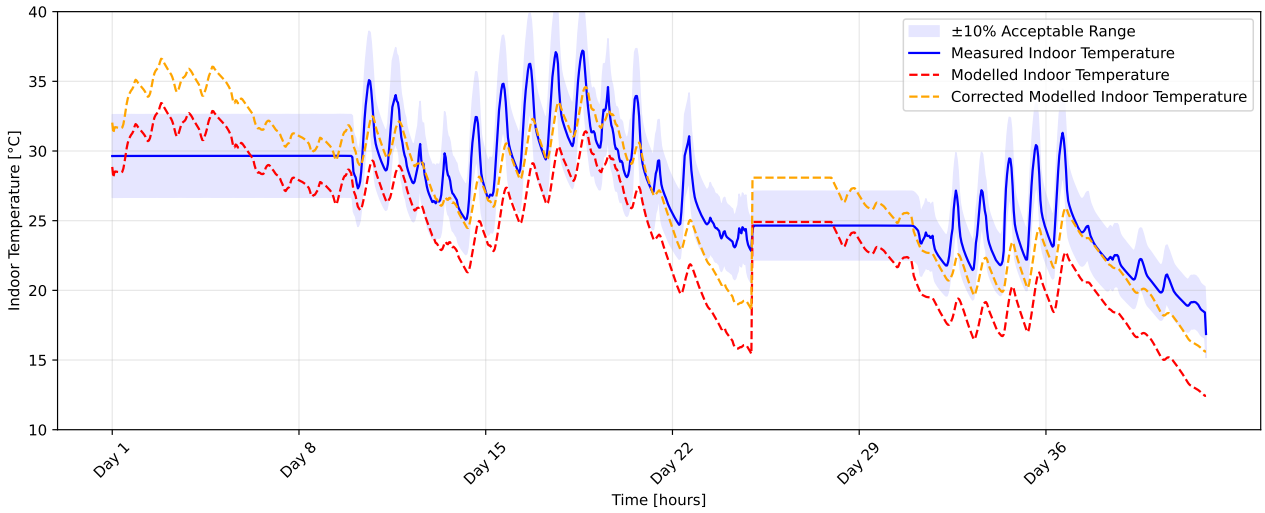

Figure 23: Comparison of measured and modelled indoor temperatures for the O5 house.

The close alignment between the corrected simulated temperature curve (in yellow) and the actual measured data (in blue) provides strong evidence that, despite simplifications, the model captures the essential thermal behaviour of the building.

Table 5 below shows the result for the two statistical criteria explained in section 4.2.2, applied to the twin houses N2 and O5 between the measured indoor temperature (blue curve) and the indoor

modelled temperature (in red) without the shift upward by the constant bias of 3.18 K across the entire simulation period.

Statistical Indices	Twin house N2	Twin house O5
MBE [%]	-13.22 %	-11.3 %
Cv(RMSE) [%]	15.38 %	15.6 %

Table 5: Validation of the building model using the statistical criteria for the twin houses.

According to internationally recognised standards for building energy model validation such as ASHRAE Guideline 14 [102], the International Performance Measurement and Verification Protocol [103], and the M&V Guidelines for the U.S. Federal Energy Management Program [104], a simulation model is considered valid if the MBE remains within ± 10 % and the Cv(RMSE) is below 30% for hourly data. The Cv(RMSE) criterion is satisfied in both validation cases presented in this study. While the MBE values are slightly outside the recommended threshold. This deviation can be attributed to modelling assumptions. Nevertheless, the simulation results demonstrate strong alignment with the measured data as shown in Figures 22 and 23, indicating that the developed building model can be considered sufficiently accurate for its intended purpose.

4.3 Sensitivity analysis

A sensitivity analysis is conducted to better understand the influence of key parameters on the thermal performance of the building. This analysis focuses specifically on the evolution of indoor temperature, which is the primary output of the building energy model. The objective is to evaluate how different modelling assumptions and physical parameters affect the predicted indoor thermal environment.

The analysis is based on test house O5, as it offers a more representative configuration. Unlike house N2, which permanently blocks solar irradiation from the south through closed blinds, house O5 allows solar gains from all orientations at various stages of the test. This makes it more suitable for evaluating the combined influence of solar radiation and other internal and external parameters on indoor temperature.

The parameters examined individually in this sensitivity study include:

- The case with no active heating, $\dot{Q}_{TU}$, to assess passive thermal behaviour. In the base case, $\dot{Q}_{TU} = 531937.17\ Wh$
- The absence of solar irradiation, $\dot{Q}_{\text{irrad, tot}}$, by disabling irradiation input through windows.
- The absence of mechanical ventilation, $\dot{Q}_{\text{ventilation}}$, to isolate its influence.
- The impact of infiltration, $\dot{Q}_{\text{infiltration}}$, by testing the case where no air leakage is considered.
- The presence of internal heat gains, $\dot{Q}_{\text{int}}$: including lights, appliances, and four occupants, taking into account the proportion of time each internal heat gain will be emitting as defined in equation 25.
- The U-value of external walls, U_{walls}, by testing different thermal transmittance values. Specifically, five representative values are considered and presented in Table 6 to reflect a wide range of insulation scenarios commonly found in buildings.

U-value (W/m^2K)	**Insulation level**	**Typical building description**
0.10	Very well insulated	Passive house or cutting-edge energy-efficient buildings
0.15	Well insulated	Low-energy buildings
0.22	Reference value	Twin house O5; moderately insulated contemporary building
0.30	Moderate insulation	Older buildings from the 1980s–1990s, no major retrofit
0.45	Poor insulation	Pre-regulation buildings with little or no insulation

Table 6: U-values tested for external walls and their corresponding insulation levels and building typologies [100].

Each scenario is simulated independently, and the resulting indoor temperature profiles are compared. The comparison is based on the mean indoor temperature calculated over the entire testing period. This allows for a consistent and interpretable evaluation of each parameter's influence on the model outcome. This type of analysis is called a one-at-a-time (OAT) analysis. The impact on the mean indoor temperature calculated is quantified by computing each parameter's sensitivity index (SI). It corresponds to the average deviation in mean indoor temperature calculated between the considered parameter case (T_{x}) and the base case ($T_{\text{base case}}$). The sensitivity index is computed as follows [107].

$$SI = \frac{T_{\text{x}} - T_{\text{base case}}}{T_{\text{base case}}} \times 100\% \tag{30}$$

A parameter can be considered sensitive and therefore influential when it leads to a significant variation in the sensitivity index. A high SI value indicates that changes in this parameter have a notable impact on the mean indoor temperature of the twin house O5.

The results of the OAT analysis are illustrated in Figure 24.

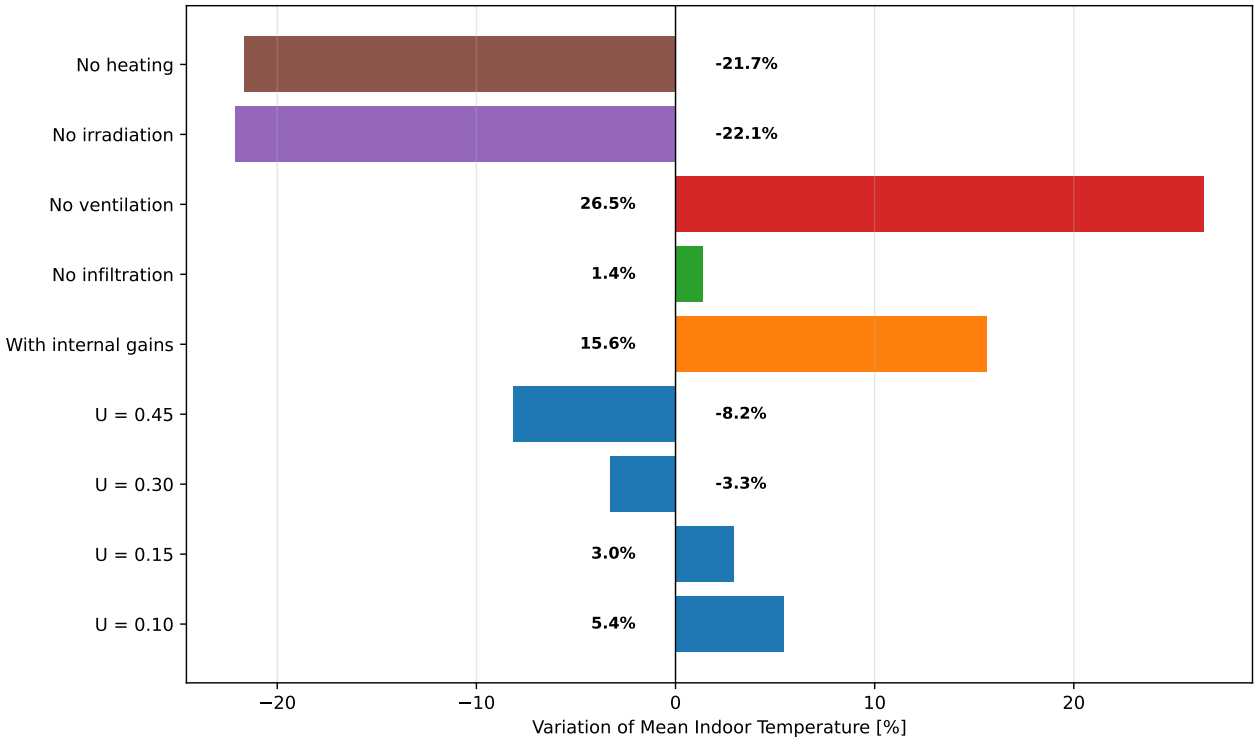

Figure 24: One-at-a-time sensitivity analysis on mean indoor temperature modelled using the sensitivity index (SI).

The parameters with the greatest influence on mean indoor temperature are mechanical ventilation, solar irradiation, the heating system, and internal heat gains, as illustrated in Figure 24. In this specific case, ventilation contributes to a temperature reduction since no heat recovery or exchange is associated with the ventilation system. In contrast, solar gains, heating input, and internal loads tend to increase indoor temperatures. The insulation level of external walls has a more moderate effect on temperature, but it plays a crucial role in determining the building's airtightness and, consequently, the required ventilation rates. Indeed, better-insulated buildings typically allow less natural infiltration, making mechanical ventilation more critical to ensure indoor air quality [108].

4.4 Buildings characteristics

To evaluate the impact of global warming on cooling demand across the various climates presented in Figure 16, a representative building is used as a baseline. The building's geometry, including its floor area and volume, is kept constant across all locations to ensure a consistent and unbiased comparison between the studied cities. Only the physical characteristics of the building envelope are adjusted to reflect regional construction practices. These include the thermal properties of the walls, roof, and floor, the window-to-wall ratio (WWR), the solar factor (SF), and the infiltration rate. By modifying only these parameters while maintaining the same overall building size, the analysis aims to isolate and compare the influence of future climate conditions on indoor cooling demand in a coherent and geographically relevant manner.

4.4.1 Building geometry

The key geometric characteristics of the building needed for the model include surface area, height, volume, and window area for the four orientations. These values serve as foundational inputs for the simulation model. An important assumption made in the model, as already explained, is that the internal walls are not considered in the model. This has an impact on the modelled indoor temperature as explained in Section 4.2.3. For a more accurate comparison across the studied cities, key building geometry parameters, including floor area, exterior surface area, height, and volume, are set to representative worldwide average values. They are shown in Table 7.

Floor area (m^2)	**Total exterior surface area (walls+windows) (m^2)**	**Height (m)**	**Volume (m^3)**
90 [109, 110]	95	2.5 [111]	225

Table 7: Standardized building geometry considered across all studied cities.

The varying WWR, wall surfaces and window surfaces in function of the orientation for the studied cities are shown in Table 8. For countries located near the equator, such as Singapore, the window areas are distributed equally across all four orientations (north, south, east, and west), as the sun's path remains relatively constant throughout the year. In contrast, for countries in the Southern Hemisphere, specifically Guayaquil, São Paulo, and Buenos Aires, the sun predominantly shines from the north. Therefore, 40 % of the total window surface is placed on the north-facing walls, while the remaining 60 % is evenly distributed across the east, west, and south orientations (20 % each). Conversely, for countries in the Northern Hemisphere, the south-facing walls receive the most sunlight. As a result, 40 % of the total window surface is allocated to the south, with 20 % on the north, east, and west orientations. This orientation-based distribution of window surfaces reflects typical architectural design strategies aimed at optimizing passive solar gains depending on the geographic location of the building.

City	**WWR (–)**	**Total Wall Area (m^2)**	**North-oriented Window (m^2)**	**South-oriented Window (m^2)**	**East-oriented Window (m^2)**	**West-oriented Window (m^2)**
Singapore	0.24 [112]	72.2	5.7	5.7	5.7	5.7
Abu Dhabi	0.20 [113]	76	3.8	7.6	3.8	3.8
Guayaquil	0.30 [114]	66.5	11.4	5.7	5.7	5.7
São Paulo	0.56 [115]	41.8	21.28	10.64	10.64	10.64
Buenos Aires	0.30 [116]	66.5	11.4	5.7	5.7	5.7
Los Angeles	0.50 [117]	47.5	9.5	19	9.5	9.5
Brussels	0.30 [118]	66.5	5.7	11.4	5.7	5.7
Vancouver	0.20 [119]	76	3.8	7.6	3.8	3.8
Copenhagen	0.15 [120]	80.75	2.85	5.7	2.85	2.85
Montreal	0.176 [121, 122]	78.28	3.344	6.688	3.344	3.344

Table 8: Comparison of WWR, wall surfaces (m^2) and window surfaces for the four orientations (m^2) for residential buildings in different climates.

4.4.2 Buildings envelope

The U-values of walls, roof, floor and window are adapted to the local construction techniques of the studied cities, as the level of insulation varies from one city to another. The values are shown in Table 9. The values for Brussels are almost the same as those for the twin houses of Germany shown in Appendix B.2. The values were confirmed and adapted thanks to other sources shown in Table 9.

City	Wall U-value ($W/m^2 \cdot K$)	Roof U-value ($W/m^2 \cdot K$)	Floor U-value ($W/m^2 \cdot K$)	Window U-value ($W/m^2 \cdot K$)
Singapore	0.67 [123, 124]	0.80 (based on certification standard)	0.35 [125]	5.70 [123]
Abu Dhabi	0.32 [126]	0.14 [126]	0.15 [126]	2.20 [126]
Guayaquil	1.14 [127]	0.75 [127]	0.75 [127]	5.70 [127]
São Paulo	2.17 [128]	2.88 [128]	2.40 [128]	5.70 [128]
Buenos Aires	1.00 [129]	0.80 [129]	1.20 [129]	5.70 [129]
Los Angeles	0.40 [130]	0.30 [130]	0.50 [130]	0.30 [131]
Brussels	0.20 [118]	0.235 [132]	0.28 [132]	1.20 [118]
Vancouver	0.45 [133]	0.30 [133]	0.40 [133]	1.42 [133]
Copenhagen	0.16 [120]	0.08 [120]	0.12 [120]	0.80 [134]
Montreal	0.47 [121, 135]	0.30 [121, 135]	0.28 [121, 135]	2.51 [121, 136]

Table 9: Comparison of U-values ($W/m^2 \cdot K$) for residential buildings in different climates.

The values of capacitance of the wall, roof and floor are fixed to the same global values for all the locations, except for Brussels, where the values are the same as those for the twin houses shown in Appendix B.2. These thermal capacitance values (C) are kept constant across all cities because the structural elements of the building, namely the load-bearing components such as concrete walls, floors, and roofs, are assumed to remain unchanged regardless of location. In other words, the thermal mass of the building is based on a common structural design using similar materials and thicknesses for the core construction. On the other hand, U-values are adapted according to local construction practices and insulation standards, as they reflect the level of thermal insulation rather than the mass of the structure. By fixing the capacitance and only varying the U-values, the effect of local insulation strategies is isolated while maintaining a consistent structural envelope for the building.

The global values of capacitance are shown in Table 10.

Capacitance:	C_{wall} ($kJ/m^2 \cdot K$)	C_{roof} ($kJ/m^2 \cdot K$)	C_{floor} ($kJ/m^2 \cdot K$)
	240 [137]	110 [137]	195 [137]

Table 10: Standardized thermal capacitance values of envelope elements considered across all studied cities except Brussels.

The values of ϕ and θ fixed for all the cities are the same as those used in the twin houses shown in Appendix B.2.

4.4.3 Ventilation system

The mechanical ventilation is fixed at 120 m^3/h for all studied cities to ensure consistent boundary conditions. This approach eliminates the influence of ventilation on cooling demand, allowing for more accurate comparisons between locations.

4.4.4 Infiltration

The infiltration rates in the cities are expressed in air changes per hour (ACH) and are adapted to the studied location. The values are shown in Table 11.

4.4.5 Solar gains

The solar factors of the windows (SF) for the cities are adapted to the studied location. The values are shown in Table 11.

City	Air Infiltration (ACH)	Window SF (–)
Singapore	0.20 [138]	0.35 [139]
Abu Dhabi	5.24 [140]	0.22 [141]
Guayaquil	1.40 [127]	0.40 [127]
São Paulo	5.70 [142]	0.32 [115]
Buenos Aires	5.70 [142]	0.50 [129]
Los Angeles	0.50 [143]	0.23 [131]
Brussels	1.15 [144]	0.35 [118]
Vancouver	3.50 [145]	0.40 [133]
Copenhagen	0.25 [146]	0.37 [134]
Montreal	2.30 [121, 147]	0.50 [121, 136]

Table 11: Comparison of air infiltration rates (ACH) and SF values (–) for residential buildings in different climates.

4.4.6 Internal gains

To ensure a fair and meaningful comparison of cooling demand across the different cities studied, internal heat gains from occupants, lighting, and appliances are not considered in the simulations. Internal gains can vary significantly from one region to another due to differences in access to electrical appliances, lighting usage patterns, and levels of technological development [148, 149]. By excluding this parameter, the analysis eliminates a potential source of bias that could distort the comparative assessment between locations. This approach enhances the accuracy of the climate-based evaluation by isolating the influence of external environmental factors on indoor thermal conditions.

4.4.7 Heating/cooling system

To calculate the cooling demand, a uniform indoor comfort temperature range is applied across all locations, set between 20°C and 25°C. If the indoor temperature exceeds 25°C, cooling is activated, whereas heating is triggered when the temperature drops below 20°C. The respective heating and cooling loads are computed as detailed in Section 4.1.6 with C, the control coefficient that modulates the response of the system based on the temperature deviation fixed to 0.5. The nominal capacities of the heating and cooling systems, $P_{\text{nom, heat}}$ and $P_{\text{nom, cold}}$, are fixed for the different locations to the same values.

$$P_{\text{nom, heat}} = 100 \text{ W/m}^2 \cdot 90 \text{ m}^2 = 9000 \text{ W} \tag{31}$$

$$P_{\text{nom, cold}} = 500 \text{ W/m}^2 \cdot 90 \text{ m}^2 = 45000 \text{ W} \tag{32}$$

4.5 Conclusion

The developed model enables dynamic simulation of the thermal behaviour of a residential building by incorporating key energy exchanges and physical parameters. Its validation using real experimental data increases confidence in its ability to replicate real-world conditions. This robust methodological framework serves as a solid foundation for quantifying the future impact of climate change on residential cooling demand across different climates.

5 Results and discussion

5.1 Comparison of present and future cooling load for the different studied cities

The building model is applied to the studied cities using the parameters defined in Section 4.4 and based on the equations presented in Section 4.1. The results are summarised in Table 12 and also illustrated in Figure 25 for a more visual representation.

City	Present (kWh/year)	Future (kWh/year)	Increase (%)
Singapore	12 888.27	15 859.35	+23.0%
Abu Dhabi	7 598.19	8 862.41	+16.6%
Guayaquil	18 386.88	21 663.85	+17.8%
São Paulo	7 177.62	12 037.60	+67.7%
Buenos Aires	5 425.17	6 014.01	+10.8%
Los Angeles	4 520.70	4 850.35	+7.3%
Brussels	1 255.73	1 085.52	-13.6%
Vancouver	1 479.32	1 942.38	+31.3%
Copenhagen	263.29	369.27	+40.3%
Montreal	1 636.06	2 155.87	+31.7%

Table 12: Comparison of present and future cooling load for the different studied cities (in kWh/year and % increase)

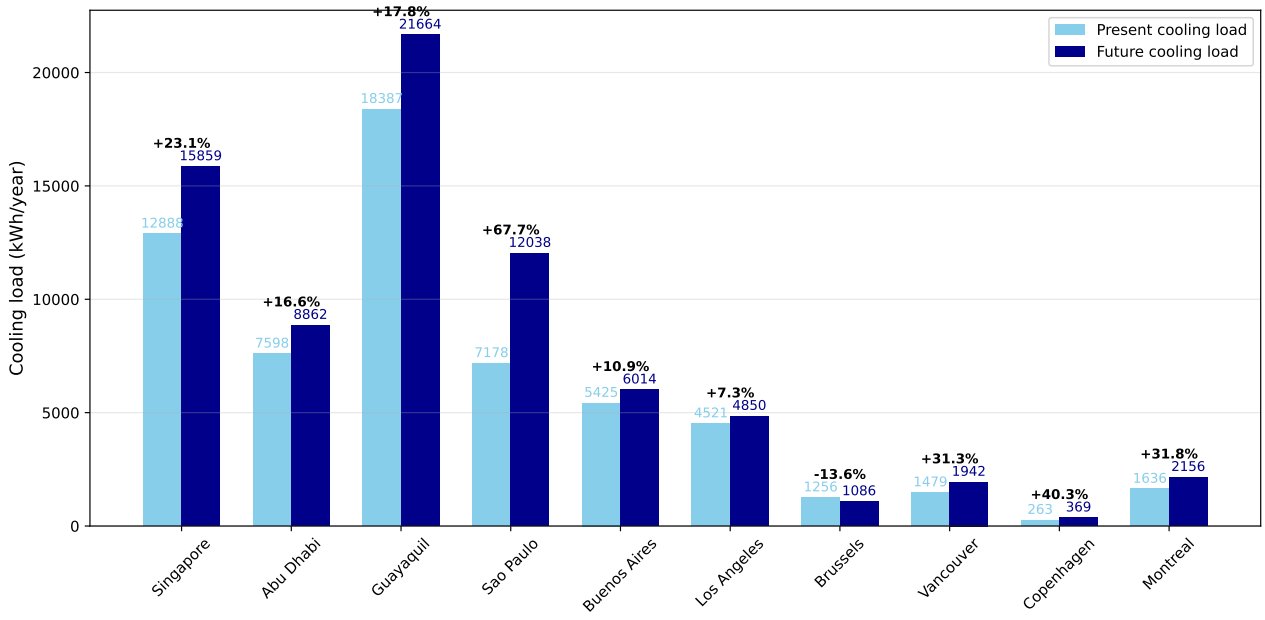

Figure 25: Comparison of present and future cooling load for the different studied cities.

As anticipated from the Cooling Degree Days (CDD) analysis presented in Section 3.3 with Figure 17, cooling loads are particularly high in hot and humid climates such as Singapore, Guayaquil, and São Paulo. These cities also show substantial future increases in cooling load, with projected rises of 23.1%, 17.8%, and 67.7% respectively. São Paulo exhibits the largest projected increase in cooling load, which aligns with its significant rise in CDD.

Surprisingly, despite having the highest CDD, Abu Dhabi, which represents extremely hot and dry climates, shows relatively moderate cooling load both in present and future projections. This can be attributed to more efficient building envelope characteristics, including lower U-values and a smaller Window-to-Wall Ratio (WWR), compared to cities such as Guayaquil and São Paulo, as shown in Tables 8 and 9.

In mixed humid climates, Brussels demonstrates the lowest increase in average outdoor temperature (+1.43%) along with a 2.86% decrease in solar irradiation as shown in Table 4, resulting in a projected decrease of 13.6% (from 1256 to 1086 kWh/year) in future cooling load.

Buenos Aires experiences a 19.8% increase in CDD as seen in Section 3.3, yet the cooling demand rises by only 10.9%. This lower-than-expected increase suggests that the relatively conservative WWR (0.3) in Argentine buildings may help buffer the effect of rising outdoor temperatures.

In Los Angeles, despite a substantial +46.4% increase in CDD, the cooling load increases by just 7.3%. This may indicate that existing envelope characteristics, such as moderate insulation, already offer good resistance to heat gains.

In contrast, Vancouver shows a +46.3% rise in CDD and a +31.3% increase in cooling load, which is proportionally higher than in L.A. This reflects the fact that buildings in Vancouver are traditionally not designed for significant cooling.

A similar trend is observed in Montreal (+37.1% CDD, +31.8% cooling load) and Copenhagen (+36.7% CDD, +40.3% cooling load), where even temperate or cold-climate cities start showing a marked sensitivity to rising temperatures. The building designs, which historically focused on heating performance, make these cities particularly vulnerable to climate change, induced cooling needs.

Overall, this analysis highlights that the response of a building to climate change is not solely determined by the magnitude of temperature rise (CDD), but also by its intrinsic thermal characteristics. The regions showing the largest increases in future cooling loads are also those most affected by global warming. In such climates, rising outdoor temperatures (as shown in Table 4) and the increased frequency and intensity of heatwaves will significantly challenge indoor thermal comfort [150]. This underscores the need for effective cooling solutions, particularly passive strategies, to maintain habitable indoor environments and avoid excessive reliance on energy-intensive active systems [11, 13, 150].

The same analysis can be made for the heating load and is presented in Appendix C.1.

5.2 Daily cooling load and temperatures for a representative cooling day for the different studied cities

Figures 26, 27 and from Figure 51 to 68 show the daily cooling load and temperatures for a representative cooling day for the studied cities. For countries in the Northern Hemisphere, this day is selected in July, when cooling demand typically peaks due to summer temperatures. The specific date, July 3^{rd}, is chosen arbitrarily. For countries in the Southern Hemisphere, where the seasons are inverted, the representative cooling day is selected in January, which corresponds to their summer. January 30^{th} is chosen arbitrarily as the representative date.

The cases of Singapore nowadays and in the future are respectively illustrated in Figures 26 and 27.

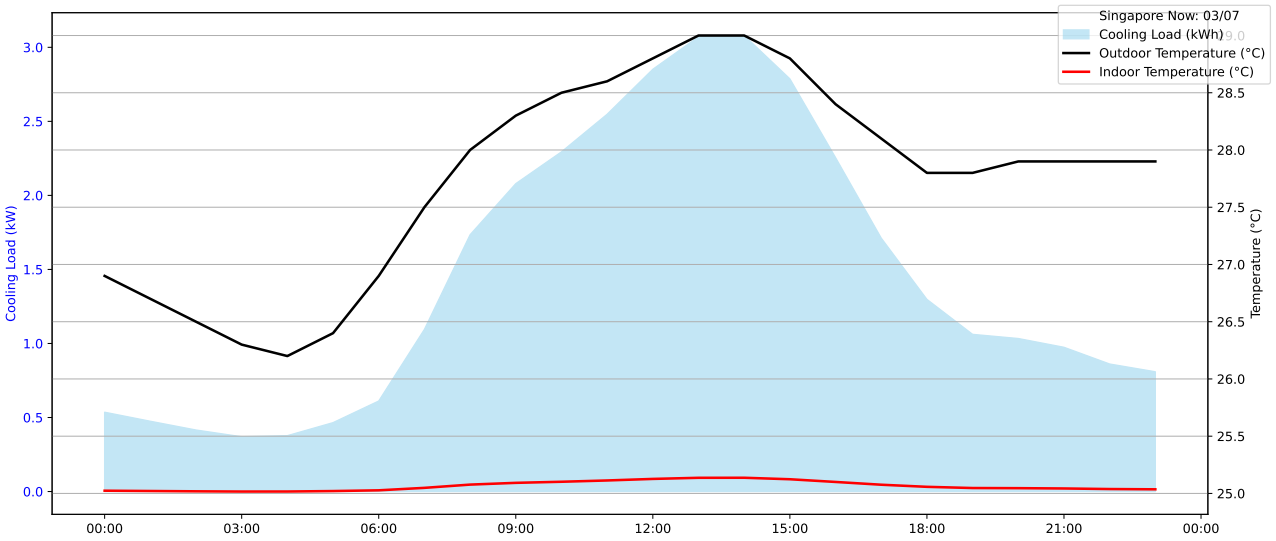

Figure 26: Present daily cooling load and temperatures in Singapore on July 3^{rd}.

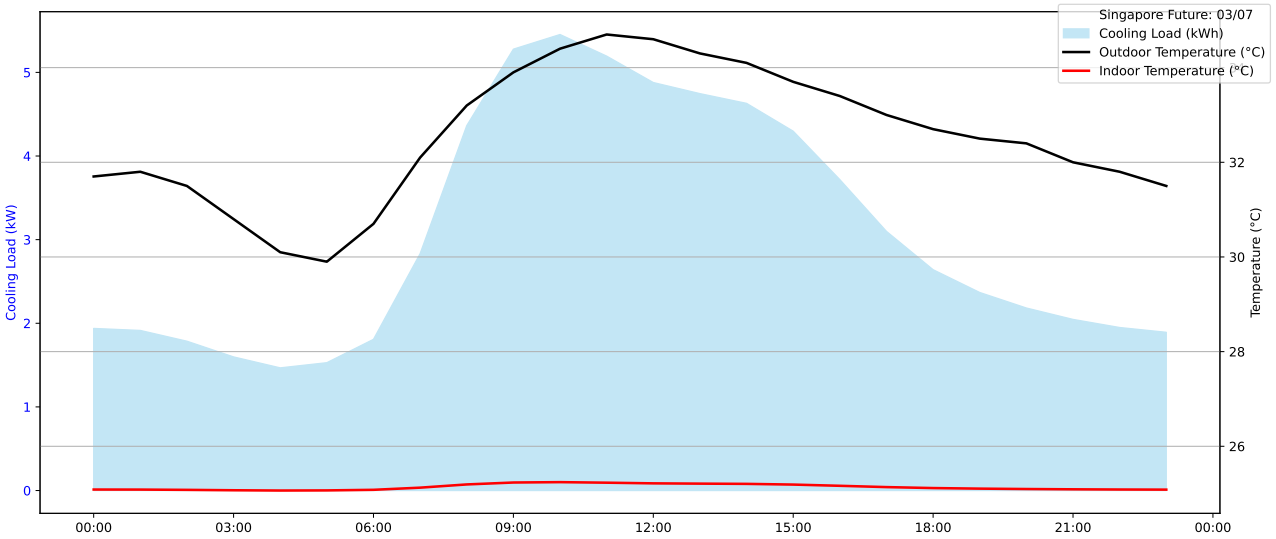

Figure 27: Future daily cooling load and temperatures in Singapore on July 3^{rd}.

Figures 26 and 27 clearly show that the model performs well in maintaining indoor temperatures below 25°C, as specified as the maximum comfort temperature, both in present and future scenarios. As expected, the cooling load increases significantly in the future, with a peak demand exceeding 5 kW, compared to approximately 3 kW under current conditions.

The increase in outdoor temperature throughout the day is mainly driven by the rise in solar irradiation, which reaches its peak around midday. This gradual increase in solar input leads to a corresponding rise in ambient outdoor air temperature. The cooling load closely follows a similar pattern, increasing as the outdoor temperature rises, indicating a strong correlation between outdoor temperature and cooling demand.

This observation suggests that implementing cold storage solutions could be beneficial. The operation of the cooling system could be shifted to nighttime hours, when conditions are more favourable. At night, the coefficient of performance (COP) is generally higher because the temperature difference between the ambient outdoor air and the target cooling temperature is smaller. By doing so, cooling energy can be stored and used later during the day. This approach reduces the need to operate cooling systems during peak demand hours, which coincide with the hottest part of the day and the lowest

COP. As a result, cold storage can improve overall system efficiency, help lower peak electricity demand, and reduce stress on the electricity grid, especially under future climate conditions.

$$COP_{\text{Carnot}} = \frac{T_{\text{in, wanted}}}{T_{\text{out}} - T_{\text{in, wanted}}} = \frac{298.15\ K}{T_{\text{out}} - 298.15\ K} \tag{33}$$

The Figures for the other studied cities can be found in Appendix D.1. The same analysis can be made for those figures.

5.3 Conclusion

The results show a significant increase in cooling demand across all studied climates by the 2041–2060 period, expected in mixed humid climates represented by Brussels, with the most pronounced rises occurring in historically temperate regions. Hourly and daily analyses also reveal a shift in peak loads, particularly in the afternoon hours. These findings emphasise the urgency of adapting buildings to future climate conditions and support the exploration of effective mitigation strategies to control the growing cooling demand.

6 Cooling technologies

To mitigate the risk of indoor overheating and maintain thermal comfort, buildings increasingly rely on both active and passive cooling strategies. Active systems employ mechanical types of equipment, such as air conditioners, heat pumps, or electric fans, to extract heat from indoor spaces [93]. These systems are often highly effective, but they are energy-intensive and can lead to significant operational costs. According to the International Energy Agency (IEA), approximately 20% of the electricity consumed in buildings globally is attributed to cooling equipment such as air conditioning and ventilation systems [11].

In contrast, passive cooling approaches prioritize architectural design and the use of natural environmental forces, such as shading, night ventilation, thermal mass, and natural airflow, to regulate indoor temperatures [151]. These strategies typically involve little to no energy consumption, making them more sustainable and economically attractive, particularly in temperate or moderately warm climates. However, their effectiveness can be limited in regions with extremely high outdoor temperatures or in buildings with substantial internal heat gains, where passive measures alone may not be sufficient to ensure thermal comfort.

6.1 Active cooling technologies

Active cooling systems can be categorized based on the energy source that powers the cooling process. A common classification distinguishes between electricity-driven systems, such as traditional vapour-compression units, fans or heat pumps, and thermally driven systems, which may use heat from natural gas, solar thermal collectors, or district heating networks to drive cooling cycles. This distinction, illustrated in Figure 28, underscores the technological diversity within active cooling technologies and the potential for integration with renewable or low-carbon energy sources to produce the necessary cooling in buildings [14, 152]. For example, solar photovoltaic panels can be placed on the roof of buildings to produce the necessary energy to run the active cooling during the day. The solar photovoltaic panels would have a double positive impact on the cooling of the building as they will produce the energy necessary for the active cooling technology, but they will also reduce the absorbed solar irradiation by the roof.

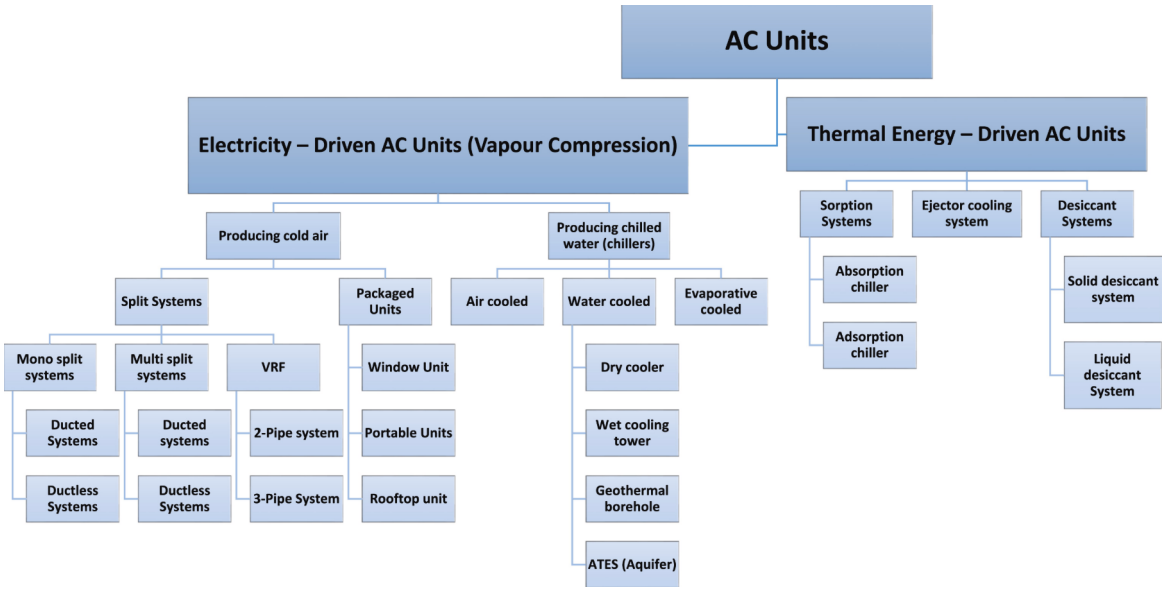

Figure 28: Classification of active cooling systems [152].

6.2 Passive cooling technologies

In contrast to active systems, passive cooling strategies rely on naturally available environmental sinks. These include building materials, ambient air, water vapour in the air (humidity), and even the night sky. Their role is to mitigate the effects of solar irradiation, internal heat gains, and elevated outdoor temperatures on indoor thermal conditions. These approaches aim to maintain indoor comfort with minimal or no energy consumption, making them highly relevant for sustainable building design. Passive cooling strategies, when effectively implemented, can significantly reduce cooling loads by limiting heat gains and enhancing natural thermal regulation [14, 153].

As illustrated in Figure 29, passive cooling techniques can be broadly categorized into three complementary approaches: solar protection, thermal modulation, and heat dissipation [154, 155].

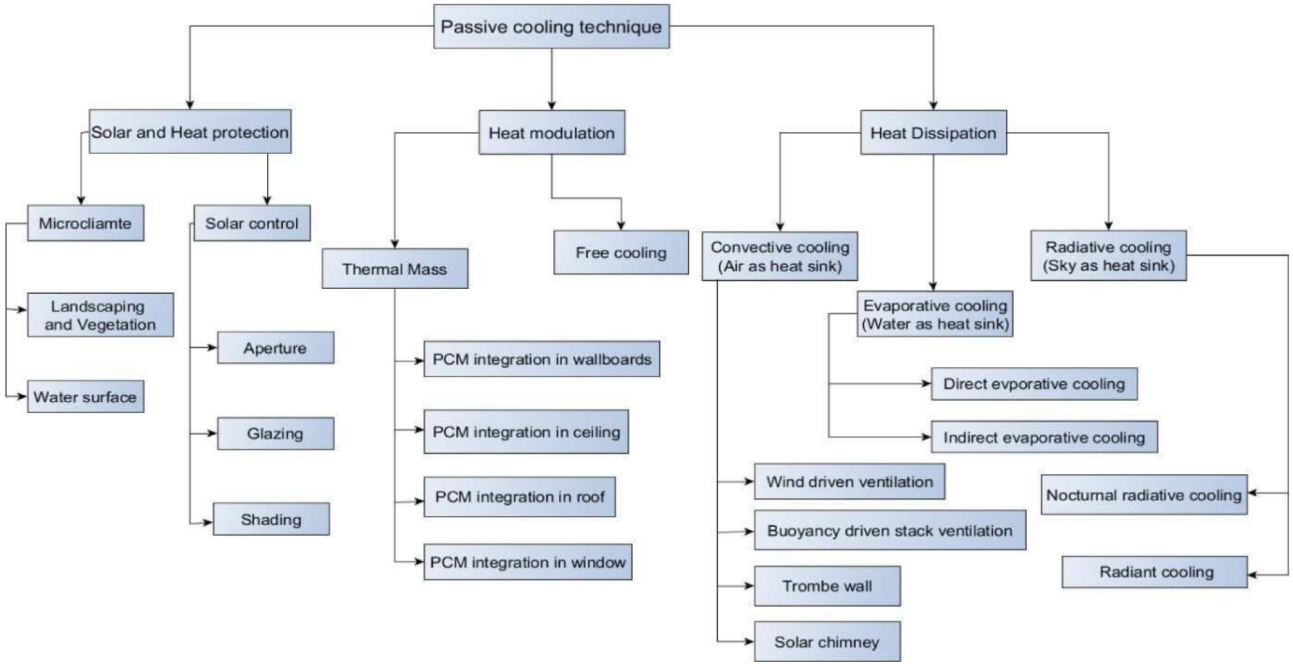

Figure 29: Classification of passive cooling techniques [154].

Solar protection aims to minimize the amount of solar radiation entering the building through interventions such as external shading devices, reflective or low-emissivity materials like white roofs, and microclimatic strategies such as vegetated landscaping and water surfaces. These methods reduce direct solar exposure and consequently lower the cooling loads imposed on the building envelope [14].

The effect of applying shading to 50 % of window surfaces is illustrated in Figure 30. In Guayaquil and São Paulo, the cooling loads decrease by 25.6 % and 38.9 %, respectively. In Brussels, Copenhagen, and Los Angeles, the reduction is particularly significant, with respective decreases of 87.4 %, 83.5 %, and 75.3 %.

In regions with very high outdoor temperatures, such as Singapore and Abu Dhabi, the relative effectiveness of shading is lower, with annual cooling load reductions of 17.7 % and 18.1 %, respectively. For Buenos Aires, Vancouver, and Montreal, shading still shows a notable impact, with respective decreases of 57.8 %, 60.5 %, and 61.3 %.

Solar protection methods such as shading can therefore significantly reduce cooling loads, often at relatively low cost, as summarised in Figure 39.

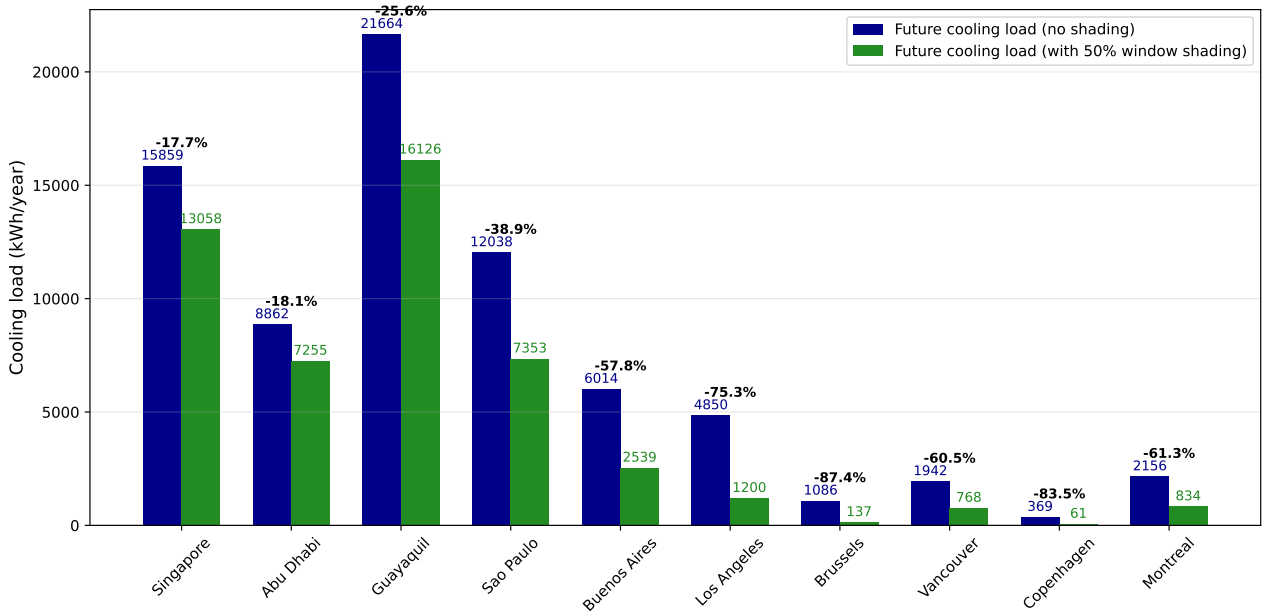

Figure 30: Comparison of projected cooling loads with and without 50% window shading for the different studied cities.

Thermal modulation, on the other hand, utilises the building's thermal mass to absorb and store excess heat during peak periods and release it when ambient conditions are cooler. By smoothing out temperature fluctuations over time, thermal modulation helps maintain more stable indoor conditions. Its effectiveness depends on the properties and placement of thermal storage materials, as well as the use of discharge methods such as natural night-time ventilation or free cooling to enhance heat release [14, 156, 157].

Thermal modulation is implemented in the model by increasing the thickness of concrete in the wall assemblies. Specifically, a 7 cm layer of concrete is added to the wall construction whose thickness is 14.4 cm if it is only constructed with concrete. This additional layer influences both the wall's thermal capacitance (C_{wall}) and its overall thermal transmittance (U_{wall}), as described by equations 11 and 13.

The thermal properties of the concrete used in the model are summarised in Table 13:

Property	**Symbol**	**Value**	**Unit**
Thermal conductivity	k	0.6	W/(m·K)
Density	ρ	2600	kg/m^3
Specific heat capacity	c_p	640	J/(kg·K)

Table 13: Thermal properties of concrete used in the simulation [158].

Using these properties and the updated wall composition, the modified values of C_{wall} and U_{wall} are computed for each studied city in Table 14.

City	Wall U-value (W/m^2·K)	C_{wall} (kJ/m^2·K)
Singapore	0.62	356.48
Abu Dhabi	0.31	356.48
Guayaquil	1.01	356.48
São Paulo	1.73	356.48
Buenos Aires	0.89	356.48
Los Angeles	0.38	356.48
Brussels	0.19	417.12
Vancouver	0.43	356.48
Copenhagen	0.157	356.48
Montreal	0.44	356.48

Table 14: Updated wall U-value and capacitance for the thermal modulation analysis with a 7 cm concrete layer added in the studied cities.

The effect of adding a 7 cm layer of concrete in the wall assembly on the annual cooling load in the studied cities is illustrated in Figure 31.

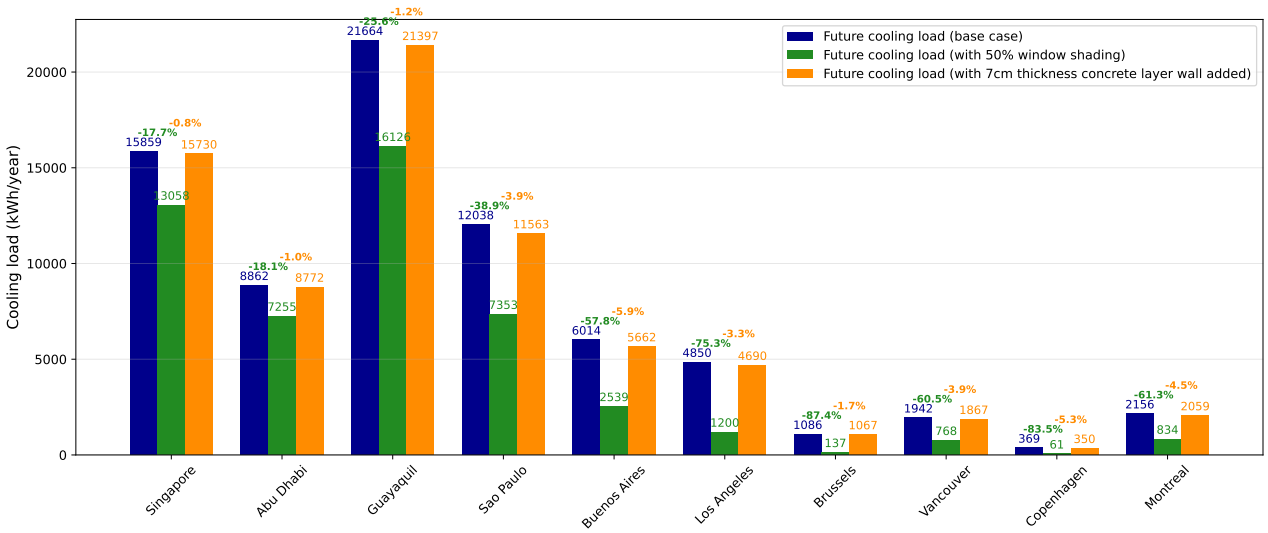

Figure 31: Comparison of projected cooling loads with and without 50% window shading and with a 7 cm thickness concrete layer wall added for the different studied cities.

The addition of a 7 cm thickness concrete wall layer in the studied cities does not have a big impact on the annual cooling loads. The biggest cooling load reduction is measured in Buenos Aires with a decrease of 5.9 %. This limited impact is expected, as the purpose of thermal mass is not to directly reduce the total annual cooling demand, unlike shading, but rather to shift the timing of the heat flow. Thermal mass absorbs and stores heat during peak periods (typically daytime), and releases it later when ambient conditions are cooler, such as at night. As a result, the stored heat must eventually be released, meaning the total cooling load over the year remains similar if not coupled with heat discharge methods. The true benefit of thermal mass is visible when analysing the daily cooling load profiles, where it helps to reduce peak demand and smooth fluctuations. This effect is illustrated for the future Buenos Aires scenario in Figure 32, and is not captured by annual values alone.

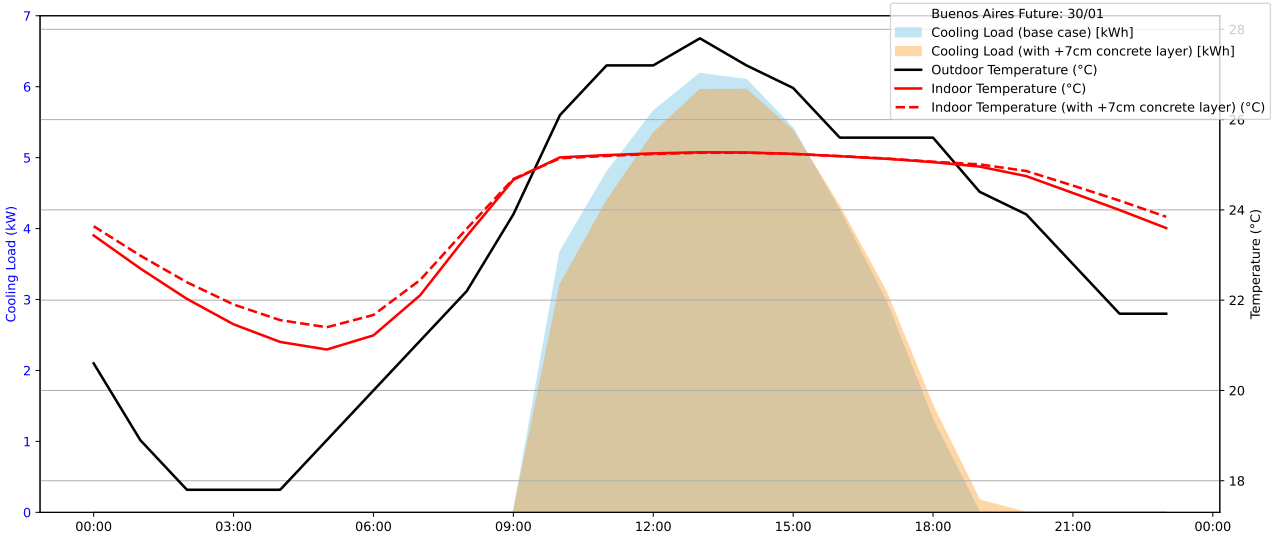

Figure 32: Comparison of future daily cooling load with and without a 7 cm thickness concrete layer wall added in Buenos Aires on January 30^{th}.

In Figure 32, a shift in the cooling demand is observed, along with a reduction in the peak value as expected.

However, the addition of a 7 cm concrete layer shows only a modest effect. The absolute impact remains limited at this thickness. A more significant thermal mass would be required to achieve a substantial influence on overall performance.

An alternative to increasing the wall's concrete thickness by 7 cm is to enhance its thermal mass through the integration of a 4 cm layer of phase change material (PCM). PCMs improve the building's capacity to store and release heat by exploiting their latent heat during phase transitions, typically between solid and liquid states. This allows a large amount of thermal energy to be absorbed or released at nearly constant temperature, which makes PCMs highly effective for moderating indoor temperature fluctuations [159, 160].

In this analysis, the selected PCM is *Rubitherm RT24*, a purely organic material with a phase change temperature between 21°C and 25°C, which is well suited to the indoor comfort range [20°C; 25°C] chosen in this work. Unlike conventional materials such as concrete, the specific heat capacity of PCMs is temperature-dependent, as shown in Figure 33. The thermal properties of RT24 used in the simulation are summarised in Table 15.

Property	**Symbol**	**Value**	**Unit**
Phase change range		21-25	°C
Thermal conductivity	k	0.2	W/(m·K)
Solid Density	ρ_s	880	kg/m^3
Liquid Density	ρ_l	770	kg/m^3

Table 15: Thermal properties of RT24 used in the simulation [161].

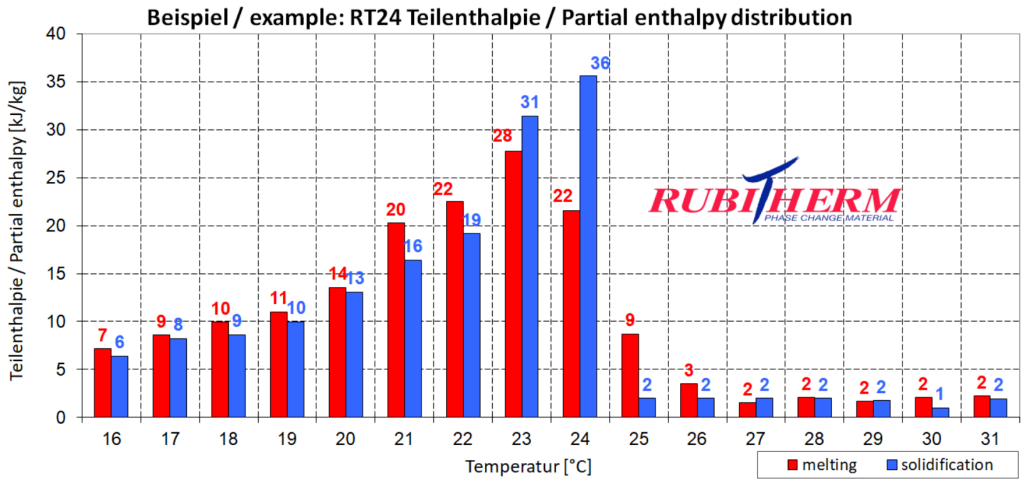

Figure 33: Specific heat capacity (c_p) of RT24 in function of the temperature [161].

Using these properties and the updated wall composition, the modified values of U_{wall} are computed based on equation 11 for each studied city in Table 16.

City	**Wall U-value (W/m^2·K)**
Singapore	0.59
Abu Dhabi	0.30
Guayaquil	0.93
São Paulo	1.51
Buenos Aires	0.83
Los Angeles	0.37
Brussels	0.19
Vancouver	0.41
Copenhagen	0.155
Montreal	0.43

Table 16: Updated wall U-value for the thermal modulation analysis using PCM in the studied cities.

The values of C_{wall} for each studied city are calculated as a function of the wall temperature, based on Equation 13.

The effect of adding a 4 cm PCM layer in the wall assembly on the annual cooling load in the studied cities is illustrated in Figure 34.

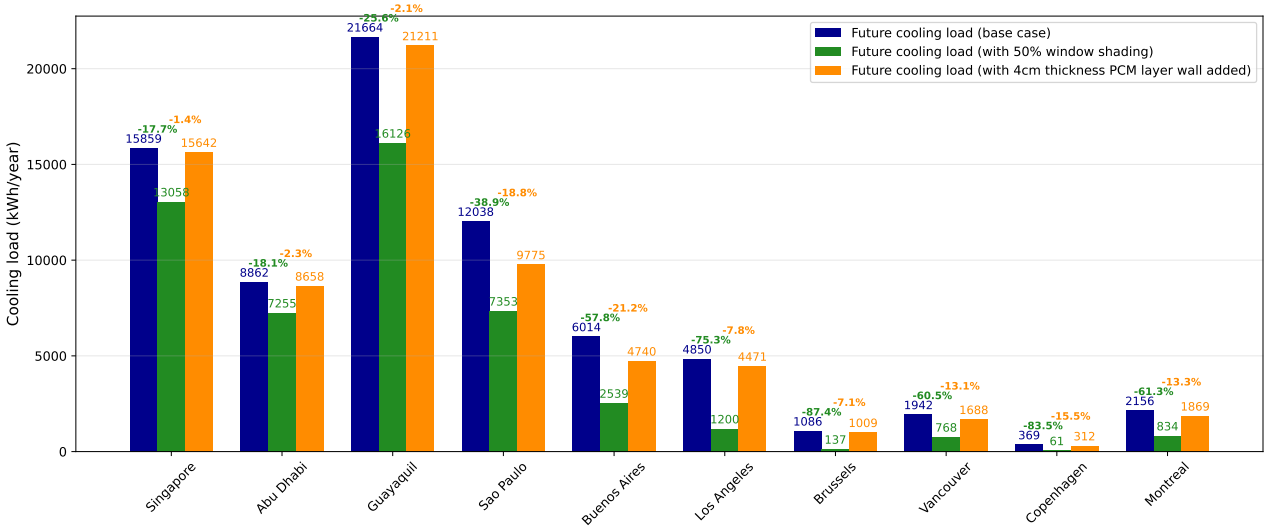

Figure 34: Comparison of projected cooling loads with and without 50% window shading and with a 4 cm thickness PCM layer wall added for the different studied cities.

The addition of a 4 cm thickness PCM (RT24) wall layer in the studied cities does not have a big impact on the annual cooling loads compared to shading devices. The biggest cooling load reduction is measured in Buenos Aires and São Paulo with a decrease of 21.2 % and 18.8 % respectively. The true benefit of thermal mass is visible when analysing the daily cooling load profiles, where it helps to reduce peak demand and smooth fluctuations. This effect is illustrated for the future Buenos Aires scenario in Figure 35.

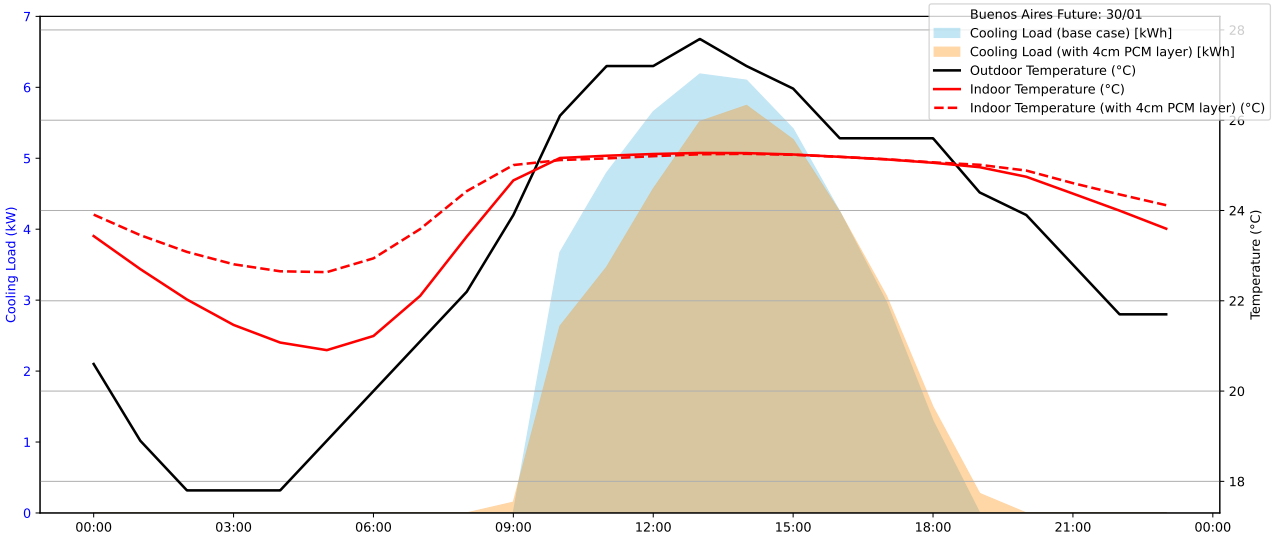

Figure 35: Comparison of future daily cooling load with and without a 4 cm thickness PCM layer wall added in Buenos Aires on January 30^{th}.

In Figure 35, a shift in the cooling demand is observed, along with a reduction in the peak value from 6.19 kW to 5.74 kW as expected. This reduction in the peak cooling load can allow the downsizing of active cooling technology, which has positive implications for both investment, operational efficiency, with a lower peak cooling value to develop and therefore lower the electrical consumption.

Increasing the thickness of the walls with concrete or adding a PCM layer can only realistically be applied to new constructions, as retrofitting existing buildings by modifying their structural components is generally unfeasible. Moreover, implementing thermal mass strategies through additional concrete

is more complex and costly than passive solar protection alternatives such as external shading. From an environmental standpoint, concrete production has a high carbon footprint [162], whereas shading systems have a much lower environmental impact. These factors must be taken into account when evaluating thermal modulation strategies in building design.

When the previous techniques are insufficient to maintain acceptable thermal conditions, excess heat must be actively rejected to an external sink thanks to heat dissipation technique. This technique involves transferring excess internal heat to environmental sinks like the night sky, ambient air, or water bodies. The performance of this strategy depends on the availability of an effective environmental sink and the efficiency of the thermal exchange between the building and its surroundings [14].

Night-time free cooling is implemented by setting the air change rate (ACH) to 12 between 8:00 p.m. and 6:00 a.m., provided that the indoor temperature exceeds the lower bound of the thermal comfort range (20°C), and that the outdoor temperature is lower than the indoor temperature [163]. The effect of night-time free cooling on the annual cooling load in the studied cities is illustrated in Figure 36.

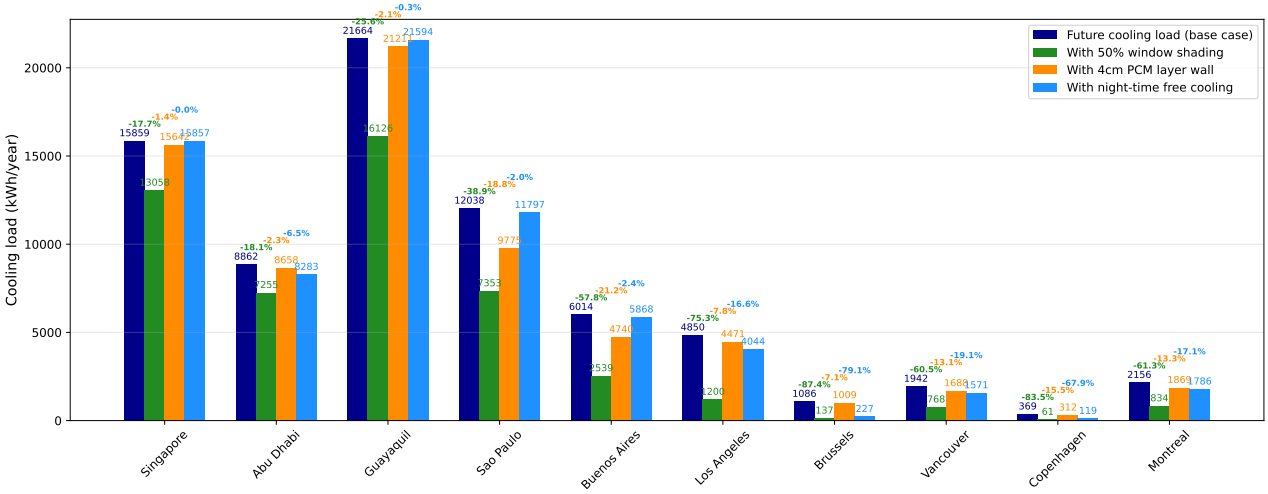

Figure 36: Comparison of projected cooling loads with and without 50% window shading; with a 4 cm thickness PCM layer wall added and with night-time free cooling for the different studied cities.

The effectiveness of night-time free cooling strongly depends on the diurnal temperature variation. In temperate climates, where outdoor temperatures drop significantly at night, this strategy results in substantial reductions in annual cooling loads. For instance, future scenarios for Brussels and Copenhagen show respective decreases of 79.1 % and 67.9 % in annual cooling demand.

In contrast, in equatorial regions such as Singapore and Guayaquil, where the outdoor temperature remains nearly constant throughout the day and night, night-time free cooling proves to be ineffective. For example, in Guayaquil, the reduction in annual cooling load is only 0.3 % and 0 % for Singapore. In climates where night-time temperatures drop slightly but not significantly, the impact of night-time free cooling remains limited. For example, in Abu Dhabi, the future annual cooling demand decreases by only 6.5 % because outdoor temperatures remain relatively high even during the night. In São Paulo and Buenos Aires, the effect is also modest, with reductions of 2.0 % and 2.4 %, respectively.

On the other hand, Los Angeles, Vancouver, and Montreal show more noticeable benefits, with reductions of 16.6 %, 19.1 %, and 17.1 % in annual cooling demand. Although these results are not as dramatic as in Brussels or Copenhagen, they still highlight the potential of this passive strategy in climates with moderate diurnal temperature ranges.

These results confirm that night-time free cooling is most effective in climates with a significant drop in temperature during the night.

The modification in the daily cooling load profile for Brussels on July 3^{rd} is illustrated in Figure 37.

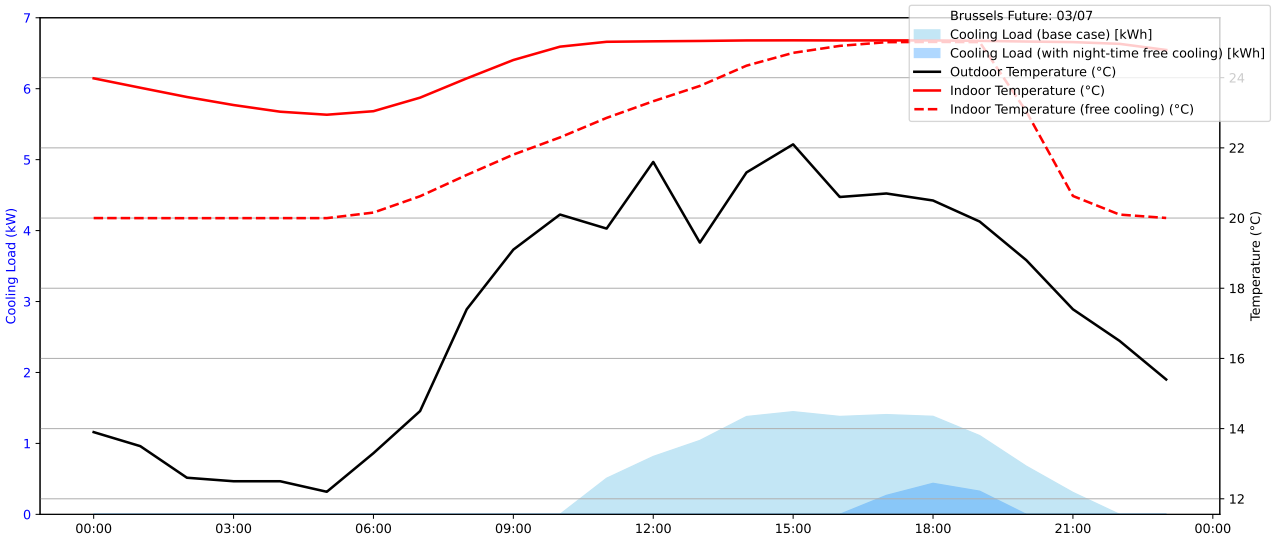

Figure 37: Comparison of future daily cooling load with and without night-time free cooling in Brussels on July 3^{rd}.

As shown in Figure 37, night-time free cooling has a significant impact on reducing indoor temperatures during summer in temperate climates such as Brussels. The indoor temperature drops to around 20°C at night, improving thermal comfort for sleeping. Additionally, this night-time ventilation reduces the cooling load during the day by pre-cooling the building and its structure, thereby limiting the temperature rise in the morning.

Together, these passive strategies offer significant potential to reduce reliance on energy-intensive mechanical systems. Their implementation plays a crucial role in enhancing building resilience to rising temperatures and contributes to long-term energy efficiency and indoor comfort, especially in a warming climate [14].

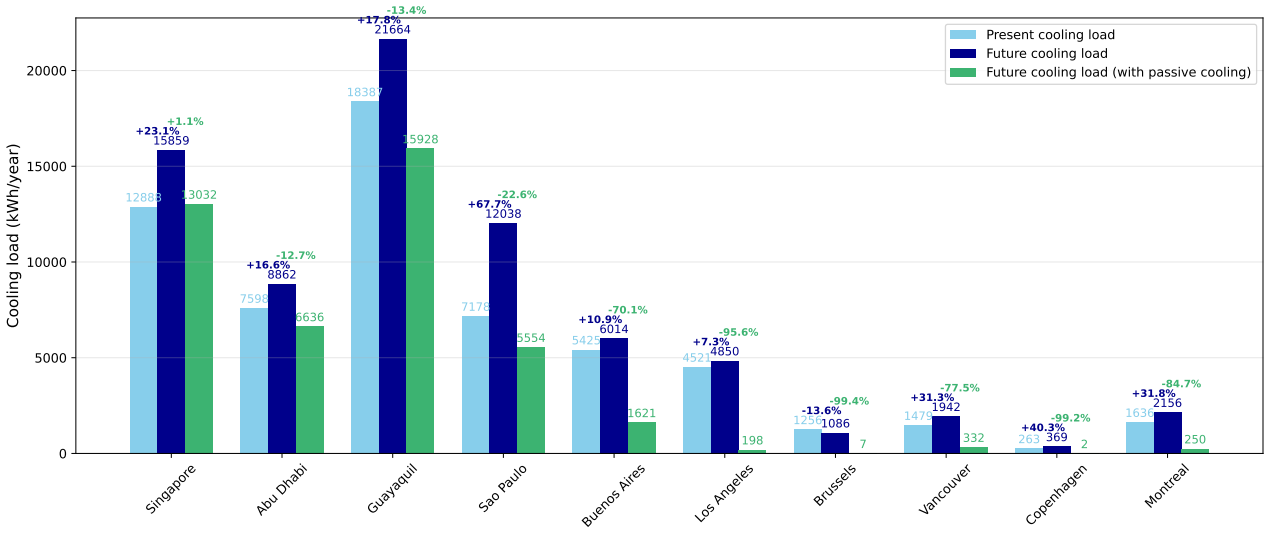

Figure 38: Comparison of present and future cooling load with and without passive cooling technologies (50% window shading, a 4 cm thickness PCM layer wall added and night-time free cooling) for the different studied cities.

The effectiveness of passive approaches has been widely studied in the literature [164–168]. Design interventions such as natural ventilation, improved insulation (e.g., low U-values), the use of building thermal mass, green roofs, and optimized shading devices have demonstrated significant potential to

enhance thermal comfort while reducing reliance on mechanical systems [169]. This effect is illustrated in Figure 38, which even shows a decrease in future cooling demand when passive technologies are implemented, compared to the actual cooling demand. This trend is observed across all studied climate types, except for extremely hot and humid climates, such as Singapore.

Natural ventilation, in particular, enables high air exchange rates with minimal energy input, contributing to comfort during the warmer months [170–172]. Similarly, the use of low-infiltration building envelopes increases the air tightness, improving both energy efficiency in winter when heating is necessary and indoor air quality in highly polluted cities [173–176]. On the other hand, buildings with low infiltration rates need mechanical ventilation to keep a good air quality. The mechanical ventilation can be coupled with an air filter and a heat exchanger to guarantee proper air and keep the heat inside the building in the colder months, and let the heat outside the building in the warmer months. Moreover, this additional mechanical ventilation increases the electrical consumption of the building. High-performance envelope materials with low thermal transmittance values minimize heat exchange with the exterior environment, reducing the need for active heating, but have a negative effect when cooling is needed [14, 177–179].

Green roofs not only reduce the conductive heat flow through roof assemblies but also offer enhanced stormwater management, biodiversity, and noise management [180]. Thermal mass plays a critical role in absorbing excess daytime heat and releasing it during cooler night hours, thus decreasing peak cooling load [181, 182]. Shading devices, especially those adapted to occupant behaviour and seasonal solar paths, are highly effective in reducing direct solar gains, with roller blinds being particularly efficient in temperate climates like Belgium's, for example as can be seen in Figure 30 [14].

6.3 Future cooling requirements and implementation challenges

The selection and implementation of appropriate cooling strategies, whether passive, active, or a combination of both, are crucial for ensuring thermal comfort in buildings, particularly in the context of global climate change. These strategies must be tailored to a range of interrelated factors, including climatic conditions, building design, occupancy patterns, economic constraints, cultural practices, and the availability of local resources. Climatic context is especially significant, as it governs not only the intensity of external heat gains but also the effectiveness of natural cooling resources. For instance, in high-density urban environments or regions with high temperature and limited temperature variation, passive techniques alone may prove insufficient, necessitating the integration of mechanical systems [14, 183].

Despite passive strategies' proven efficacy as illustrated in Figures 38 and 39, their performance inherently depends on prevailing environmental conditions. As climate change intensifies, outdoor temperatures are projected to rise, as shown in Section 2.2.1, reducing the temperature differential that drives natural ventilation and limiting the capacity of passive dissipation strategies. Increased outdoor temperatures also negatively affect the performance of active cooling systems by increasing thermal and mechanical stress on key components. Higher ambient temperatures lead to reduced heat rejection efficiency in condensers, causing a drop in the coefficient of performance (COP). As a result, cooling systems operate less efficiently. This reduced efficiency can lead to accelerated wear of components and more frequent maintenance needs. Together, these factors contribute to higher operational costs.

Moreover, elevated cooling load during peak periods can strain electricity grids, leading to potential outages and exacerbating greenhouse gas emissions if the energy is sourced from fossil fuels [13, 14].

Technique	Power [W] [a]	Maximum ΔT [°C] [b]	Cost [€] [c]	Maintenance [d]	Retrofit	Required space
Active methods						
Fans	50–185	~6	20–250	Medium	High	Low
Evaporative coolers	285–1500	~7	80–1400	Medium	High	Low
AC	800–4000	> 28	400–2200	Medium	High	Medium
Passive methods						
Shading systems	0	~1	20–500	Low	High	Low
PCM	0	~7	20000–50000	Medium	Low	Medium
Passive cooling shelter	10–500	~17	500–20000	High	Low	High
Heat sinks	10–100	~4	300–3000	Medium	Low	High
Thermal capacity	0	~16	500–3000	Low	Low	Medium
Radiant heat barriers	0	~13	30–9600	High	Medium	Low
Eco-evaporation cooling	0–100	~7	100–1800	Medium	Medium	Medium
Natural ventilation	0	~13	0–1000	Low	Low	Medium
Solar-assisted AC		> 28	5000–7000	Medium	High	High
Intelligent facades	100–800	~5	8000–26000	High	Medium	High

[a] Indicative range.
[b] Indicative values. The temperature depends on various factors such as relative humidity and wind speed.
[c] Indicative costs. The costs can vary from region to region.
[d] Maintenance is ranged according to the expenditure, invested work and occupied time.

Figure 39: Comparison between active and passive cooling methods for a 120 m^2 dwelling [184].

Consequently, the integration of active cooling systems becomes increasingly essential in scenarios where passive strategies alone cannot guarantee thermal comfort. This is particularly true in regions with consistently high outdoor temperatures, such as Singapore or Guayaquil. The need for active systems is even more pronounced during periods of extreme heat (heatwaves) or in buildings with high internal heat gains. Among the most promising active systems are heat pumps, especially reversible air-to-water models, which have shown superior performance over conventional gas-fired boilers and separate air conditioning systems [185, 186]. When powered by renewable electricity, heat pumps offer a low-emission solution to the growing cooling demand [187]. Nevertheless, their environmental impact must be carefully considered, particularly concerning the carbon intensity of the electricity mix and the use of refrigerants with high global warming potentials, such as hydrofluorocarbons (HFCs) as seen in Table 1 [14, 188].

Adaptation to climate change requires a forward-looking, flexible approach to building design and operation. Passive strategies should be routinely evaluated under future weather scenarios to ensure continued effectiveness. At the same time, active systems must be optimised for efficiency and integrated with renewable energy sources wherever possible. Backup solutions, such as mini-split systems, battery storage, or emergency generators, should also be considered to enhance resilience during concurrent heat waves and power outages [14].

6.4 Conclusion

In conclusion, this chapter demonstrated the potential of passive cooling strategies to mitigate the projected increase in energy demand due to global warming. Although their effectiveness varies by climate zone, their low energy consumption makes them a promising component of future adaptation strategies. The comparative study also showed that combining multiple passive techniques, such as window shading, thermal mass enhancement, and night-time ventilation, can lead to substantial reductions in cooling loads. These solutions must, however, be seen as part of a broader approach to building adaptation. A well-balanced combination of passive and active cooling strategies, adapted to local conditions and informed by robust simulation models and measurements, offers a viable pathway to climate-resilient buildings. This integrated approach enhances thermal comfort and contributes to energy efficiency and long-term sustainability goals.

7 Conclusion and future work

7.1 Conclusion

In the context of climate change, this thesis first aimed to present the root causes, observed effects, and likely future developments of global warming. The analysis emphasised the accelerating pace of climate disruption, driven by the growing global population, increasing greenhouse gas emissions, and energy-intensive lifestyles. In particular, it highlighted how these systemic factors reinforce one another in a "snowball effect" that amplifies global temperature increases.

To quantify one of the key consequences of this trend, the rising demand for cooling in residential buildings, a dynamic thermal simulation model was developed, validated, and applied to cities across a broad range of climate zones. Using present-day and projected Typical Meteorological Year (TMY) data for the period 2041–2060, the study evaluated how climate change will influence cooling needs in diverse geographic contexts.

The simulation results confirmed a general and significant increase in cooling demand across most studied cities. For instance, São Paulo and Copenhagen are expected to experience increases of +67.7 % and +40.3 % respectively, while even cooler cities like Montreal and Vancouver show future increases of over +30 %. In contrast, historically hot and humid cities such as Singapore and Abu Dhabi see more moderate increases (around +23 % and +16 %) but remain among the cities with the highest absolute demand. Surprisingly, Brussels is one of the rare cities to show a slight decrease in simulated future cooling demand.

A sensitivity analysis helped identify the most influential physical parameters affecting indoor temperature regulation, including solar gains, insulation performance (U-values), internal heat gains, and infiltration rates. The simulation model showed good alignment with real-world temperature data collected from twin test houses, achieving Cv(RMSE) values below 16 %, well within the accepted accuracy thresholds for hourly simulations.

To mitigate the future rise in cooling loads, the study also examined passive cooling strategies such as window shading, night-time ventilation, and phase change materials (PCM) integrated into walls. When applied collectively, these measures can lead to dramatic reductions in future cooling loads, up to 99 % in some cases (e.g., Brussels) and at least 20–80 % in most others. This underscores the powerful role that building design can play in climate adaptation.

However, the effectiveness of these strategies is highly dependent on local climate conditions. In cities with extreme heat and humidity, such as Singapore, passive measures alone are insufficient. In such cases, hybrid systems or well-designed active cooling will remain essential.

7.2 Future work

While this thesis provided valuable insights into the evolution of cooling demand in residential buildings under future climate scenarios, several extensions and improvements could be explored in future work. First, the scope of this study was limited to a representative residential building typology. However, expanding the analysis to include other building types, such as offices, hospitals, schools, elderly care homes, or sports facilities, would provide a more comprehensive understanding of how global warming affects different occupancy profiles and usage patterns. Each of these buildings has distinct internal gains, occupancy schedules, ventilation needs, and comfort requirements, making their thermal behaviour under climate stress significantly different from that of dwellings.

Moreover, within the residential sector itself, a broader range of case studies could be considered. The current model is based on a single standardised house geometry and insulation level per climate

zone, but future work could explore variations in construction quality (e.g., poorly insulated vs. high-performance homes), architectural typologies (apartments, detached houses, etc.), and window-to-wall ratios. This would allow for a more detailed sensitivity analysis and help identify the most vulnerable building types under different climate trajectories.

In addition to expanding the building stock, further work could also investigate the impact of active cooling systems. This study focused on passive techniques, but incorporating air conditioning systems of different efficiencies, control strategies, and seasonal performance factors would allow for a more realistic assessment of how future energy demand may evolve. This is especially relevant in extremely hot and humid climates as Singapore, where passive solutions alone are insufficient to ensure thermal comfort.

Furthermore, the study tested only three passive cooling strategies: window shading, phase change materials, and night ventilation. While effective, these represent only a small subset of the available strategies. Future research could include green roofs, evaporative cooling, thermal mass optimisation, light-coloured façades (albedo effect), and smart ventilation controls using PCM. Testing the synergistic effects of combining several techniques would also provide valuable guidance for integrated design approaches.

Another limitation lies in the use of Typical Meteorological Year (TMY) weather files, which are designed to represent "average" conditions and do not capture short-term extreme events such as heatwaves. Future work could simulate actual historical or projected heatwave episodes to analyse thermal resilience under extreme conditions. This would offer deeper insight into potential overheating risks, especially for vulnerable populations and building typologies with low thermal inertia.

7.3 Personal reflection

This work invites a deeper reflection: while technology is part of the solution, it cannot be the only answer to global warming. This is particularly true when viewed through the lens of Jean-Marc Jancovici's words:

"Most of today's technological progress is absolutely not aimed at solving environmental problems." (Interview, Le Monde, 2024 [189])

The belief that innovation alone will "fix" climate change is a dangerous illusion. As Jancovici sharply puts it:

"We don't have an energy problem, we have a civilisation problem. The issue is not that we will run out of solutions, but that we refuse to accept that there are limits." (Interview, France Inter, 2019 [190])

Addressing climate change will require more than engineering ingenuity. It demands a fundamental shift in how we live, consume, and organise our societies. Buildings are one piece of the puzzle, but so are our habits, expectations, and collective ambitions. If we truly want to limit global warming and preserve liveable conditions on Earth, we must transition toward energy sobriety and rethink the notion of infinite growth on a finite planet. This means embracing a form of controlled, planned degrowth in energy use, especially in wealthy nations, rather than blindly scaling up consumption and hoping technology will catch up.

In short, this thesis not only highlights technical strategies to adapt buildings to a changing climate, but also echoes a broader truth: adapting our models is not enough. We must also adapt ourselves.

Appendix A: Additional meteorological graphs of daily temperature anomalies comparing present (2001-2020) and future projections (2041-2060) in the studied cities

A.4 Graphs

The comparison between present and future projections outdoor temperatures are made for the studied countries with in black the present case and in colour (red if increase, blue if decrease) the future projections in the following Figures.

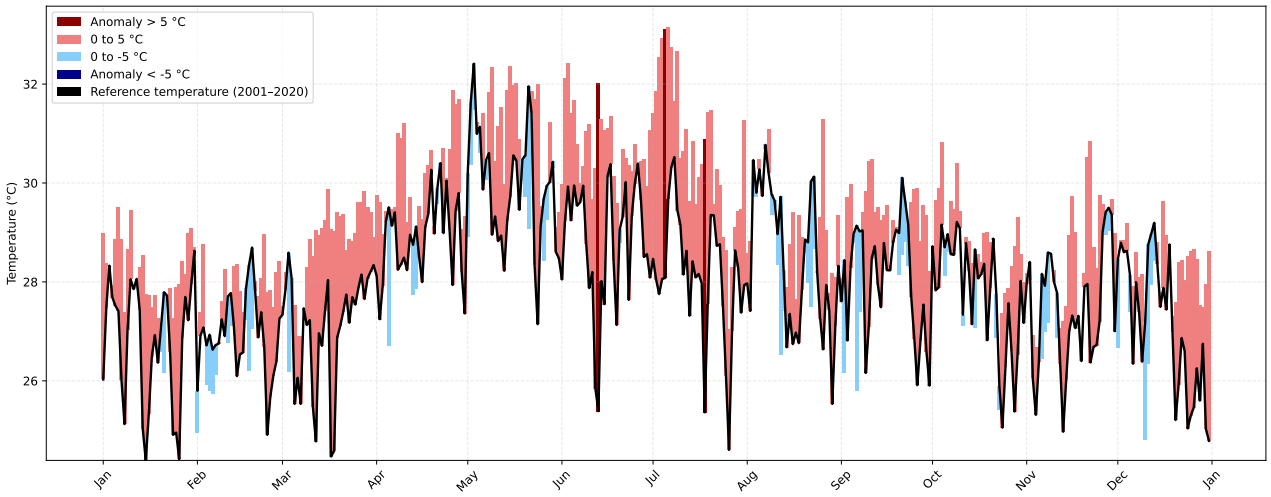

Figure 40: Daily temperature anomalies in Singapore comparing present data (2001-2020) and future climate projections (2041-2060).

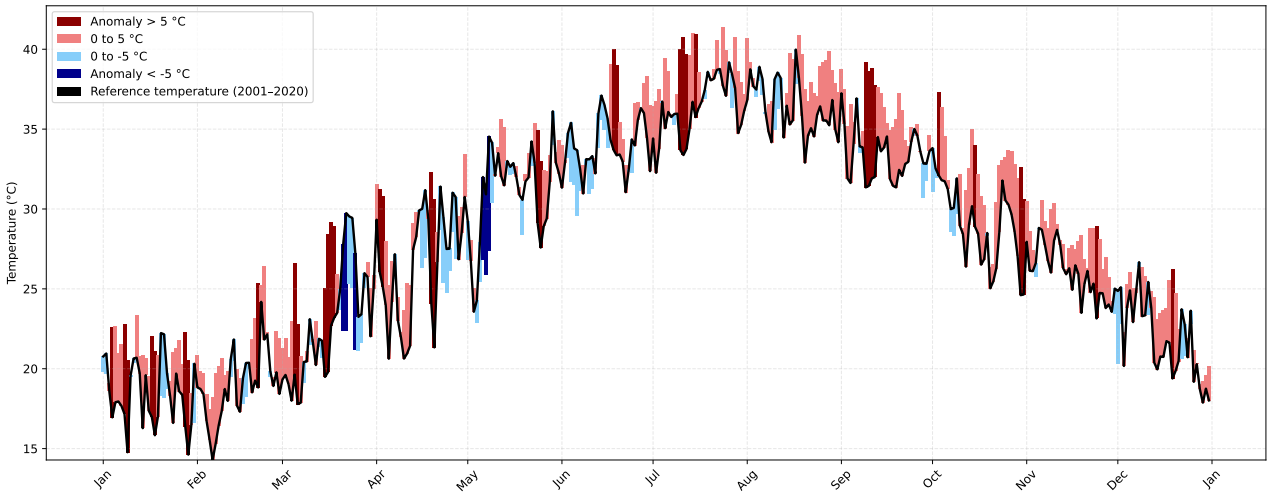

Figure 41: Daily temperature anomalies in Abu Dhabi comparing present data (2001-2020) and future climate projections (2041-2060).

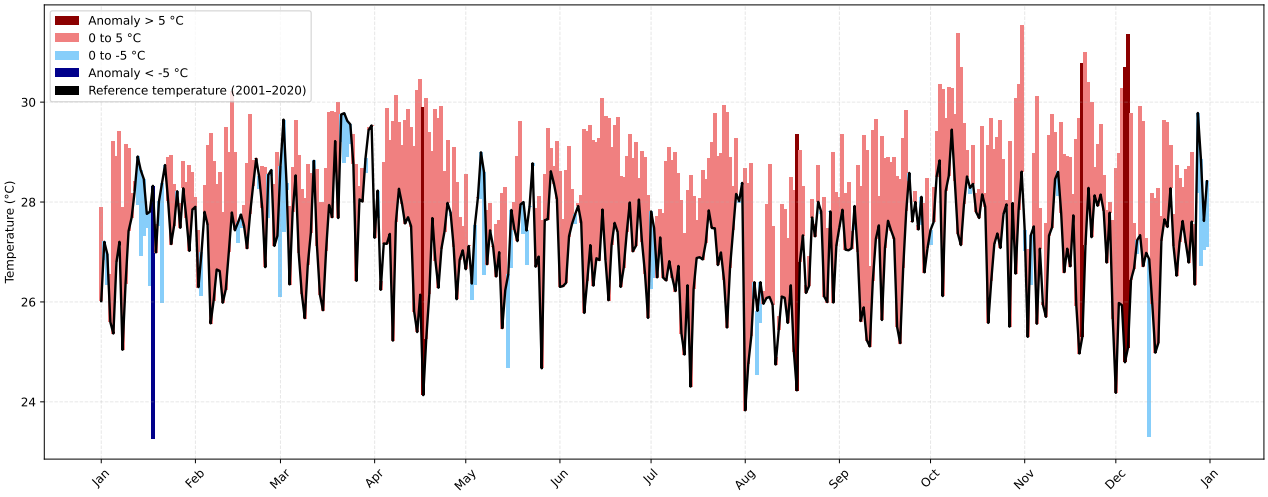

Figure 42: Daily temperature anomalies in Guayaquil comparing present data (2001-2020) and future climate projections (2041-2060).

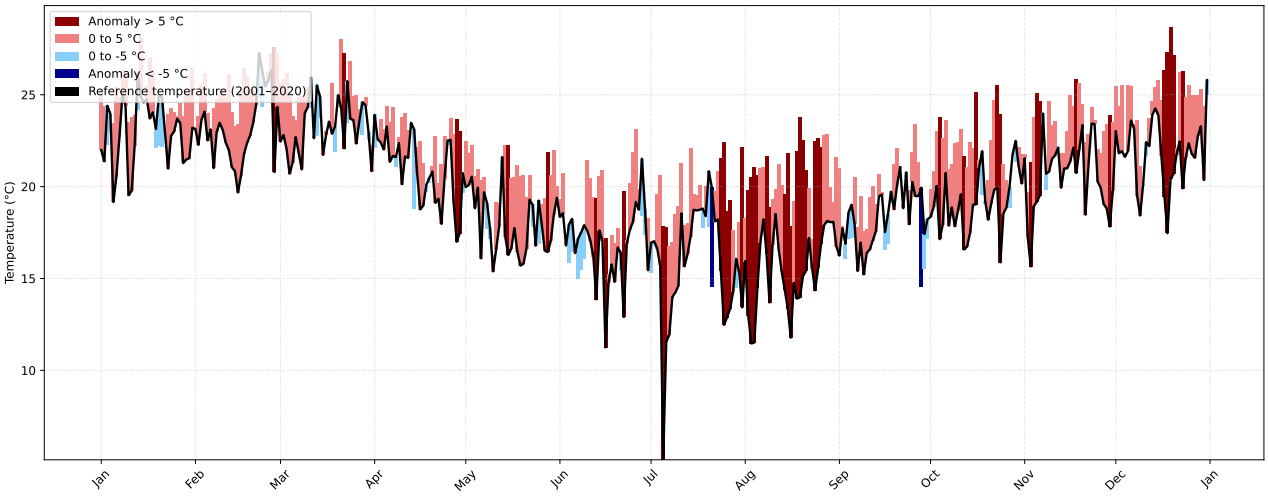

Figure 43: Daily temperature anomalies in Sao Paulo comparing present data (2001-2020) and future climate projections (2041-2060).

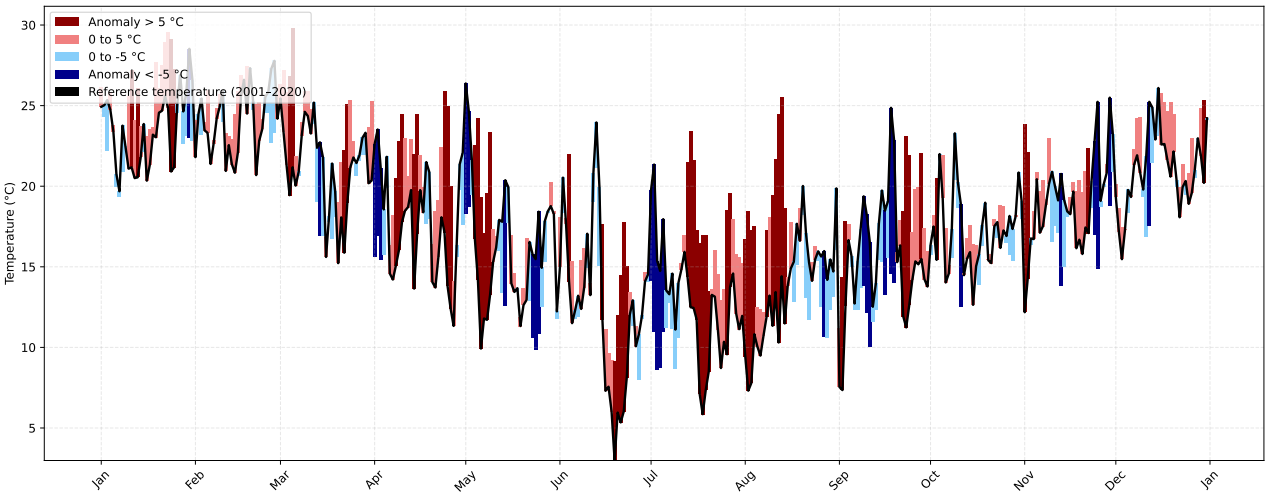

Figure 44: Daily temperature anomalies in Buenos Aires comparing present data (2001-2020) and future climate projections (2041-2060).

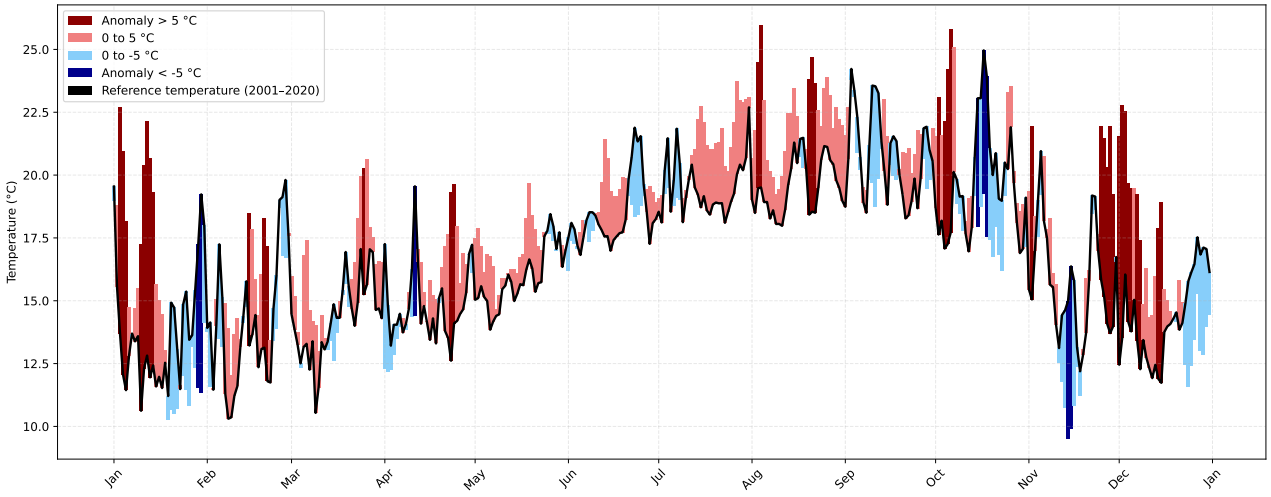

Figure 45: Daily temperature anomalies in Los Angeles comparing present data (2001-2020) and future climate projections (2041-2060).

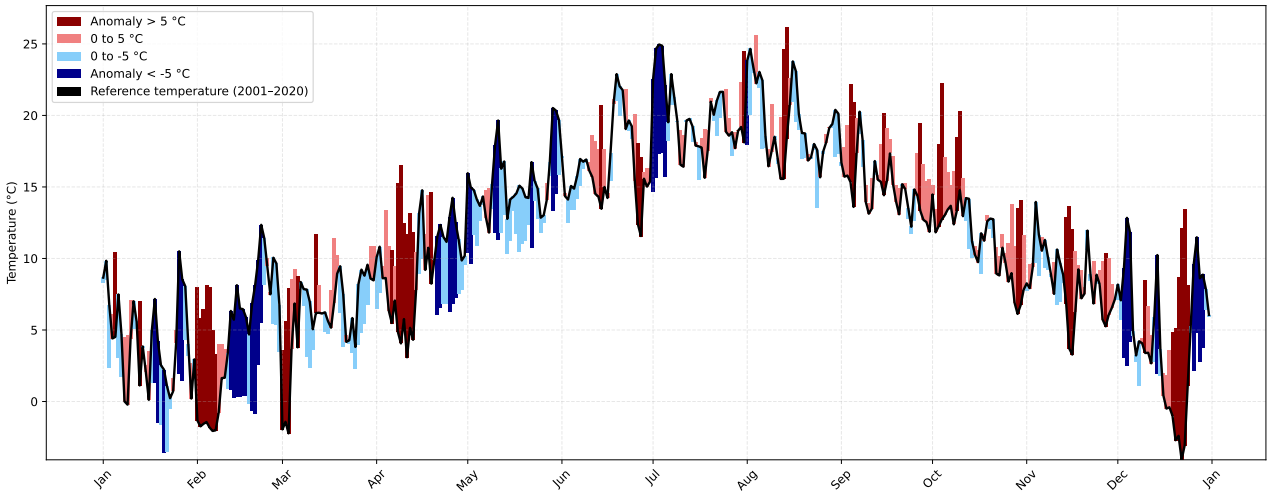

Figure 46: Daily temperature anomalies in Brussels comparing present data (2001-2020) and future climate projections (2041-2060).

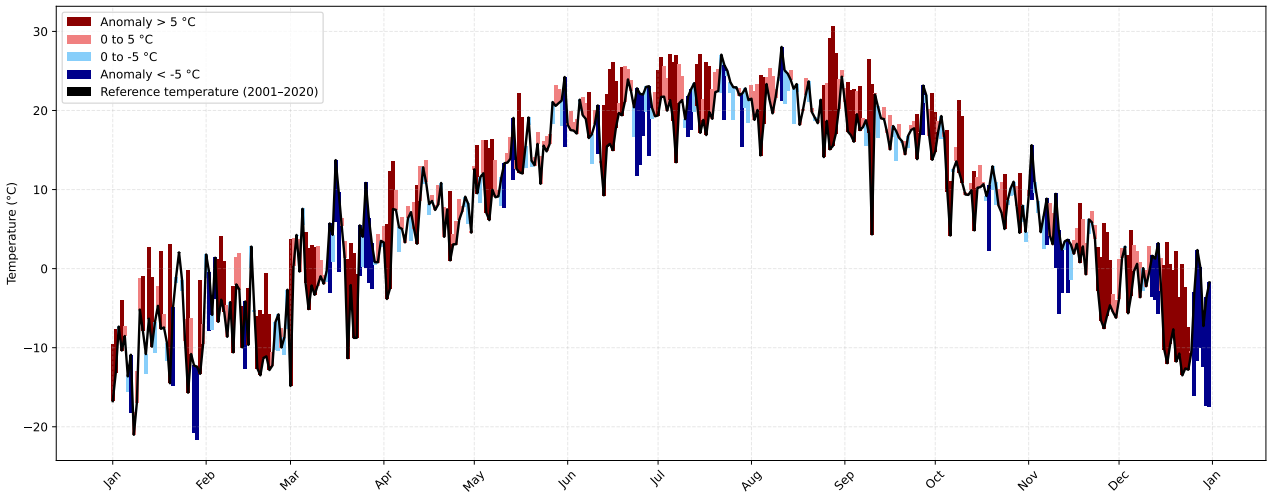

Figure 47: Daily temperature anomalies in Vancouver comparing present data (2001-2020) and future climate projections (2041-2060).

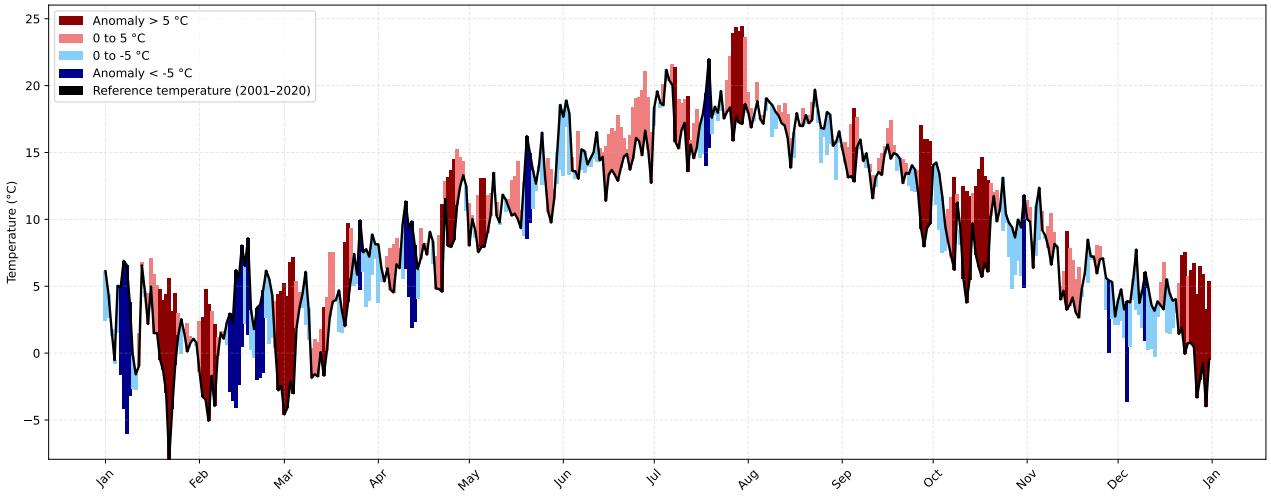

Figure 48: Daily temperature anomalies in Copenhagen comparing present data (2001-2020) and future climate projections (2041-2060).

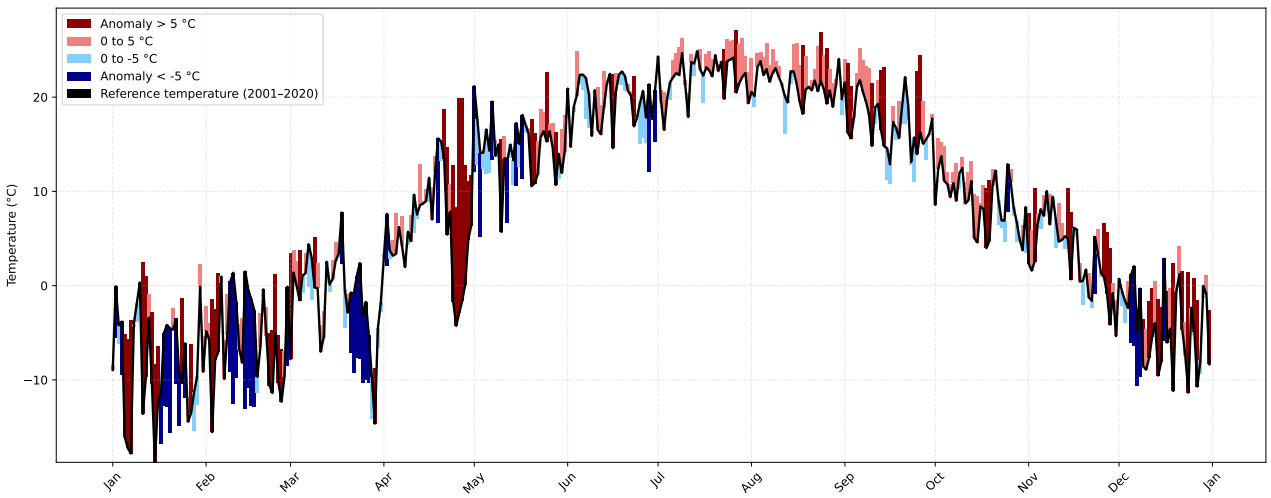

Figure 49: Daily temperature anomalies in Montreal comparing present data (2001-2020) and future climate projections (2041-2060).

Appendix B: Additional data of twin houses used for building model validation

B.1 Geometry

Table B.1 summarises the key geometric characteristics of the twin houses, including surface area, height, volume, and window area as a function of their orientation. These values serve as foundational inputs for the simulation model. An important assumption made is that the internal walls are not considered in the model.

Zone surface (m^2)	Exterior wall surface (m^2)	North-oriented wall area (m^2)	South-oriented wall area (m^2)	West-oriented wall area (m^2)	East-oriented wall area (m^2)	Height (m)	Volume (m^3)	North-oriented window area (m^2)	South-oriented window area (m^2)	West-oriented window area (m^2)	East-oriented window area (m^2)
101.0025	102.49	28.26	19.6	26.37	28.26	3	303.0075	1.29	7.24	2.58	1.29

Table B.1: Geometry of the twin houses studied for the building model validation.

B.2 Envelope parameters

Table B.2 summarises the key physical characteristics of the twin houses, including U, C, θ, ϕ factors, and the solar factor(SF). These values are foundational inputs for the simulation model. The ceiling corresponds to the roof in the equations, and the floor to the ground.

	U ($W/m^2 \cdot K$)	**C ($J/m^2 \cdot K$)**	θ	ϕ	SF
Floor	0.2837	664 182	0.039 98	0.1964	/
Ceiling	0.2350	629 409	0.4252	0.0158	/
Wall S.	0.1995	300 768	0.053 12	0.2397	/
Wall W.	0.2730	300 512	0.071 38	0.2395	/
Wall N.	0.1995	300 768	0.0512	0.2397	/
Wall E.	0.1915	300 512	0.0511	0.2399	/
Windows	1.2	/	/	/	0.51

Table B.2: Thermal characteristics of the twin houses studied for the building model validation.

The other parameters needed for the different interactions between the twin houses and the exterior, such as the infiltration and the mechanical ventilation air flow rate, are presented in the following Table B.3:

$V_{infiltration}$	V_{mech}	η_{HEX}	ICF	$\dot{Q}_{\text{int}}$
9.32 m^3/h	120 m^3/h	0	4	0 W

Table B.3: Essential parameters for the twin houses interactions with the environment.

Appendix C: Additional comparison of present (2001-2020) and future (2041-2060) heating load for the studied cities

C.1 Graph

The building model is applied to the studied cities using the parameters defined in Section 4.4 and based on the equations presented in Section 4.1. The results are illustrated in Figure 50 for the heating loads.

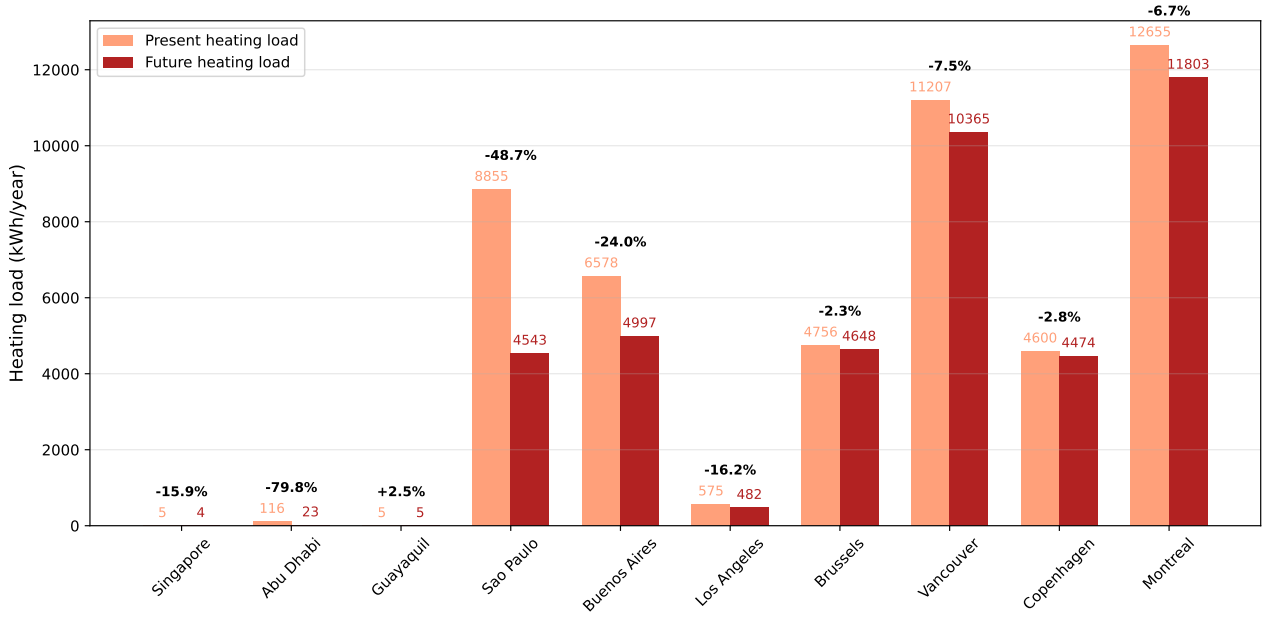

Figure 50: Comparison of present and future heating load for the different studied cities.

As expected, the heating loads decrease in all the studied cities when considering future climatic conditions. This reduction is primarily due to the projected increase in outdoor temperatures caused by global warming, which reduces the need for indoor heating during colder periods.

However, when comparing this decrease in heating demand with the increase in cooling demand shown in Figure 25, it becomes clear that the reduction in heating loads is smaller than the rise in cooling loads in each studied city. This means that the overall energy demand for thermal comfort (heating and cooling combined) is expected to increase.

Furthermore, if heat pumps are used to meet both heating and cooling needs, their performance in each mode must be considered. Heat pumps are generally more efficient in heating mode than in cooling mode. This is because, in heating mode, the system extracts heat from the outdoor air, which requires less energy input than rejecting heat to hot outdoor conditions in cooling mode. As outdoor temperatures rise due to global warming, the efficiency of cooling decreases further, as the heat pump must work against a higher temperature gradient. Therefore, despite a reduction in heating demand, the increased cooling demand, combined with lower efficiency in cooling mode, will lead to a net rise in electricity consumption for thermal regulation in the studied cities. Since these cities were selected to represent a variety of global climate zones, the trends observed can be extended to draw broader conclusions about the likely evolution of building energy needs worldwide.

Appendix D: Additional graphs of daily cooling load and temperatures in the different studied cities on a representative cooling day

D.1 Graphs

The cases of Abu Dhabi nowadays and in the future are respectively illustrated in Figures 51 and 52.

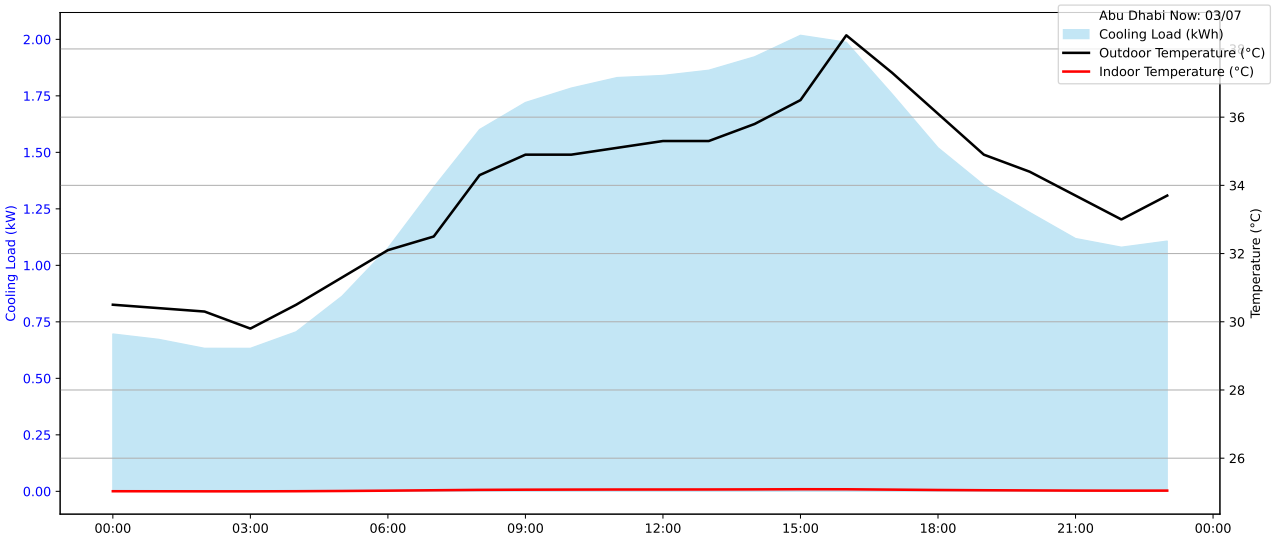

Figure 51: Present daily cooling load and temperatures in Abu Dhabi on July 3^{rd}.

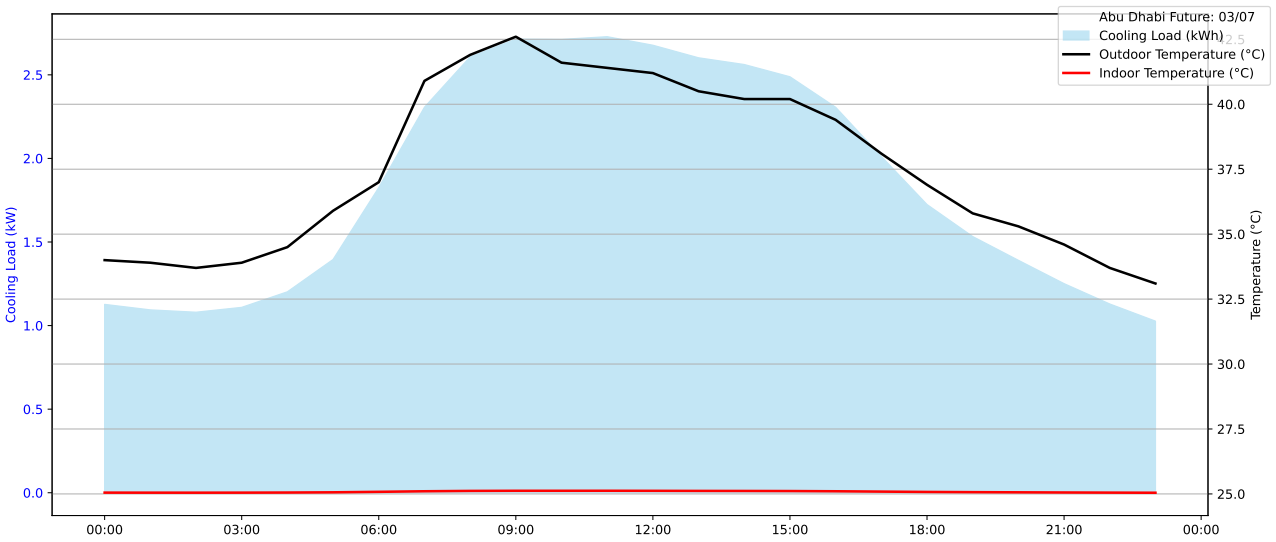

Figure 52: Future daily cooling load and temperatures in Abu Dhabi on July 3^{rd}.

The cases of Guayaquil nowadays and in the future are respectively illustrated in Figures 53 and 54.

The cases of Sao Paulo nowadays and in the future are respectively illustrated in Figures 55 and 56.

The cases of Buenos Aires nowadays and in the future are respectively illustrated in Figures 57 and 58.

The cases of Los Angeles nowadays and in the future are respectively illustrated in Figures 59 and 60.

The cases of Brussels nowadays and in the future are respectively illustrated in Figures 61 and 62.

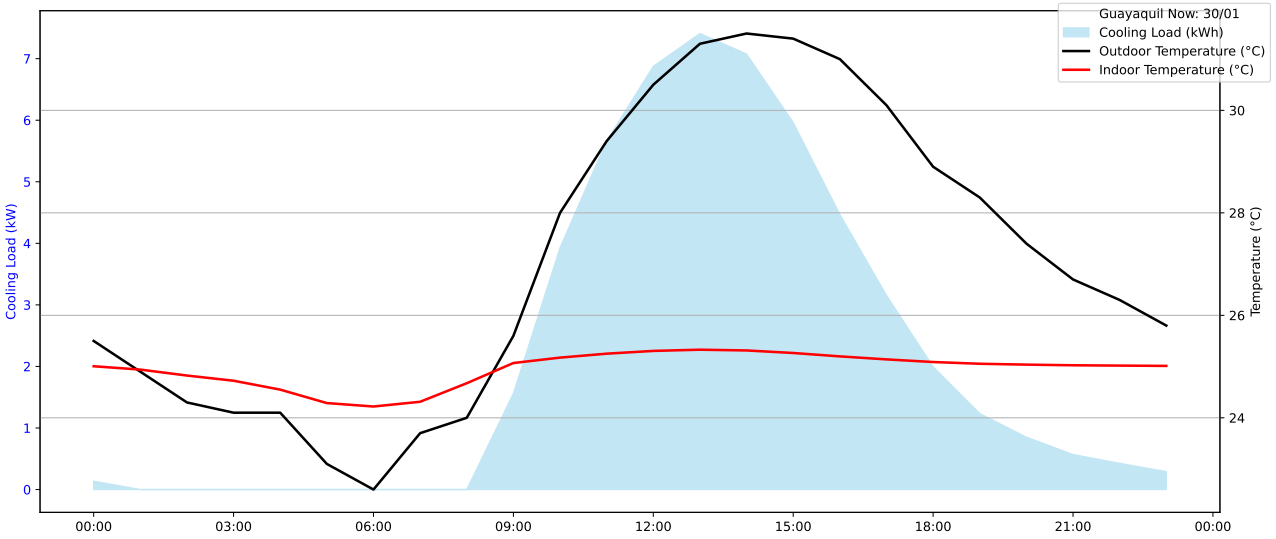

Figure 53: Present daily cooling load and temperatures in Guayaquil on January 30^{th}.

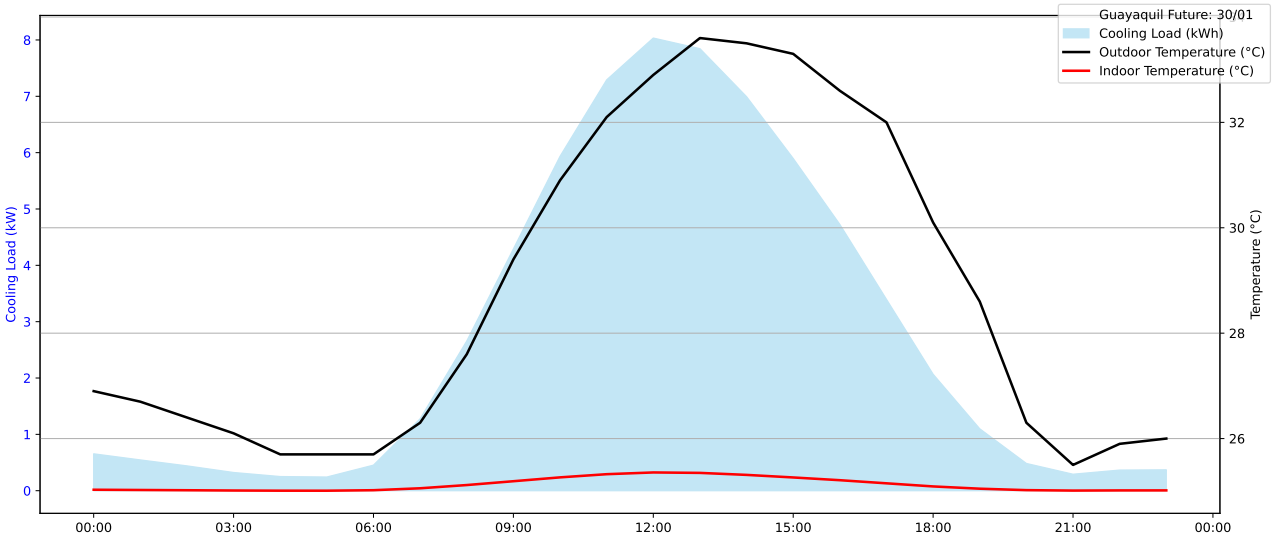

Figure 54: Future daily cooling load and temperatures in Guayaquil on January 30^{th}.

The cases of Vancouver nowadays and in the future are respectively illustrated in Figures 63 and 64.
The cases of Copenhagen nowadays and in the future are respectively illustrated in Figures 65 and 66.
The cases of Montreal nowadays and in the future are respectively illustrated in Figures 67 and 68.

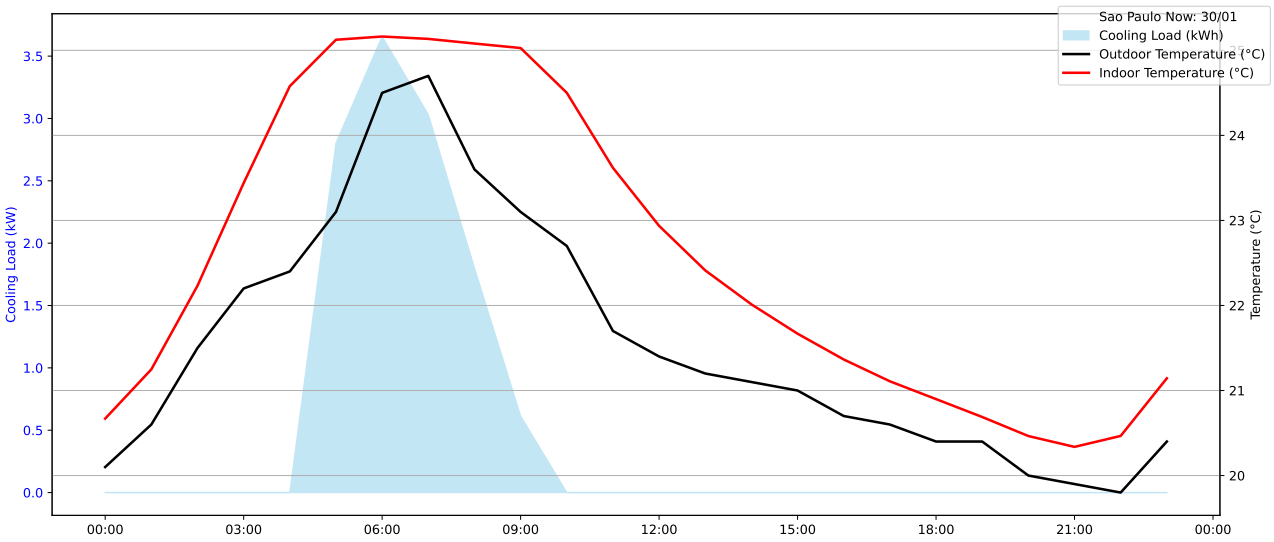

Figure 55: Present daily cooling load and temperatures in Sao Paulo on January 30^{th}.

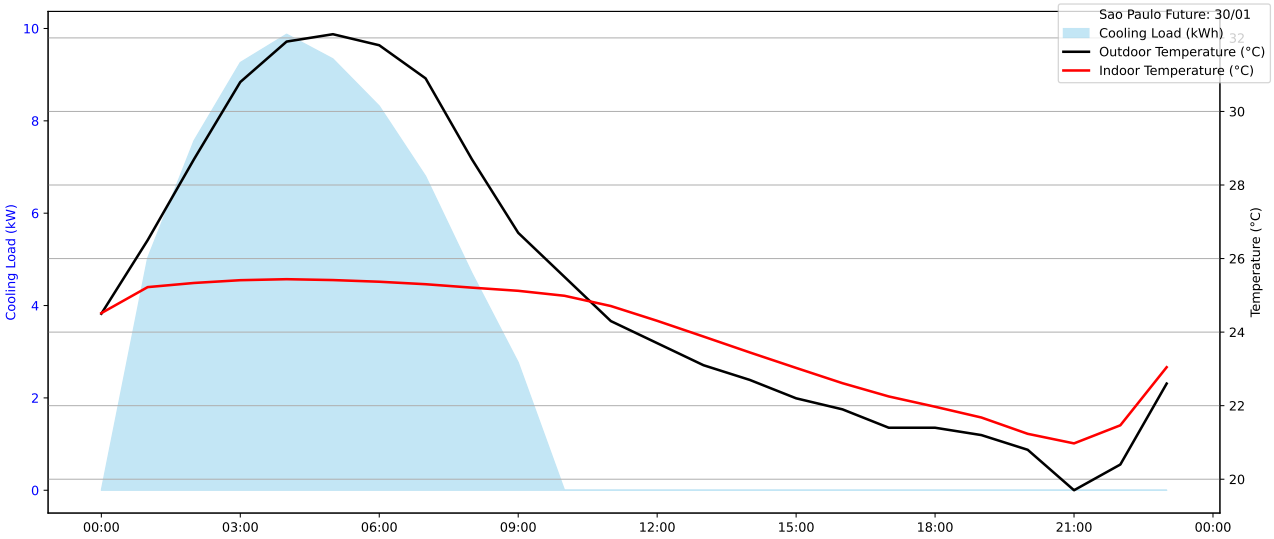

Figure 56: Future daily cooling load and temperatures in Sao Paulo on January 30^{th}.

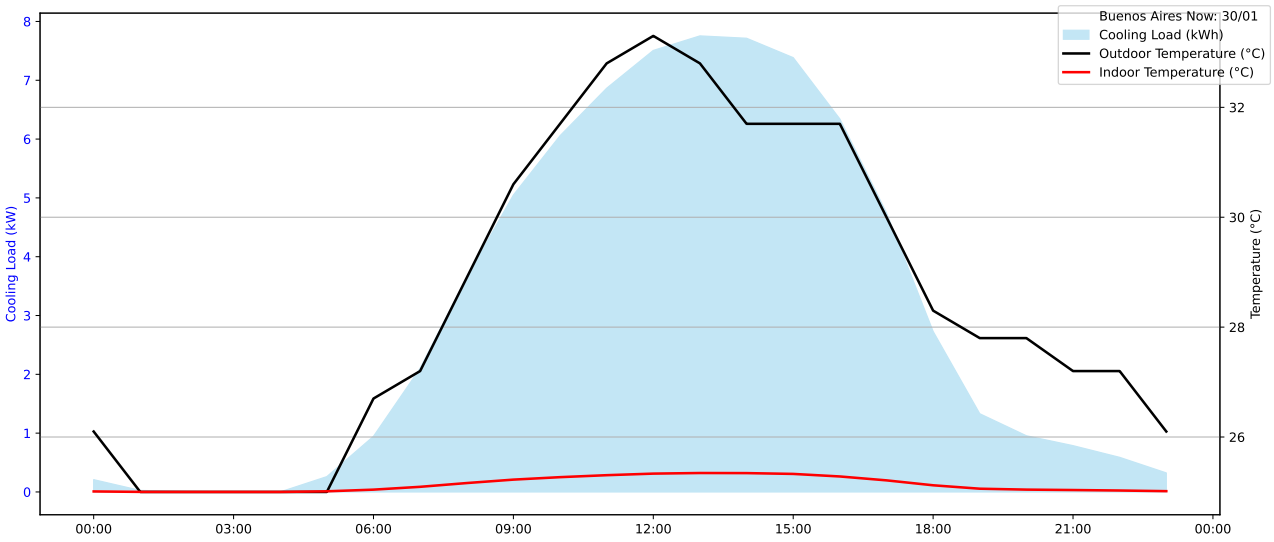

Figure 57: Present daily cooling load and temperatures in Buenos Aires on January 30^{th}.

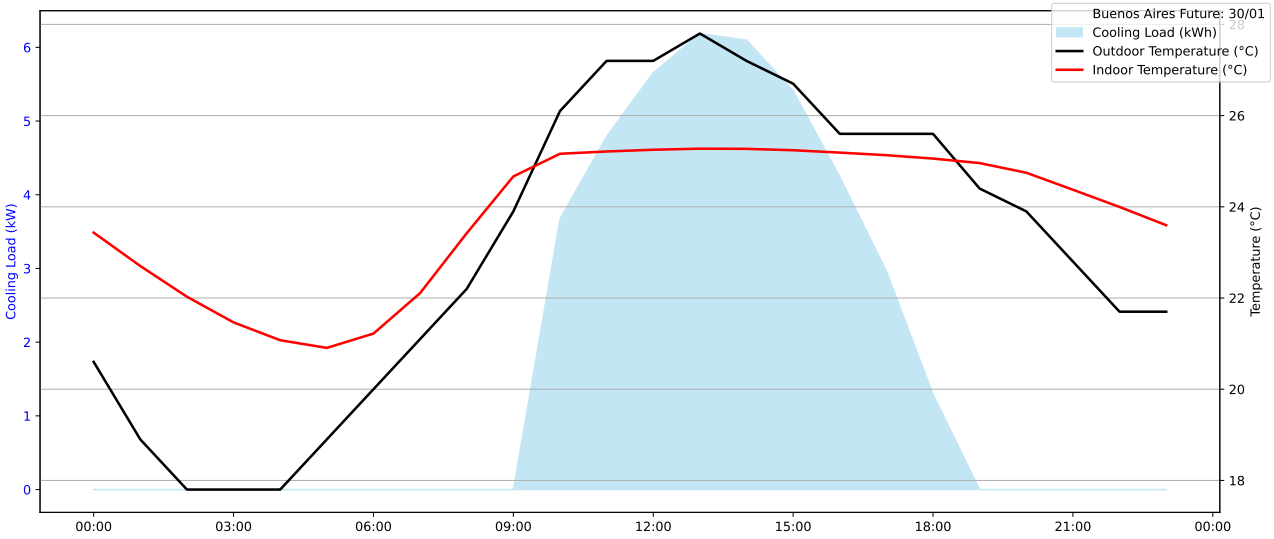

Figure 58: Future daily cooling load and temperatures in Buenos Aires on January 30^{th}.

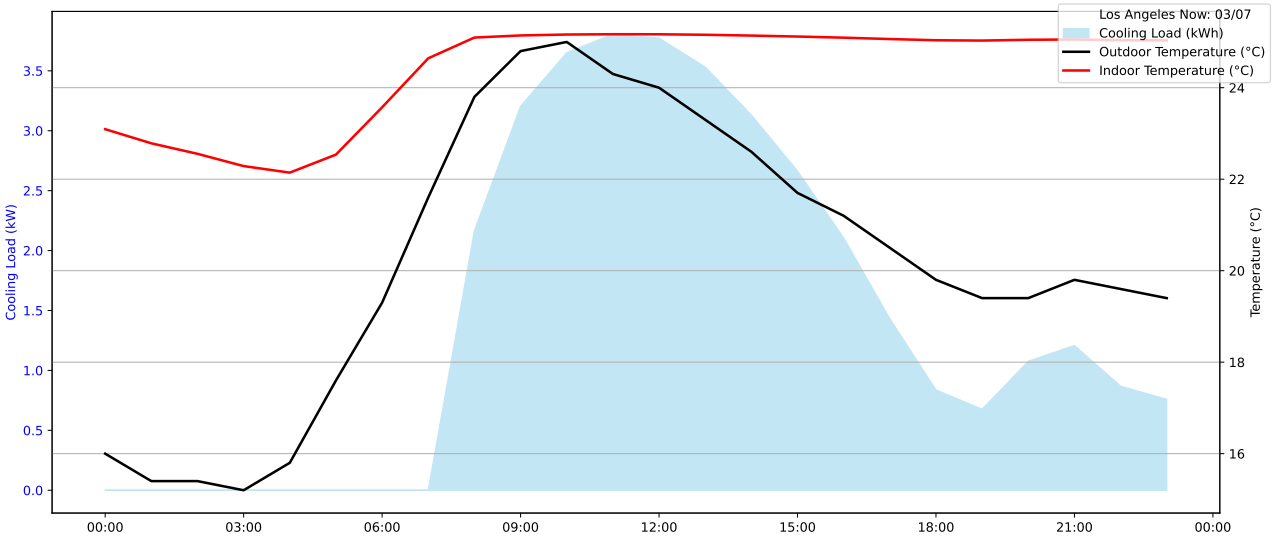

Figure 59: Present daily cooling load and temperatures in Los Angeles on July 3^{rd}.

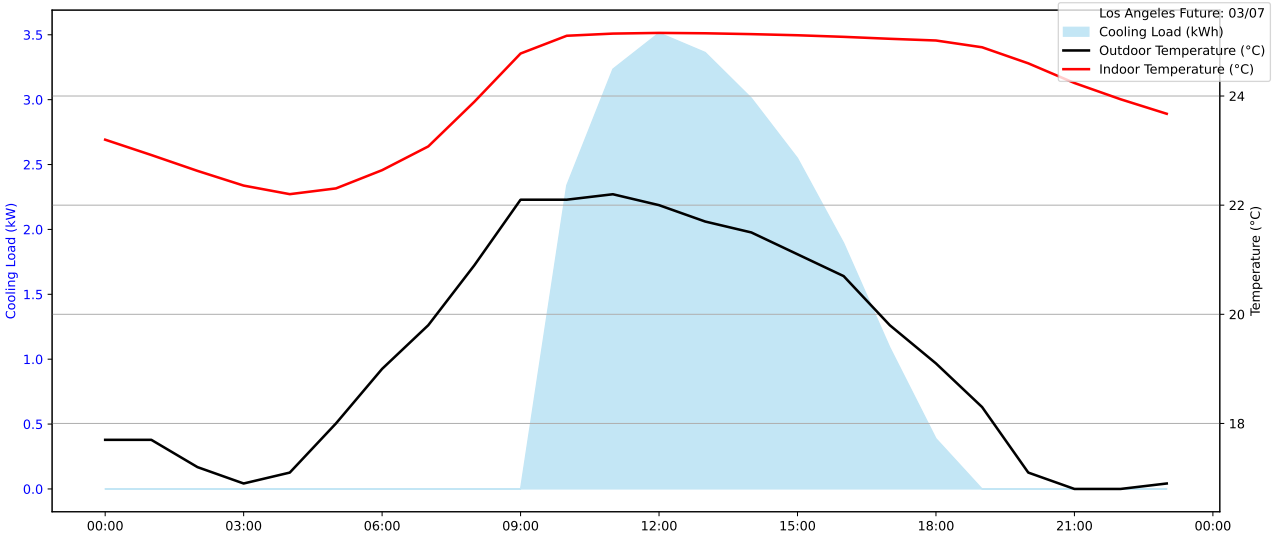

Figure 60: Future daily cooling load and temperatures in Los Angeles on July 3^{rd}.

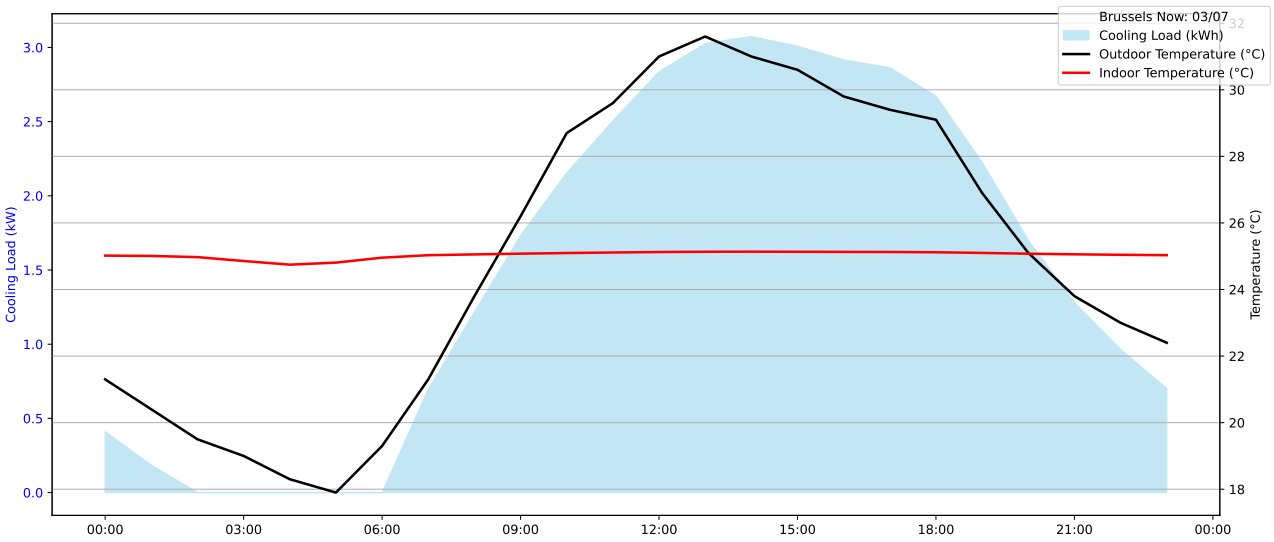

Figure 61: Present daily cooling load and temperatures in Brussels on July 3^{rd}.

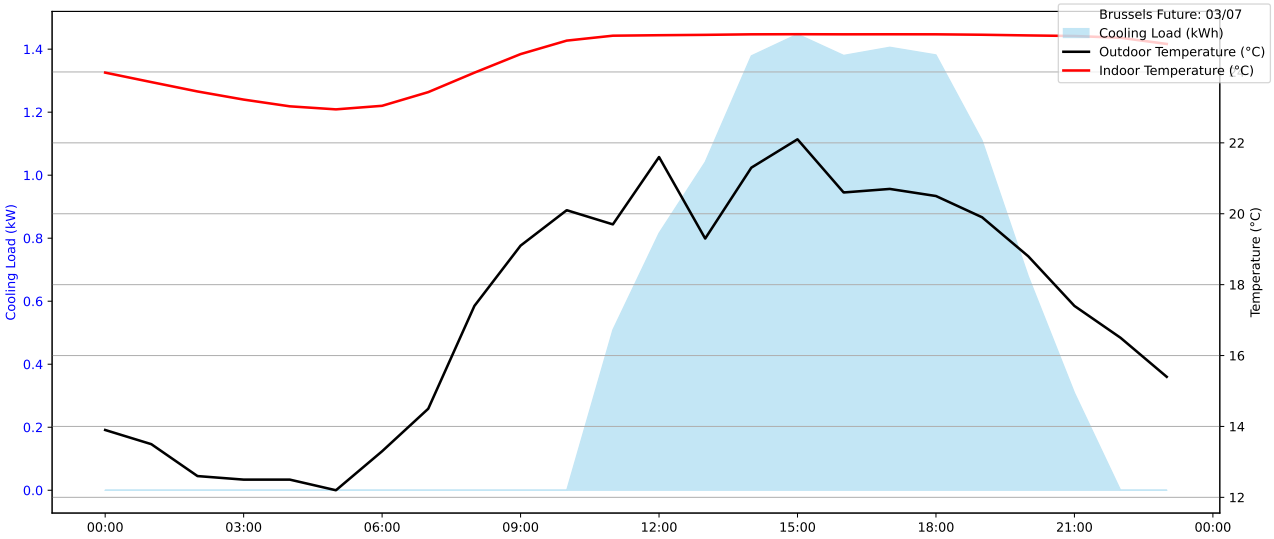

Figure 62: Future daily cooling load and temperatures in Brussels on July 3^{rd}.

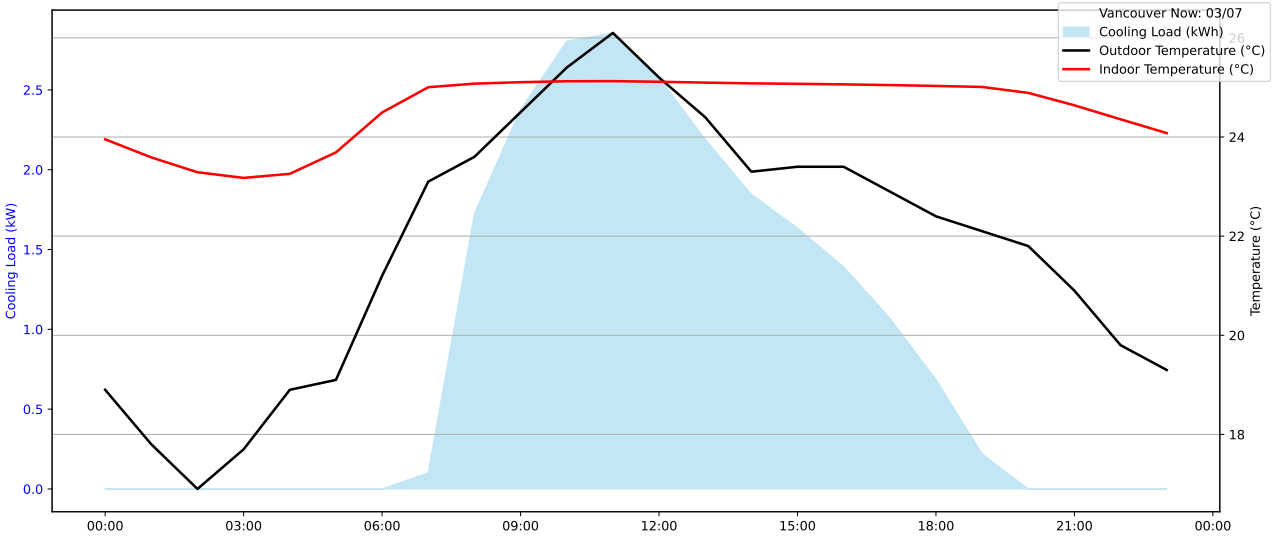

Figure 63: Present daily cooling load and temperatures in Vancouver on July 3^{rd}.

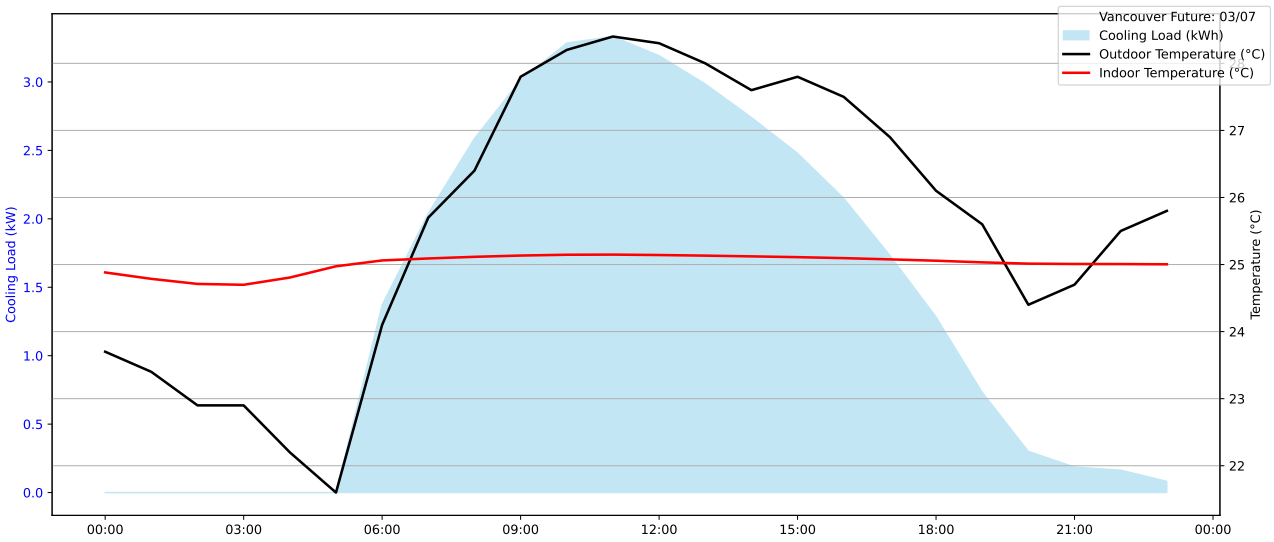

Figure 64: Future daily cooling load and temperatures in Vancouver on July 3^{rd}.

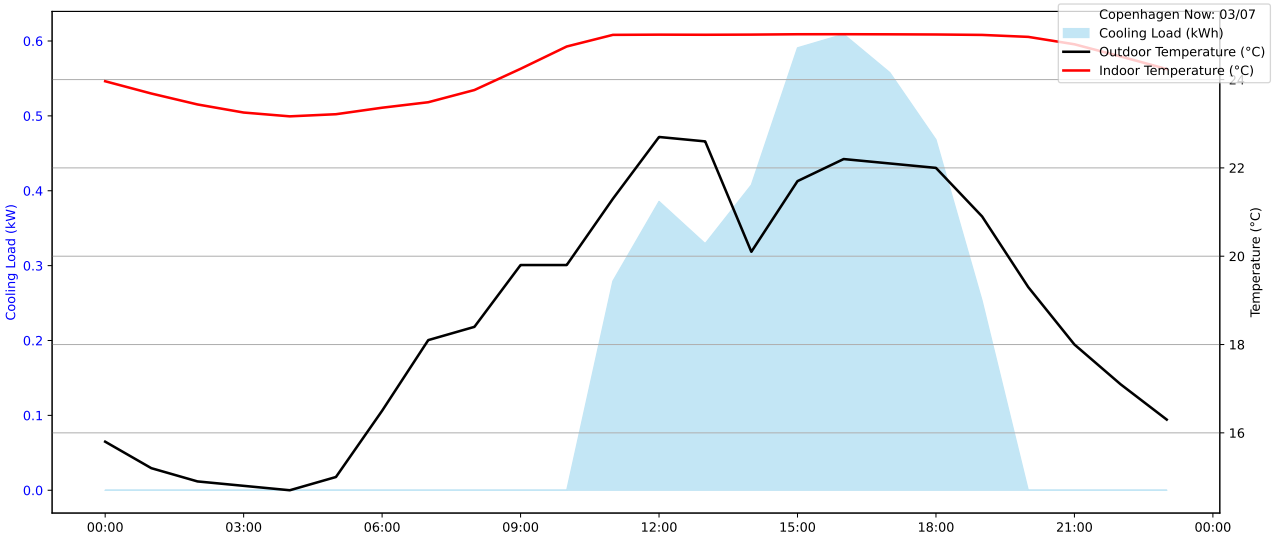

Figure 65: Present daily cooling load and temperatures in Copenhagen on July 3^{rd}.

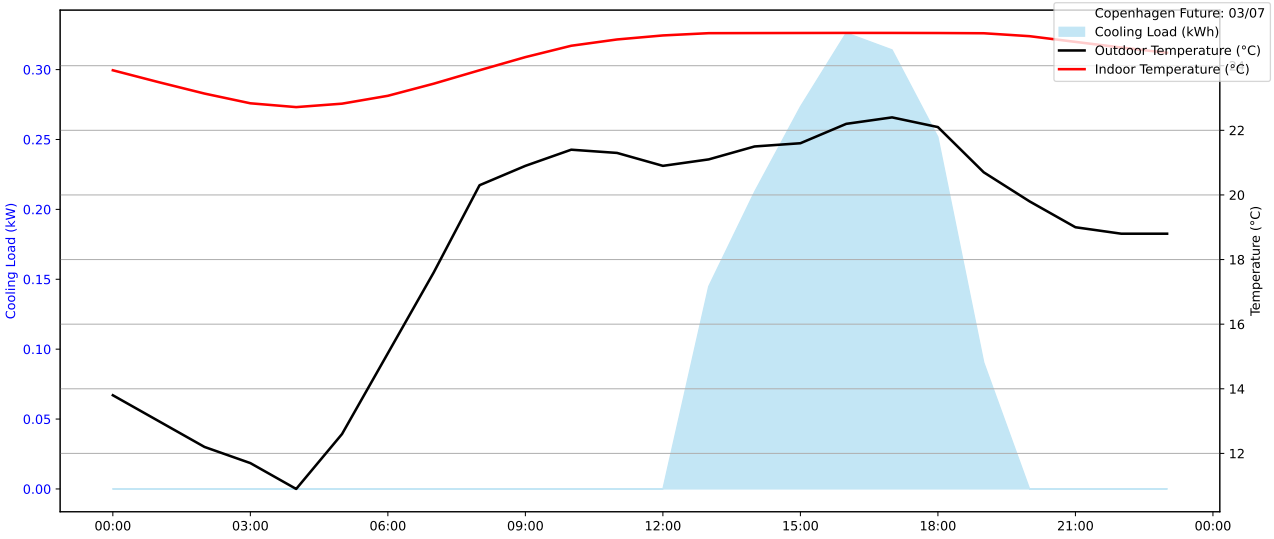

Figure 66: Future daily cooling load and temperatures in Copenhagen on July 3^{rd}.

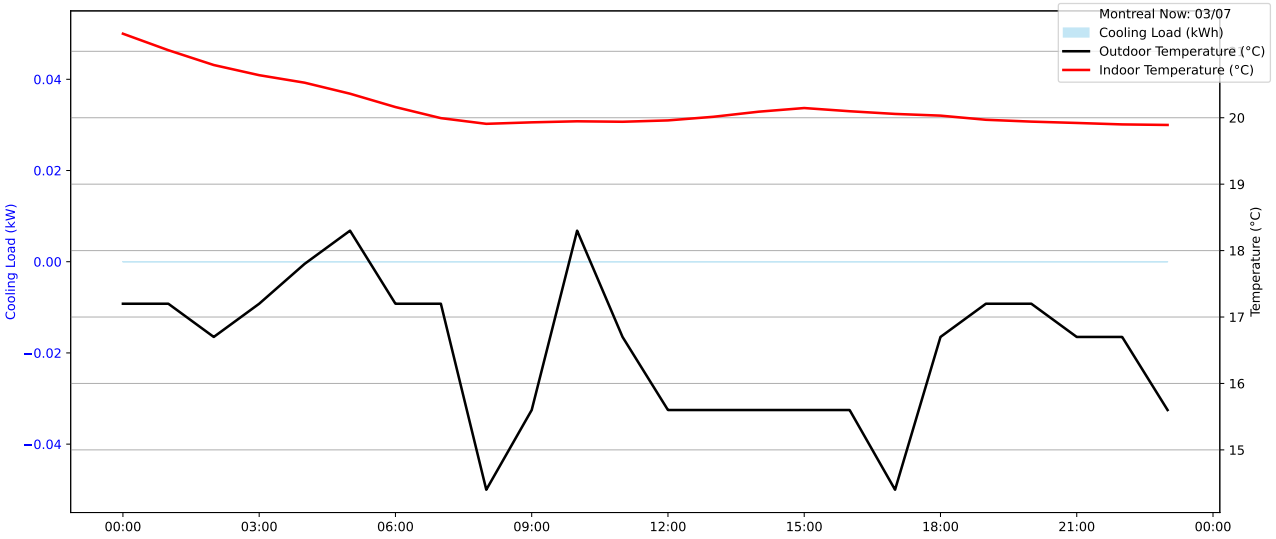

Figure 67: Present daily cooling load and temperatures in Montreal on July 3^{rd}.

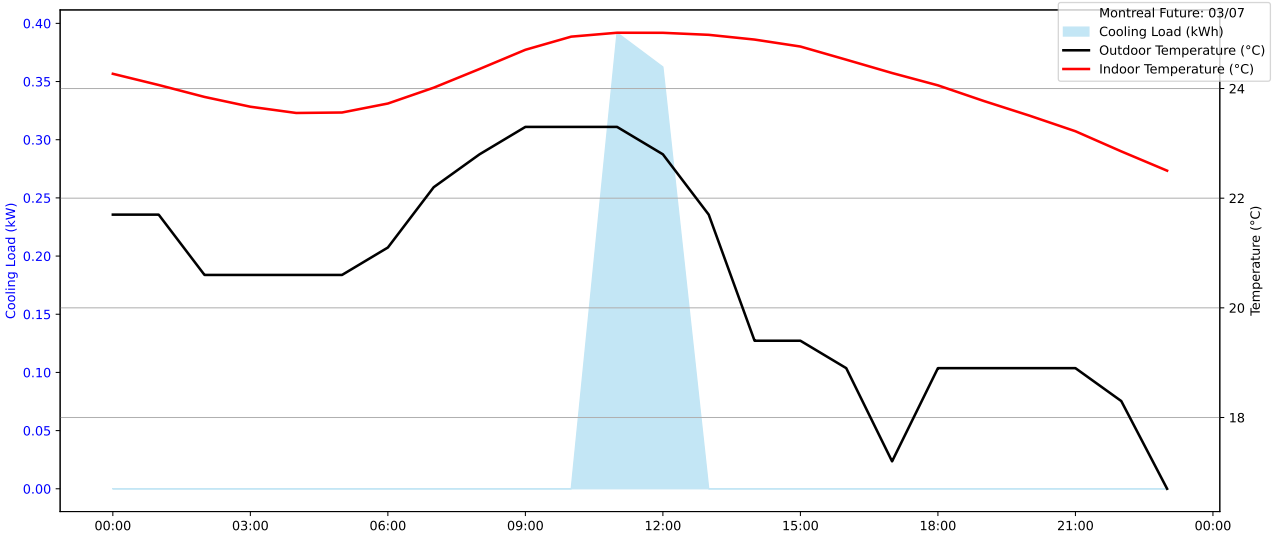

Figure 68: Future daily cooling load and temperatures in Montreal on July 3^{rd}.

References

[1] United Nations. *Population*. United Nations. Publisher: United Nations. URL: https://www.un.org/en/global-issues/population (visited on 02/12/2025).

[2] Ministère de la transition écologique français. *Émissions de CO2 hors UTCATF dans le monde*. Consulted the: 22 November 2024. URL: https://www.statistiques.developpement-durable.gouv.fr/edition-numerique/chiffres-cles-du-climat-2022/6-emissions-de-co2-hors-utcatf.

[3] GIEC. *Changements Climatiques 2014, rapport de synthèse*. Consulted the: 21 November 2024. 2014. URL: https://www.ipcc.ch/site/assets/uploads/2018/02/SYR_AR5_FINAL_full_fr.pdf.

[4] *Réchauffement planétaire*. Klimaat | Climat. URL: https://climat.be/changements-climatiques/changements-observes/rechauffement-planetaire (visited on 02/12/2025).

[5] Katherine Calvin et al. *IPCC, 2023: Climate Change 2023: Synthesis Report. Contribution of Working Groups I, II and III to the Sixth Assessment Report of the Intergovernmental Panel on Climate Change [Core Writing Team, H. Lee and J. Romero (eds.)]. IPCC, Geneva, Switzerland.* Edition: First. Intergovernmental Panel on Climate Change (IPCC), July 25, 2023. DOI: 10.59327/IPCC/AR6-9789291691647. URL: https://www.ipcc.ch/report/ar6/syr/ (visited on 02/12/2025).

[6] *Energy statistics - an overview*. URL: https://ec.europa.eu/eurostat/statistics-explained/index.php?title=Energy_statistics_-_an_overview (visited on 02/12/2025).

[7] *Final energy consumption by energy sector in EU | ODYSSEE-MURE*. URL: https://www.odyssee-mure.eu/publications/efficiency-by-sector/overview/final-energy-consumption-by-sector.html (visited on 02/17/2025).

[8] *EU-27: GHG emissions breakdown by sector*. Statista. URL: https://www.statista.com/statistics/1325132/ghg-emissions-shares-sector-european-union-eu/ (visited on 02/17/2025).

[9] eurostat. *Final energy consumption*. Consulted the: 21 November 2024. URL: https://ec.europa.eu/eurostat/statistics-explained/index.php?title=Energy_statistics_-_an_overview.

[10] *The Future of Cooling – Analysis*. IEA. May 15, 2018. URL: https://www.iea.org/reports/the-future-of-cooling (visited on 05/06/2025).

[11] Dr Fatih Birol. "The Future of Cooling". In: (2018).

[12] Mat Santamouris. "Cooling the buildings – past, present and future". In: *Energy and Buildings* 128 (Sept. 15, 2016), pp. 617–638. ISSN: 0378-7788. DOI: 10.1016/j.enbuild.2016.07.034. URL: https://www.sciencedirect.com/science/article/pii/S0378778816306314 (visited on 05/06/2025).

[13] David M. Ward. "The effect of weather on grid systems and the reliability of electricity supply". In: *Climatic Change* 121.1 (Nov. 1, 2013), pp. 103–113. ISSN: 1573-1480. DOI: 10.1007/s10584-013-0916-z. URL: https://doi.org/10.1007/s10584-013-0916-z.

[14] Ramin Rahif. “Impact of Climate Change on High-Performance Belgian Houses: Thermal Comfort, HVAC Energy Performance, and HVAC GHG Emissions”. In: (Sept. 15, 2023). Publisher: ULiège - University of Liège [Applied Sciences], Liege, Belgium. URL: https://orbi.uliege.be/handle/2268/303336 (visited on 03/11/2025).

[15] John T. Hardy. *Climate Change: Causes, Effects, and Solutions*. Google-Books-ID: YCijEAAAQBAJ. John Wiley & Sons, June 27, 2003. 281 pp. ISBN: 978-0-470-85019-0.

[16] *layers-atmosphere-Earth-yellow-line-height-response.jpg (1480×1600)*. URL: https://cdn.britannica.com/56/97256-050-C79BB432/layers-atmosphere-Earth-yellow-line-height-response.jpg (visited on 05/01/2025).

[17] OAR US EPA. *Climate Change Indicators: Greenhouse Gases*. Dec. 16, 2015. URL: https://www.epa.gov/climate-indicators/greenhouse-gases (visited on 02/13/2025).

[18] *CO2 equivalents | Climate Change Connection*. Climate Change Connection | Connecting Manitobans to climate change facts and solutions. Aug. 17, 2014. URL: https://climatechangeco
org/emissions/co2-equivalents/ (visited on 02/12/2025).

[19] *What Is the Greenhouse Effect?* NASA Climate Kids. URL: https://climatekids.nasa.gov/greenhouse-effect/ (visited on 02/11/2025).

[20] OAR US EPA. *Ultraviolet (UV) Radiation and Sun Exposure*. Nov. 26, 2018. URL: https://www.epa.gov/radtown/ultraviolet-uv-radiation-and-sun-exposure (visited on 02/11/2025).

[21] *Sunbeds: 3. How can different types of ultraviolet radiation affect health?* URL: https://ec.europa.eu/health/scientific_committees/opinions_layman/en/sunbeds/l-2/3-health-effects-uva-uvb-uvc.htm (visited on 02/11/2025).

[22] *Global Warming*. Publisher: NASA Earth Observatory. June 3, 2010. URL: https://earthobservatory.nasa.gov/features/GlobalWarming/page2.php (visited on 02/11/2025).

[23] *The Sun’s impact on the Earth*. World Meteorological Organization. Mar. 21, 2023. URL: https://wmo.int/suns-impact-earth (visited on 02/11/2025).

[24] *Climate change: evidence and causes | Royal Society*. URL: https://royalsociety.org/news-resources/projects/climate-change-evidence-causes/basics-of-climate-change/ (visited on 02/18/2025).

[25] *Methane | Vital Signs*. Climate Change: Vital Signs of the Planet. URL: https://climate.nasa.gov/vital-signs/methane?intent=121 (visited on 02/12/2025).

[26] Bo Nordell. “Thermal pollution causes global warming”. In: *Global and Planetary Change* 38.3 (Sept. 1, 2003), pp. 305–312. ISSN: 0921-8181. DOI: 10.1016/S0921-8181(03)00113-9. URL: https://www.sciencedirect.com/science/article/pii/S0921818103001139 (visited on 02/07/2025).

[27] NASA Global Climate Change. *Carbon Dioxide Concentration | NASA Global Climate Change*. Climate Change: Vital Signs of the Planet. URL: https://climate.nasa.gov/vital-signs/carbon-dioxide?intent=121 (visited on 02/11/2025).

[28] NASA Global Climate Change. *Carbon Dioxide Concentration | NASA Global Climate Change*. Climate Change: Vital Signs of the Planet. URL: https://climate.nasa.gov/vital-signs/carbon-dioxide?intent=121 (visited on 05/01/2025).

[29] *WMO confirms 2024 as warmest year on record at about 1.55°C above pre-industrial level*. World Meteorological Organization. Jan. 10, 2025. URL: https://wmo.int/news/media-centre/wmo-confirms-2024-warmest-year-record-about-155degc-above-pre-industrial-level (visited on 02/11/2025).

[30] NASA Global Climate Change. *Global Surface Temperature | NASA Global Climate Change*. Climate Change: Vital Signs of the Planet. URL: https://climate.nasa.gov/vital-signs/global-temperature?intent=121 (visited on 02/12/2025).

[31] United Nations. *What Is Climate Change?* United Nations. Publisher: United Nations. URL: https://www.un.org/en/climatechange/what-is-climate-change (visited on 02/12/2025).

[32] *The Ozone Layer | Center for Science Education*. URL: https://scied.ucar.edu/learning-zone/atmosphere/ozone-layer (visited on 02/18/2025).

[33] *What is the current state of the ozone layer?* Dec. 5, 2024. URL: https://www.eea.europa.eu/en/topics/in-depth/climate-change-mitigation-reducing-emissions/current-state-of-the-ozone-layer (visited on 02/11/2025).

[34] *Ozone depletion | Facts, Effects, & Solutions | Britannica*. URL: https://www.britannica.com/science/ozone-depletion (visited on 02/17/2025).

[35] U. N. Environment. *About Montreal Protocol*. Oct. 29, 2018. URL: https://www.unep.org/ozonaction/who-we-are/about-montreal-protocol (visited on 02/17/2025).

[36] *World of Change: Antarctic Ozone Hole*. Publisher: NASA Earth Observatory. June 1, 2009. URL: https://earthobservatory.nasa.gov/world-of-change/Ozone (visited on 02/11/2025).

[37] supportadmin@onceinteractive.com. *AC Refrigerant Types: What's In Use Today*. The Cooling Company. Dec. 26, 2023. URL: https://thecoolingco.com/blog/what-types-of-refrigerant-are-used-in-ac-nowadays/ (visited on 02/11/2025).

[38] Karen Mohr. *Aerosols and Their Importance | Earth*. Publisher: 610 Web Dev. URL: https://earth.gsfc.nasa.gov/climate/data/deep-blue/aerosols (visited on 02/12/2025).

[39] *World Bank Open Data*. World Bank Open Data. URL: https://data.worldbank.org (visited on 02/12/2025).

[40] Max Roser et al. "Economic Growth". In: *Our World in Data* (July 14, 2023). URL: https://ourworldindata.org/economic-growth (visited on 02/12/2025).

[41] *World Population Clock: 8.2 Billion People (LIVE, 2025) - Worldometer*. URL: https://www.worldometers.info/world-population/ (visited on 02/12/2025).

[42] Hannah Ritchie et al. "Population Growth". In: *Our World in Data* (July 11, 2023). URL: https://ourworldindata.org/population-growth (visited on 02/12/2025).

[43] *World Population Clock: 8.2 Billion People (LIVE, 2025) - Worldometer*. URL: https://www.worldometers.info/world-population/#growthrate (visited on 02/12/2025).

[44] *Climate change: why the oceans matter*. en-US. URL: https://www.scienceinschool.org/article/2017/climate-change-why-oceans-matter/ (visited on 06/03/2025).

[45] IPCC. *Climate change 2001: Synthesis Report*. URL: https://archive.ipcc.ch/ipccreports/tar/vol4/011.htm (visited on 02/13/2025).

[46] *Earth's Big Heat Bucket*. Publisher: NASA Earth Observatory. Apr. 24, 2006. URL: https://earthobservatory.nasa.gov/features/HeatBucket/heatbucket4.php (visited on 02/13/2025).

[47] John Abraham et al. "The ocean response to climate change guides both adaptation and mitigation efforts". In: *Atmospheric and Oceanic Science Letters* 15.4 (July 1, 2022), p. 100221. ISSN: 1674-2834. DOI: 10.1016/j.aosl.2022.100221. URL: https://www.sciencedirect.com/science/article/pii/S1674283422000964 (visited on 02/13/2025).

[48] Richard J. de Dear and Gail S. Brager. "Thermal comfort in naturally ventilated buildings: revisions to ASHRAE Standard 55". In: *Energy and Buildings*. Special Issue on Thermal Comfort Standards 34.6 (July 1, 2002), pp. 549–561. ISSN: 0378-7788. DOI: 10.1016/S0378-7788(02)00005-1. URL: https://www.sciencedirect.com/science/article/pii/S0378778802000051 (visited on 05/06/2025).

[49] *Standard 55 – Thermal Environmental Conditions for Human Occupancy*. URL: https://www.ashrae.org/technical-resources/bookstore/standard-55-thermal-environmental-conditions-for-human-occupancy (visited on 05/06/2025).

[50] Cong Song et al. "Effects of phased sleeping thermal environment regulation on human thermal comfort and sleep quality". In: *Building and Environment* 181 (Aug. 15, 2020), p. 107108. ISSN: 0360-1323. DOI: 10.1016/j.buildenv.2020.107108. URL: https://www.sciencedirect.com/science/article/pii/S0360132320304832 (visited on 05/06/2025).

[51] D. Lush, K. Butcher, and P. Appleby. "Environmental design: CIBSE Guide A". In: (Oct. 1, 1999). URL: https://www.osti.gov/etdeweb/biblio/20133944 (visited on 05/06/2025).

[52] Faith S. Luyster et al. "Sleep: A Health Imperative". In: *Sleep* 35.6 (June 1, 2012), pp. 727–734. ISSN: 0161-8105. DOI: 10.5665/sleep.1846. URL: https://doi.org/10.5665/sleep.1846 (visited on 05/06/2025).

[53] Mark R. Rosekind. "Underestimating the societal costs of impaired alertness: safety, health and productivity risks". In: *Sleep Medicine*. The Art of Goods Sleep. Proceedings of the 2nd International Sleep Disorders Forum. A yearly event made possible by sanofi-aventis 6 (Jan. 1, 2005), S21–S25. ISSN: 1389-9457. DOI: 10.1016/S1389-9457(05)80005-X. URL: https://www.sciencedirect.com/science/article/pii/S138994570580005X (visited on 05/06/2025).

[54] *Working Memory: Theories, Models, and Controversies | Annual Reviews*. URL: https://www.annualreviews.org/content/journals/10.1146/annurev-psych-120710-100422 (visited on 05/06/2025).

[55] Olli Seppanen, William J Fisk, and Q H Lei. "Effect of temperature on task performance in office environment". In: ().

[56] Pawel Wargocki, Jose Ali Porras-Salazar, and Sergio Contreras-Espinoza. "The relationship between classroom temperature and children's performance in school". In: *Building and Environment* 157 (June 15, 2019), pp. 197–204. ISSN: 0360-1323. DOI: 10.1016/j.buildenv.2019.04.046. URL: https://www.sciencedirect.com/science/article/pii/S0360132319302987 (visited on 05/06/2025).

[57] Pawel Wargocki et al. “Perceived Air Quality, Sick Building Syndrome (SBS) Symptoms and Productivity in an Office with Two Different Pollution Loads.” In: *Indoor Air* 9.3 (Sept. 1, 1999). Publisher: Wiley-Blackwell, p. 165. ISSN: 0905-6947. DOI: 10.1111/j.1600-0668.1999.t01-1-00003.x. URL: https://research.ebsco.com/linkprocessor/plink?id=ae04c0c2-0945-3fa7-bda4-d5d1fd3887f7 (visited on 05/06/2025).

[58] *Research Report on Effects of HVAC On Student Performance - ProQuest*. URL: https://www.proquest.com/openview/cfe6ee40439b3a263f7a7523dc89af77/1?cbl=41118&pq-origsite=gscholar (visited on 05/06/2025).

[59] Paul Roelofsen. “The impact of office environments on employee performance: The design of the workplace as a strategy for productivity enhancement productivity enhancement”. In: *Journal of Facilities Management* 1.3 (Jan. 1, 2002). Publisher: MCB UP Ltd, pp. 247–264. ISSN: 1472-5967. DOI: 10.1108/14725960310807944. URL: https://doi.org/10.1108/14725960310807944 (visited on 05/06/2025).

[60] Stephen Phillips. “Working through the pandemic: Accelerating the transition to remote working”. In: *Business Information Review* 37.3 (Sept. 1, 2020). Publisher: SAGE Publications Ltd, pp. 129–134. ISSN: 0266-3821. DOI: 10.1177/0266382120953087. URL: https://doi.org/10.1177/0266382120953087 (visited on 05/06/2025).

[61] *Heatwaves*. URL: https://www.who.int/health-topics/heatwaves (visited on 02/14/2025).

[62] Daniela D’Ippoliti et al. “The impact of heat waves on mortality in 9 European cities: results from the EuroHEAT project”. In: *Environmental Health* 9.1 (July 16, 2010), p. 37. ISSN: 1476-069X. DOI: 10.1186/1476-069X-9-37. URL: https://doi.org/10.1186/1476-069X-9-37 (visited on 05/06/2025).

[63] NASA Global Climate Change. *Sea Level | NASA Global Climate Change*. Climate Change: Vital Signs of the Planet. URL: https://climate.nasa.gov/vital-signs/sea-level?intent=121 (visited on 02/14/2025).

[64] *Thermal Expansion of Solids and Liquids | Physics*. URL: https://courses.lumenlearning.com/suny-physics/chapter/13-2-thermal-expansion-of-solids-and-liquids/ (visited on 02/14/2025).

[65] *NASA Sea Level Change Portal: Thermal Expansion*. NASA Sea Level Change Portal. URL: https://sealevel.nasa.gov/understanding-sea-level/global-sea-level/thermal-expansion (visited on 02/14/2025).

[66] National Oceanic {and} Atmospheric Administration US Department of Commerce. *What is Ocean Acidification?* URL: https://oceanservice.noaa.gov/facts/acidification.html (visited on 02/14/2025).

[67] *What is Ocean Acidification?* Publisher: IAEA. June 8, 2022. URL: https://www.iaea.org/newscenter/news/what-is-ocean-acidification (visited on 02/14/2025).

[68] *Impacts des activités économiques sur la biodiversité marine : quels outils de mesure et quelles limites ? | Carbone 4*. URL: https://carbone4.com/fr/analyse-impact-activite-economique-biodiversite-marine (visited on 02/18/2025).

[69] *Océan & climat | Ifremer*. URL: https://www.ifremer.fr/fr/ocean-climat (visited on 02/14/2025).

[70] National Oceanic {and} Atmospheric Administration US Department of Commerce. *How do hurricanes form?* URL: https://oceanservice.noaa.gov/facts/how-hurricanes-form.html (visited on 02/14/2025).

[71] OAR US EPA. *Climate Change Indicators: Heat Waves*. Feb. 4, 2021. URL: https://www.epa.gov/climate-indicators/climate-change-indicators-heat-waves (visited on 02/14/2025).

[72] *European heat wave of 2003 | 2003 Heatwave, Record Temperatures, France | Britannica*. URL: https://www.britannica.com/event/European-heat-wave-of-2003 (visited on 02/14/2025).

[73] F. Gemenne. *Climate geopolitics. Negotiations, strategies, impacts*. Editions Armand Colin. URL: https://inis.iaea.org/records/b889q-xxp39 (visited on 02/14/2025).

[74] NASA Global Climate Change. *Ice Sheets | NASA Global Climate Change*. Climate Change: Vital Signs of the Planet. URL: https://climate.nasa.gov/vital-signs/ice-sheets?intent=121 (visited on 02/14/2025).

[75] NASA Global Climate Change. *Arctic Sea Ice Minimum | NASA Global Climate Change*. Climate Change: Vital Signs of the Planet. URL: https://climate.nasa.gov/vital-signs/arctic-sea-ice?intent=121 (visited on 02/14/2025).

[76] OAR US EPA. *Climate Change Indicators: Permafrost*. Mar. 18, 2021. URL: https://www.epa.gov/climate-indicators/climate-change-indicators-permafrost (visited on 02/14/2025).

[77] *Thawing permafrost*. WWF Arctic. URL: https://www.arcticwwf.org/the-circle/stories/thawing-permafrost/ (visited on 02/14/2025).

[78] *Arctic permafrost is thawing fast. That affects us all.* Environment. Section: Environment. Aug. 13, 2019. URL: https://www.nationalgeographic.com/environment/article/arctic-permafrost-is-thawing-it-could-speed-up-climate-change-feature (visited on 02/14/2025).

[79] *Why Frozen Ground Matters*. National Snow and Ice Data Center. URL: https://nsidc.org/learn/parts-cryosphere/frozen-ground-permafrost/why-frozen-ground-matters (visited on 02/14/2025).

[80] *2023 Annual Report*. Rainforest Alliance. URL: https://www.rainforest-alliance.org/annual_report/2023/ (visited on 02/17/2025).

[81] *Deforestation in the Amazon*. Amazon Conservation Association. URL: https://www.amazonconservation.org/the-challenge/threats/ (visited on 02/17/2025).

[82] Sibélia Zanon. *Deforestation in the Amazon: past, present and future*. InfoAmazonia. Mar. 21, 2023. URL: http://infoamazonia.org/en/2023/03/21/deforestation-in-the-amazon-past-present-and-future/ (visited on 02/17/2025).

[83] *L'Accord de Paris | CCNUCC*. URL: https://unfccc.int/fr/a-propos-des-ndcs/l-accord-de-paris (visited on 02/13/2025).

[84] *Global Warming of 1.5 ºC —*. URL: https://www.ipcc.ch/sr15/ (visited on 02/13/2025).

[85] R. K. Pachauri, Leo Mayer, and Intergovernmental Panel on Climate Change, eds. *Climate change 2014: synthesis report*. Geneva, Switzerland: Intergovernmental Panel on Climate Change, 2015. 151 pp. ISBN: 978-92-9169-143-2.

[86] "ANSI/ASHRAE Addendum a to ANSI/ASHRAE Standard 169-2020". In: ().

[87] J. M. FINKELSTEIN and R. E. SCHAFER. "Improved goodness-of-fit tests". In: *Biometrika* 58.3 (Dec. 1, 1971), pp. 641–645. ISSN: 0006-3444. DOI: 10.1093/biomet/58.3.641. URL: https://doi.org/10.1093/biomet/58.3.641 (visited on 04/17/2025).

[88] Alanis Zeoli et al. *Feasibility Analysis of Desiccant Evaporative Cooling Technologies in Various Climate Conditions: Present and Future Potential*. Rochester, NY, Dec. 27, 2024. DOI: 10.2139/ssrn.5073756. URL: https://papers.ssrn.com/abstract=5073756 (visited on 05/05/2025).

[89] *IEA EBC || Annex 80 || Resilient Cooling || IEA EBC || Annex 80*. URL: https://annex80.iea-ebc.org/ (visited on 05/05/2025).

[90] *IEA – International Energy Agency*. IEA. URL: https://www.iea.org (visited on 05/05/2025).

[91] Sébastien Doutreloup et al. "Historical and future weather data for dynamic building simulations in Belgium using the regional climate model MAR: typical and extreme meteorological year and heatwaves". In: *Earth System Science Data* 14.7 (July 6, 2022). Publisher: Copernicus GmbH, pp. 3039–3051. ISSN: 1866-3508. DOI: 10.5194/essd-14-3039-2022. URL: https://essd.copernicus.org/articles/14/3039/2022/ (visited on 04/16/2025).

[92] NOAA US Department of Commerce. *What Are Heating and Cooling Degree Days*. EN-US. Publisher: NOAA's National Weather Service. URL: https://www.weather.gov/key/climate_heat_cool (visited on 05/26/2025).

[93] *Refroidissement actif*. In: *Wikipédia*. Page Version ID: 223988493. Mar. 17, 2025. URL: https://fr.wikipedia.org/w/index.php?title=Refroidissement_actif&oldid=223988493 (visited on 05/06/2025).

[94] G. Masy et al. "Lessons Learned from Heat Balance Analysis for Holzkirchen Twin Houses Experiment". In: *Energy Procedia*. 6th International Building Physics Conference, IBPC 2015 78 (Nov. 1, 2015), pp. 3270–3275. ISSN: 1876-6102. DOI: 10.1016/j.egypro.2015.11.718. URL: https://www.sciencedirect.com/science/article/pii/S1876610215024509 (visited on 05/12/2025).

[95] Anne-Laure Robert. *Chauffage à la maison : pour le calcul de vos besoins, c'est ici !* fr-FR. Feb. 2022. URL: https://www.sowee.fr/conseils/chauffage-connecte/chauffage-a-la-maison-pour-le-calcul-de-vos-besoins-c-est-ici/ (visited on 06/01/2025).

[96] >*Comment calculer la puissance de son chauffage ?* fr-FR. URL: https://www.izi-by-edf-renov.fr/blog/quelle-puissance-chauffage-par-metre-carre (visited on 06/01/2025).

[97] *Guide : quelle puissance de radiateur par m2 choisir ? | ENGIE*. fr-FR. URL: https://particuliers.engie.fr/depannages-services/conseils-equipements-chauffage/conseils-radiateurs/quelle-puissance-radiateur-par-m2.html (visited on 06/01/2025).

[98] *Calcul des déperditions thermiques et de la puissance de chauffe*. URL: https://www.cedeo.fr/conseils/comment-calculer-les-deperditions-thermiques-et-la-puissance-de-chauffe-dun-batiment (visited on 06/01/2025).

[99] *Climatisation : comment évaluer la puissance nécessaire ?* fr. URL: https://www.climatisationreversible.net/climatisation-bien-evaluer-la-puissance-necessaire.htm (visited on 06/01/2025).

[100] *ChatGPT*. URL: https://chatgpt.com (visited on 05/15/2025).

[101] Paul Strachan et al. "Whole model empirical validation on a full-scale building". In: *Journal of Building Performance Simulation* 9.4 (July 2016). Publisher: Taylor & Francis, pp. 331–350. DOI: 10.1080/19401493.2015.1064480. URL: https://doi.org/10.1080/19401493.2015.1064480 (visited on 05/12/2025).

[102] Jeff S Haberl, Charles Culp, and David E Claridge. “ASHRAE’s GUIDELINE 14-2002 FOR MEASUREMENT OF ENERGY AND DEMAND SAVINGS: HOW TO DETERMINE WHAT WAS REALLY SAVED BY THE RETROFIT.” In: (2005).

[103] Daniel Coakley, Paul Raftery, and Marcus Keane. “A review of methods to match building energy simulation models to measured data”. In: *Renewable and Sustainable Energy Reviews* 37 (Sept. 1, 2014), pp. 123–141. ISSN: 1364-0321. DOI: 10.1016/j.rser.2014.05.007. URL: https://www.sciencedirect.com/science/article/pii/S1364032114003232 (visited on 05/19/2025).

[104] “M&V Guidelines: Measurement and Verification for Federal Energy Projects”. In: ().

[105] Enrico Fabrizio and Valentina Monetti. “Methodologies and Advancements in the Calibration of Building Energy Models”. In: *Energies* 8.4 (Apr. 2015). Number: 4 Publisher: Multidisciplinary Digital Publishing Institute, pp. 2548–2574. ISSN: 1996-1073. DOI: 10.3390/en8042548. URL: https://www.mdpi.com/1996-1073/8/4/2548 (visited on 05/19/2025).

[106] Hui Yie Teh, Andreas W. Kempa-Liehr, and Kevin I-Kai Wang. “Sensor data quality: a systematic review”. In: *Journal of Big Data* 7.1 (Feb. 11, 2020), p. 11. ISSN: 2196-1115. DOI: 10.1186/s40537-020-0285-1. URL: https://doi.org/10.1186/s40537-020-0285-1 (visited on 05/26/2025).

[107] Pamela Berkeley, Philip Haves, and Erik Kolderup. “IMPACT OF MODELER DECISIONS ON SIMULATION RESULTS”. In: ().

[108] Maxime Trocmé and Bruno Peuportier. “Analyse de cycle de vie d’un bâtiment”. In: *J3eA* 7 (2008), p. 0001. ISSN: 1638-5705. DOI: 10.1051/j3ea:2008034. URL: http://www.j3ea.org/10.1051/j3ea:2008034 (visited on 05/26/2025).

[109] *Average home sizes: living space per person?* en-US. URL: https://thundersaidenergy.com/downloads/average-home-sizes/ (visited on 06/01/2025).

[110] *House Size by Country 2025*. en. URL: https://worldpopulationreview.com/country-rankings/house-size-by-country?utm_source=chatgpt.com (visited on 06/01/2025).

[111] *Understanding Standard Wall Height for Homes*. URL: https://www.coohom.com/article/standard-wall-height?utm_source=chatgpt.com (visited on 06/01/2025).

[112] Wang Liping and Wong Nyuk Hien. *(PDF) The impact of façade designs: Orientations, window to wall ratios and shading devices on indoor environment for naturally ventilated residential buildings in Singapore*. ResearchGate. URL: https://www.researchgate.net/publication/237476905_The_impact_of_facade_designs_Orientations_window_to_wall_ratios_and_shading_devices_on_indoor_environment_for_naturally_ventilated_residential_buildings_in_Singapore (visited on 05/30/2025).

[113] Abdullah Khalid Abdullah et al. “Thermal Performance Evaluation of Window Shutters for Residential Buildings: A Case Study of Abu Dhabi, UAE”. In: *Energies* 15.16 (Jan. 2022). Number: 16 Publisher: Multidisciplinary Digital Publishing Institute, p. 5858. ISSN: 1996-1073. DOI: 10.3390/en15165858. URL: https://www.mdpi.com/1996-1073/15/16/5858 (visited on 05/30/2025).

[114] Fang'ai Chi et al. "An investigation of optimal window-to-wall ratio based on changes in building orientations for traditional dwellings". In: *Solar Energy* 195 (Jan. 1, 2020), pp. 64–81. ISSN: 0038-092X. DOI: 10.1016/j.solener.2019.11.033. URL: https://www.sciencedirect.com/science/article/pii/S0038092X19311429 (visited on 05/30/2025).

[115] Leticia Neves. "(PDF) Building Envelope Energy Performance of High-rise Office buildings in Sao Paulo City, Brazil". In: *ResearchGate* (). DOI: 10.1016/j.proenv.2017.03.167. URL: https://www.researchgate.net/publication/316049141_Building_Envelope_Energy_Performance_of_High-rise_Office_buildings_in_Sao_Paulo_City_Brazil (visited on 05/30/2025).

[116] *Window-to-Wall Ratio*. Building Thermal Rating Assessors. Aug. 19, 2024. URL: https://vstarenergy.com.au/2024/08/19/window-to-wall-ratio/ (visited on 05/30/2025).

[117] Laure Michelon and Brian Stern. *Balancing energy efficiency and aesthetics at Wilshire Grand*. Consulting - Specifying Engineer. Accessed on 2025-05-30. Feb. 2017. URL: https://www.csemag.com/balancing-energy-efficiency-and-aesthetics-at-wilshire-grand/.

[118] Kaiser Ahmed and Jarek Kurnitski. "New Equation for Optimal Insulation Dependency on the Climate for Office Buildings". In: *Energies* 14.2 (Jan. 2021). Number: 2 Publisher: Multidisciplinary Digital Publishing Institute, p. 321. ISSN: 1996-1073. DOI: 10.3390/en14020321. URL: https://www.mdpi.com/1996-1073/14/2/321 (visited on 05/30/2025).

[119] JELD-WEN Canada. *Windows in the Spotlight: Building Code Changes 101 | JELD-WEN Windows & Doors*. URL: https://www.jeld-wen.ca/en-ca/blogs/windows-in-the-spotlight-building-code-changes-101 (visited on 05/31/2025).

[120] Anker Nielsen. "Energy efficient houses in Denmark and moisture conditions in highly insulated constructions - rules, practice and education". In: (Jan. 1, 2015). URL: https://www.academia.edu/113676591/Energy_efficient_houses_in_Denmark_and_moisture_conditions_in_highly_insulated_constructions_rules_practice_and_education (visited on 05/31/2025).

[121] Farid Boudali Errebai et al. "Impact of urban heat island on cooling energy demand for residential building in Montreal using meteorological simulations and weather station observations". In: *Energy and Buildings* 273 (Oct. 15, 2022), p. 112410. ISSN: 0378-7788. DOI: 10.1016/j.enbuild.2022.112410. URL: https://www.sciencedirect.com/science/article/pii/S0378778822005813 (visited on 02/24/2025).

[122] *The Quebec Building Code | AMENDMENTS TO THE CODE*. URL: https://www.buildingcode.online/qbc/9.html (visited on 05/31/2025).

[123] Chong Zhun Min Adrian et al. "Predicting the envelope performance of commercial office buildings in Singapore". In: *Energy and Buildings* 66 (Nov. 2013), pp. 66–76. ISSN: 03787788. DOI: 10.1016/j.enbuild.2013.07.008. URL: https://linkinghub.elsevier.com/retrieve/pii/S0378778813003964 (visited on 05/30/2025).

[124] K.J. Chua and S.K. Chou. "Energy performance of residential buildings in Singapore | Request PDF". In: *ResearchGate* (). DOI: 10.1016/j.energy.2009.10.039. URL: https://www.researchgate.net/publication/222421024_Energy_performance_of_residential_buildings_in_Singapore (visited on 05/30/2025).

[125] *Singapore: Code for Environmental Sustainability of Buildings | Global Buildings Performance Network*. URL: https://library.gbpn.org/library/bc-detail-pages/singapore (visited on 05/30/2025).

[126] K. Tabet Aoul et al. "(PDF) Building Envelope Thermal Defects in Existing and Under-Construction Housing in the UAE; Infrared Thermography Diagnosis and Qualitative Impacts Analysis". In: *ResearchGate* (Apr. 21, 2025). DOI: 10.3390/su13042230. URL: https://www.researchgate.net/publication/349445424_Building_Envelope_Thermal_Defects_in_Existing_and_Under-Construction_Housing_in_the_UAE_Infrared_Thermography_Diagnosis_and_Qualitative_Impacts_Analysis (visited on 05/30/2025).

[127] Carlos Naranjo-Mendoza, Gabriel Vicente Gaona, and Jesus Lopez-Villada. "(PDF) Performance Analysis With Future Predictions of Different Solar Cooling Systems in Guayaquil, Ecuador". In: *ResearchGate*. DOI: 10.1115/ES2014-6594. URL: https://www.researchgate.net/publication/268508153_Performance_Analysis_With_Future_Predictions_of_Different_Solar_Cooling_Systems_in_Guayaquil_Ecuador (visited on 05/30/2025).

[128] Carolina A. Alves, Denise H. S. Duarte, and Fábio L. T. Gonçalves. "Residential buildings' thermal performance and comfort for the elderly under climate changes context in the city of São Paulo, Brazil". In: *Energy and Buildings*. SI: Countermeasures to Urban Heat Island 114 (Feb. 15, 2016), pp. 62–71. ISSN: 0378-7788. DOI: 10.1016/j.enbuild.2015.06.044. URL: https://www.sciencedirect.com/science/article/pii/S0378778815300736 (visited on 02/24/2025).

[129] Celina Filippín. "(PDF) Energy Use of Buildings in Central Argentina". In: *ResearchGate* (). DOI: 10.1177/1744259105051798. URL: https://www.researchgate.net/publication/245382440_Energy_Use_of_Buildings_in_Central_Argentina (visited on 05/30/2025).

[130] *Windows and Glazing | WBDG - Whole Building Design Guide*. URL: https://www.wbdg.org/resources/windows-and-glazing (visited on 05/30/2025).

[131] *What Are Title 24 Windows? | MILGARD*. URL: https://www.milgard.com/blog/title-24-windows-and-patio-doors (visited on 05/30/2025).

[132] Sara Kunkel et al. *(PDF) Indoor air quality, thermal comfort and daylight. Analysis of residential buildings regulations in eight EU member states*. ResearchGate. URL: https://www.researchgate.net/publication/274695177_Indoor_air_quality_thermal_comfort_and_daylight_Analysis_of_residential_buildings_regulations_in_eight_EU_member_states (visited on 05/30/2025).

[133] *The Wilfred - RJC Engineers*. URL: https://www.rjc.ca/project-details/the-wilfred.html (visited on 05/31/2025).

[134] Terri Peters and Julian Weyer. "(PDF) 7. Passivhus Norden | Sustainable Cities and Buildings Brings practitioners and researchers together Architectural Design for Low Energy Housing -Experiences From Two Recent Affordable Housing Projects in Denmark". In: *ResearchGate*. URL: https://www.researchgate.net/publication/301604327_7_Passivhus_Norden_Sustainable_Cities_and_Buildings_Brings_practitioners_and_researchers_together_Architectural_Design_for_Low_Energy_Housing_-Experiences_From_Two_Recent_Affordable_Housing_Projects_i (visited on 05/31/2025).

[135] *Eliminating air leaks and insulating your home*. Hydro-Québec. URL: http://www.hydroquebec.com/ (visited on 05/31/2025).

[136] Natural Resources Canada. *Keeping The Heat In - Section 8: Upgrading windows and exterior doors*. Last Modified: 2025-01-14. Mar. 6, 2014. URL: https://natural-resources.canada.ca/energy-efficiency/home-energy-efficiency/keeping-heat-section-8-upgrading-windows-exterior-doors (visited on 05/31/2025).

[137] Christoph Reinhart. *4.401/4.464 Environmental Technologies in Buildings*. Thermal Mass and Heat Flow.

[138] Carlos Duarte, Paul Raftery, and Stefano Schiavon. "SinBerBEST Technology Energy Assessment Results". In: ().

[139] Veronika Shabunko and Thomas Reindl. "MEASUREMENT OF SOLAR HEAT GAIN COEFFICIENT FOR SEMI-TRANSPARENT BUILDING-INTEGRATED PHOTOVOLTAICS IN THE TROPICS". In: ().

[140] Mohamed H. Elnabawi, Esmail Saber, and Lindita Bande. "Passive Building Energy Saving: Building Envelope Retrofitting Measures to Reduce Cooling Requirements for a Residential Building in an Arid Climate". In: *Sustainability* 16.2 (Jan. 2024). Number: 2 Publisher: Multidisciplinary Digital Publishing Institute, p. 626. ISSN: 2071-1050. DOI: 10.3390/su16020626. URL: https://www.mdpi.com/2071-1050/16/2/626 (visited on 05/30/2025).

[141] *Sustainable Design Requirements-ADD | PDF | Hvac | Ventilation (Architecture)*. Scribd. URL: https://www.scribd.com/document/374409759/Sustainable-Design-Requirements-ADD (visited on 05/30/2025).

[142] Ben M. Roberts, Kevin J. Lomas, and David Allinson. "(PDF) Evaluating methods for estimating whole house air infiltration rates in summer: implications for overheating and indoor air quality". In: *ResearchGate* (Dec. 9, 2024). DOI: 10.1108/IJBPA-06-2021-0085. URL: https://www.researchgate.net/publication/355713917_Evaluating_methods_for_estimating_whole_house_air_infiltration_rates_in_summer_implications_for_overheating_and_indoor_air_quality (visited on 05/30/2025).

[143] *Infiltration values*. GreenBuildingAdvisor. Jan. 24, 2019. URL: https://www.greenbuildingadvi
com/question/infiltration-values (visited on 05/30/2025).

[144] Lukas Vandenbogaerde et al. "(PDF) Field study on the evolution of air tightness in 30 Belgian dwellings". In: *ResearchGate*. Jan. 3, 2025. URL: https://www.researchgate.net/publication/375411201_Field_study_on_the_evolution_of_air_tightness_in_30_Belgian_dwellings (visited on 05/30/2025).

[145] Luke Dolan. *Want to Keep Toxic Smoke Out of Your Home? Here is How We Can Help*. Capital Home Energy. Feb. 3, 2021. URL: https://capitalhomeenergy.com/help/smoke-out-of-your-home/ (visited on 05/31/2025).

[146] *Danish Dwellings with Cold Attics—Ventilation Rates and Air Exchange between Attic and Dwelling*. URL: https://www.mdpi.com/2075-5309/11/2/64 (visited on 05/31/2025).

[147] Maysoun Ismaiel et al. *Airtightness evaluation of Canadian dwellings and influencing factors based on measured data and predictive models*. 2023. URL: https://journals.sagepub.com/doi/full/10.1177/1420326X221121519 (visited on 05/31/2025).

[148] Geun Young Yun and Koen Steemers. "Time-dependent internal heat gains from office equipment, lighting and occupants in buildings: A review". In: *Renewable and Sustainable Energy Reviews* 37 (2014), pp. 317–327. DOI: 10.1016/j.rser.2014.05.056. URL: https://www.sciencedirect.com/science/article/pii/S1364032114004277.

[149] Yat Huang Yau and Boon Hong Chew. "A review on internal heat gains in buildings". In: *Renewable and Sustainable Energy Reviews* 34 (2014), pp. 358–369. DOI: 10.1016/j.rser.2014.03.024. URL: https://www.sciencedirect.com/science/article/pii/S1364032114002276.

[150] Chen Zhang et al. "Resilient cooling strategies – A critical review and qualitative assessment". In: *Energy and Buildings* 251 (Nov. 2021), p. 111312. ISSN: 0378-7788. DOI: 10.1016/j.enbuild.2021.111312. URL: https://www.sciencedirect.com/science/article/pii/S037877882100596X (visited on 06/02/2025).

[151] Akam Abdullah. *Active vs Passive Cooling: Understanding Both Systems*. Grayson Thermal Systems. Nov. 28, 2024. URL: https://www.graysonts.com/active-vs-passive-cooling-in-heavy-vehicles-and-stationary-power-applications/ (visited on 05/06/2025).

[152] Essam Elnagar et al. "A qualitative assessment of integrated active cooling systems: A review with a focus on system flexibility and climate resilience". In: *Renewable and Sustainable Energy Reviews* 175 (Apr. 1, 2023), p. 113179. ISSN: 1364-0321. DOI: 10.1016/j.rser.2023.113179. URL: https://www.sciencedirect.com/science/article/pii/S1364032123000357 (visited on 05/06/2025).

[153] Mohammad Arif Kamal. "An Overview of Passive Cooling Techniques in Buildings: Design Concepts and Architectural Interventions". In: *Civil Engineering* 55.1 (2012).

[154] Dnyandip K. Bhamare, Manish K. Rathod, and Jyotirmay Banerjee. "Passive cooling techniques for building and their applicability in different climatic zones—The state of art". In: *Energy and Buildings* 198 (Sept. 1, 2019), pp. 467–490. ISSN: 0378-7788. DOI: 10.1016/j.enbuild.2019.06.023. URL: https://www.sciencedirect.com/science/article/pii/S0378778819300210 (visited on 05/06/2025).

[155] Mattheos Santamouris and Dionysia Kolokotsa. "Passive cooling dissipation techniques for buildings and other structures: The state of the art". In: *Energy and Buildings* 57 (Feb. 1, 2013), pp. 74–94. ISSN: 0378-7788. DOI: 10.1016/j.enbuild.2012.11.002. URL: https://www.sciencedirect.com/science/article/pii/S0378778812005762 (visited on 05/06/2025).

[156] Jinghua Yu, Changzhi Yang, and Liwei Tian. "Low-energy envelope design of residential building in hot summer and cold winter zone in China". In: *Energy and Buildings* 40.8 (Jan. 1, 2008), pp. 1536–1546. ISSN: 0378-7788. DOI: 10.1016/j.enbuild.2008.02.020. URL: https://www.sciencedirect.com/science/article/pii/S0378778808000418 (visited on 02/24/2025).

[157] Essam Elnagar, Simran Munde, and Vincent Lemort. "Energy Efficiency Measures Applied to Heritage Retrofit Buildings: A Simulated Student Housing Case Study in Vienna". In: *Heritage* 4.4 (Oct. 22, 2021). Publisher: MDPI AG, Basel, Switzerland. ISSN: 2571-9408. DOI: 10.3390/heritage4040215. URL: https://orbi.uliege.be/handle/2268/264528 (visited on 03/11/2025).

[158] Frank P. Incropera et al., eds. *Foundations to heat transfer*. en. 6. ed., internat. student version. Singapore: Wiley, 2013. ISBN: 978-0-470-50196-2 978-0-470-64616-8.

[159] D. Dubert et al. "Numerical analysis of *n*-octadecane melting process in a rectangular cell under reboosting maneuver conditions". In: *Acta Astronautica* 215 (Feb. 2024), pp. 455–463. ISSN: 0094-5765. DOI: 10.1016/j.actaastro.2023.12.020. URL: https://www.sciencedirect.com/science/article/pii/S0094576523006501 (visited on 06/05/2025).

[160] Sung Ho Choi et al. “Heat penetration reduction through PCM walls via bubble injections in buildings”. In: *Energy Conversion and Management* 221 (Oct. 2020), p. 113187. ISSN: 0196-8904. DOI: 10.1016/j.enconman.2020.113187. URL: https://www.sciencedirect.com/science/article/pii/S0196890420307317 (visited on 06/05/2025).

[161] Basile Chaudoir. “Cooling Performance of Macro-Encapsulated Phase Change Material (PCM) Panels: Experimental Investigation and FEM Modelling[BR]”. en. In: (June 2023). Accepted: 2023-07-12T02:15:41Z Publisher: Université de Liège, Liège, Belgique Section: Université de Liège. URL: https://matheo.uliege.be/handle/2268.2/17561 (visited on 06/06/2025).

[162] *Cement*. en-GB. URL: https://www.iea.org/energy-system/industry/cement (visited on 06/05/2025).

[163] Nikolai Artmann, Heinrich Manz, and Per Heiselberg. “PASSIVE COOLING OF BUILDINGS BY NIGHT-TIME VENTILATION”. In: (). URL: https://www.academia.edu/8046364/PASSIVE_COOLING_OF_BUILDINGS_BY_NIGHT_TIME_VENTILATION (visited on 06/06/2025).

[164] Haider Albayyaa, Dharmappa Hagare, and Swapan Saha. “Energy conservation in residential buildings by incorporating Passive Solar and Energy Efficiency Design Strategies and higher thermal mass”. In: *Energy and Buildings* 182 (Jan. 1, 2019), pp. 205–213. ISSN: 0378-7788. DOI: 10.1016/j.enbuild.2018.09.036. URL: https://www.sciencedirect.com/science/article/pii/S0378778817340574 (visited on 05/07/2025).

[165] Emad Mushtaha et al. “The impact of passive design strategies on cooling loads of buildings in temperate climate”. In: *Case Studies in Thermal Engineering* 28 (Dec. 1, 2021), p. 101588. ISSN: 2214-157X. DOI: 10.1016/j.csite.2021.101588. URL: https://www.sciencedirect.com/science/article/pii/S2214157X21007516 (visited on 05/07/2025).

[166] Edwin Rodriguez-Ubinas et al. “Passive design strategies and performance of Net Energy Plus Houses”. In: *Energy and Buildings*. SCIENCE BEHIND AND BEYOND THE SOLAR DECATHLON EUROPE 2012 83 (Nov. 1, 2014), pp. 10–22. ISSN: 0378-7788. DOI: 10.1016/j.enbuild.2014.03.074. URL: https://www.sciencedirect.com/science/article/pii/S0378778814003430 (visited on 05/07/2025).

[167] J. Morrissey, T. Moore, and R. E. Horne. “Affordable passive solar design in a temperate climate: An experiment in residential building orientation”. In: *Renewable Energy* 36.2 (Feb. 1, 2011), pp. 568–577. ISSN: 0960-1481. DOI: 10.1016/j.renene.2010.08.013. URL: https://www.sciencedirect.com/science/article/pii/S0960148110003836 (visited on 05/07/2025).

[168] Sahar Zahiri and Hasim Altan. “The Effect of Passive Design Strategies on Thermal Performance of Female Secondary School Buildings during Warm Season in a Hot and Dry Climate”. In: *Frontiers in Built Environment* 2 (Mar. 7, 2016). Publisher: Frontiers. ISSN: 2297-3362. DOI: 10.3389/fbuil.2016.00003. URL: https://www.frontiersin.orghttps://www.frontiersin.org/journals/built-environment/articles/10.3389/fbuil.2016.00003/full (visited on 05/07/2025).

[169] A. Synnefa, M. Santamouris, and H. Akbari. “Estimating the effect of using cool coatings on energy loads and thermal comfort in residential buildings in various climatic conditions”. In: *Energy and Buildings* 39.11 (Nov. 1, 2007), pp. 1167–1174. ISSN: 0378-7788. DOI: 10.1016/j.enbuild.2007.01.004. URL: https://www.sciencedirect.com/science/article/pii/S0378778807000126 (visited on 05/08/2025).

[170] Mohamed Hamdy et al. “The impact of climate change on the overheating risk in dwellings—A Dutch case study”. In: *Building and Environment* 122 (Sept. 1, 2017), pp. 307–323. ISSN: 0360-1323. DOI: 10.1016/j.buildenv.2017.06.031. URL: https://www.sciencedirect.com/science/article/pii/S0360132317302664 (visited on 05/07/2025).

[171] Maite Gil-Baez et al. “Natural ventilation systems in 21st-century for near zero energy school buildings”. In: *Energy* 137 (Oct. 15, 2017), pp. 1186–1200. ISSN: 0360-5442. DOI: 10.1016/j.energy.2017.05.188. URL: https://www.sciencedirect.com/science/article/pii/S0360544217309842 (visited on 05/07/2025).

[172] Rachel Becker, Itamar Goldberger, and Monica Paciuk. “Improving energy performance of school buildings while ensuring indoor air quality ventilation”. In: *Building and Environment* 42.9 (Sept. 1, 2007), pp. 3261–3276. ISSN: 0360-1323. DOI: 10.1016/j.buildenv.2006.08.016. URL: https://www.sciencedirect.com/science/article/pii/S0360132306002423 (visited on 05/07/2025).

[173] Utkarsh Mathur and Rashmin Damle. “Impact of air infiltration rate on the thermal transmittance value of building envelope”. In: *Journal of Building Engineering* 40 (Aug. 1, 2021), p. 102302. ISSN: 2352-7102. DOI: 10.1016/j.jobe.2021.102302. URL: https://www.sciencedirect.com/science/article/pii/S2352710221001583 (visited on 05/07/2025).

[174] K. Hassouneh, A. Alshboul, and A. Al-Salaymeh. “Influence of infiltration on the energy losses in residential buildings in Amman”. In: *Sustainable Cities and Society*. Special Issue on Third Global Conference on Renewable Energy and Energy Efficiency for Desert Region - GCREEDER 2011 5 (Dec. 1, 2012), pp. 2–7. ISSN: 2210-6707. DOI: 10.1016/j.scs.2012.09.004. URL: https://www.sciencedirect.com/science/article/pii/S2210670712000601 (visited on 05/07/2025).

[175] Juha Jokisalo et al. “Building leakage, infiltration, and energy performance analyses for Finnish detached houses”. In: *Building and Environment* 44.2 (Feb. 1, 2009), pp. 377–387. ISSN: 0360-1323. DOI: 10.1016/j.buildenv.2008.03.014. URL: https://www.sciencedirect.com/science/article/pii/S0360132308000516 (visited on 05/07/2025).

[176] Chadi Younes, Caesar Abi Shdid, and Girma Bitsuamlak. “Air infiltration through building envelopes: A review”. In: *Journal of Building Physics* 35.3 (Jan. 1, 2012). Publisher: SAGE Publications Ltd STM, pp. 267–302. ISSN: 1744-2591. DOI: 10.1177/1744259111423085. URL: https://doi.org/10.1177/1744259111423085 (visited on 05/07/2025).

[177] Paraschiv Lizica Simona, Paraschiv Spiru, and Ion V. Ion. “Increasing the energy efficiency of buildings by thermal insulation”. In: *Energy Procedia*. International Scientific Conference “Environmental and Climate Technologies”, CONECT 2017, 10-12 May 2017, Riga, Latvia 128 (Sept. 1, 2017), pp. 393–399. ISSN: 1876-6102. DOI: 10.1016/j.egypro.2017.09.044. URL: https://www.sciencedirect.com/science/article/pii/S1876610217338882 (visited on 05/07/2025).

[178] Junghun Lee et al. “Impact of external insulation and internal thermal density upon energy consumption of buildings in a temperate climate with four distinct seasons”. In: *Renewable and Sustainable Energy Reviews* 75 (Aug. 1, 2017), pp. 1081–1088. ISSN: 1364-0321. DOI: 10.1016/j.rser.2016.11.087. URL: https://www.sciencedirect.com/science/article/pii/S1364032116308255 (visited on 05/07/2025).

[179] Jong-Jin Kim {and} Jin Woo Moon. “Impact of insulation on building energy consumption”. In: (June 20, 2009). Last Modified: 2014-06-20T10:21+02:00. URL: https://www.aivc.org/resource/impact-insulation-building-energy-consumption (visited on 05/07/2025).

[180] Umberto Berardi, AmirHosein GhaffarianHoseini, and Ali GhaffarianHoseini. “State-of-the-art analysis of the environmental benefits of green roofs”. In: *Applied Energy* 115 (Feb. 15, 2014), pp. 411–428. ISSN: 0306-2619. DOI: 10.1016/j.apenergy.2013.10.047. URL: https://www.sciencedirect.com/science/article/pii/S0306261913008775.

[181] Elisa Guelpa. “Impact of thermal masses on the peak load in district heating systems”. In: *Energy* 214 (Jan. 1, 2021), p. 118849. ISSN: 0360-5442. DOI: 10.1016/j.energy.2020.118849. URL: https://www.sciencedirect.com/science/article/pii/S0360544220319563.

[182] Simon B. Pallin, Tyler Pilet, and Renata Starostka. *Variables Influenced by Thermal Mass and its Impact on Energy Performance in Buildings*. Oak Ridge National Laboratory (ORNL), Oak Ridge, TN (United States), Dec. 1, 2019. URL: https://www.osti.gov/biblio/1649425.

[183] Azin Velashjerdi Farahani et al. “Performance assessment of ventilative and radiant cooling systems in office buildings during extreme weather conditions under a changing climate”. In: *Journal of Building Engineering* 57 (Oct. 1, 2022), p. 104951. ISSN: 2352-7102. DOI: 10.1016/j.jobe.2022.104951. URL: https://www.sciencedirect.com/science/article/pii/S2352710222009627.

[184] Ivan Oropeza-Perez and Poul Alberg Østergaard. “Active and passive cooling methods for dwellings: A review”. In: *Renewable and Sustainable Energy Reviews* 82 (Feb. 1, 2018), pp. 531–544. ISSN: 1364-0321. DOI: 10.1016/j.rser.2017.09.059. URL: https://www.sciencedirect.com/science/article/pii/S1364032117313084.

[185] *Heat Pumps - Energy System*. IEA. URL: https://www.iea.org/energy-system/buildings/heat-pumps (visited on 05/07/2025).

[186] *Decarbonising heating and cooling — a climate imperative*. European Environment Agency. URL: https://www.eea.europa.eu/publications/decarbonisation-heating-and-cooling/decarbonising-heating-and-cooling (visited on 05/07/2025).

[187] *Cooling buildings sustainably in Europe: exploring the links between climate change mitigation and adaptation, and their social impacts*. European Environment Agency. URL: https://www.eea.europa.eu/publications/cooling-buildings-sustainably-in-europe/cooling-buildings-sustainably-in-europe.

[188] William Goetzler et al. *The Future of Air Conditioning for Buildings*. DOE/EE-1394. Navigant Consulting, Burlington, MA (United States), July 1, 2016. DOI: 10.2172/1420235. URL: https://www.osti.gov/biblio/1420235.

[189] Jean-Marc Jancovici. “« L’essentiel du progrès technique aujourd’hui n’est absolument pas fait pour résoudre les problèmes d’environnement »”. In: *Le Monde* (July 2024). URL: https://www.lemonde.fr/series-d-ete/article/2024/07/24/jean-marc-jancovici-l-essentiel-du-progres-technique-n-est-pas-fait-pour-resoudre-les-problemes-d-environnement_6256728_3451060.html.

[190] Jean-Marc Jancovici. *« Nous n'avons pas un problème d'énergie, mais un problème de civilisation »*. Interview on France Inter. 2019. URL: https://www.radiofrance.fr/franceinter/podcasts/le-telephone-sonne/le-telephone-sonne-du-mercredi-16-octobre-2019-2380672.